5-3-2019

Implant-Related Osteomyelitis Models for the Assessment of Bacteriophage Therapeutics

Leah Kelley Horstemeyer

Implant-related osteomyelitis models for the assessment of bacteriophage therapeutics

By

Leah Kelley Horstemeyer

A Thesis
Submitted to the Faculty of
Mississippi State University
in Partial Fulfillment of the Requirements
for the Degree of Master of Science
in Biomedical Engineering
in the Agricultural and Biological Engineering

Mississippi State, Mississippi

May 2019

Implant-related osteomyelitis models for the assessment of bacteriophage therapeutics

By

Leah Kelley Horstemeyer

Approved:

_____

Lauren Priddy
(Major Professor)

_____

Keun Seo
(Committee Member)

_____

Elizabeth Swanson
(Committee Member)

_____

Steve Elder
(Graduate Coordinator)

_____

Jason Keith
Dean
Bagley College of Engineering

Name: Leah Kelley Horstemeyer

Date of Degree: May 3, 2019

Institution: Mississippi State University

Major Field: Biomedical Engineering

Major Professor: Lauren Priddy

Title of Study: Implant-related osteomyelitis models for the assessment of bacteriophage therapeutics

Pages in Study: 116

Candidate for Degree of Master of Science

Antibiotic resistant strains of bacteria continue to increase in prevalence, hindering the ability of clinicians to treat infection. One disease exacerbated by this trend is osteomyelitis, or bone infection. When osteomyelitis is induced by these antibiotic resistant strains, patients can experience prolonged hospital visits, greater economic burdens, amputation, and even death. Due to the limitations of antibiotics to clear these infections, we sought to identify new therapeutic options for osteomyelitis. Our aim was to first develop an *in vivo* implant-related model of osteomyelitis. We then wanted to explore the potential of novel CRISPR-Cas9 modified bacteriophage to treat infection. *in vitro* and *in vivo* investigations demonstrated that bacteriophage therapeutic may be a viable option for infection mitigation. Furthermore, our *in vivo* model of osteomyelitis proved to be reliable, consistent, and challenging. Future research will utilize this model as a platform for optimizing therapeutic regimen and delivery vehicle(s) for antimicrobial therapeutics.

DEDICATION

I dedicate the entirety of this work to my parents, Jill and Derek Horstemeyer. Every success I have in life is only possible because of the love, encouragement, and inspiration you give me every day. I can't put into words how much the late phone calls, long drives to Mississippi, and enthusiasm for my academic pursuits means, so I'll simply say that "I love you to the moon and back."

To my wonderful roommate, cousin, and therapist Darby Stanford- thank you for blindly following me here and for making this chapter of life full of so much joy. I can't imagine having anyone else by my side through all of this.

Norman Cobb; never in a million years would I have guessed that I would meet the love of my life in Starkville, MS. Thank you for supporting and loving me every single step of the way. I thank God every day that we met, and I can't wait to build my life with you.

ACKNOWLEDGEMENTS

This work is truly interdisciplinary, and as thus required the time, dedication, and passion from a large variety of people. I would like to acknowledge the students, faculty, and staff at Mississippi State who invested in this project:

I would like to first acknowledge Dr. Lauren Priddy, my wonderful advisor, mentor, and confidant. I feel so lucky to have been given the opportunity to be here, out of all of the overqualified students you could have chosen to help start up your lab. Thank for giving me so much freedom in choosing this research topic, and for respecting my thoughts, ideas, and opinions. Being trusted by you to explore various avenues of research and for expressing my creativity has made this such an enjoyable, and fun experience. Thank you to my other committee members: Dr. Steve Elder, Dr. Betsy Swanson, and Dr. Seo, for investing literal hours of your personal time in this work. Your expertise and positive guidance throughout this study has been crucial to the culmination of this document.

Thank you to the numerous folks at CVM who allowed us to perform animal studies, and assisted us throughout the late nights, early mornings, and emergencies as we developed this model. Drs. Seo and Park, thank you for letting me invade your space and for spending hours teaching me the skills necessary to handle and manipulate *Staphylococcus aureus.* I enjoyed getting to know your family, and can't wait to read the literature your lab produces over the coming years which will surely be revolutionary. Dr. Swanson, it was such an honor to work with you. I wish I had a way to properly thank you for the hours you offered your surgical

expertise to our team. I know that I speak for the rest of our lab group when I say that you are a wonderful teacher, collaborator, and surgeon. For that, I am thankful. Drs. Willeford and Senter, veterinary expertise, communication, and willingness to work with us has been such a blessing. Jamie Walker, you have been absolutely vital to our group. I have so enjoyed working with you, and wish that we had more studies together in the future. Dr. Alicia Olivier, thank you for providing histological expertise and last-minute necropsies. I enjoyed working under you, and appreciate the time you spent teaching me, and our research group, in necropsy. I would also like to acknowledge USDA- ARS Biophotonics Initiative #58-6402-3-018, and Drs. Jean Feugang and Seongbin Park, for allowing us to use the IVIS Lumina XRMS system.

I have appreciated the comradery and support offered by the entirety of the Priddy lab group over the past three years: Weitong Chen, Emily McCabe, Mary Catherine Beard, Anna Rourke, Kristen Lacy, Bethany Foust, Kali Sebastian, Chris Grant, Heather White, Luke Tucker, Luke Nichols, Liam McDougal, Landon Teer, and Sarah Heller. I have so enjoyed working with you all and being given the responsibility and the joy serve as a mentor and friend to the many undergraduates in our lab group. You all have truly made research fun!

Last but not least, thank you to the many friends I have made over the past few years who have made me fall in love with Mississippi State, through late night conversations, football games, trivia, and even a kickball recreation league team: Darby Stanford, Norman Cobb, Anna Marie Dulaney, Parker Berthelson, Ty Smith, Will Williams, Alex Smith, Shelby Baird, Pratik Parajuli, Sonja Jensen, Kali Sebastian, Hannah Bateman, the Vaughn family, Katie Rose Anthony, Allen Barbour, and so many others.

TABLE OF CONTENTS

LIST OF TABLES

LIST OF FIGURES

CHAPTER I

MOTIVATION

The prevalence of antibiotic resistant pathogens is increasing, whereas the rate of novel antibiotic production by pharmaceutical companies is dwindling. Furthermore, osteomyelitis is especially prevalent in the diabetic population, with one 1 in every 15 patients requiring amputation.[1] This is concerning, as there are currently over 11 million people in the United States alone with this disease, with new diagnoses each day.[1] It may be assumed that the rate of osteomyelitis infections may thus increase, due to the widespread diagnosis of these diseases and antibiotic resistant bacterial strains across the United States. Thus, there exists a great need to develop novel therapeutics which can effectively kill bacteria, but are not susceptible to bacterial resistance.

Research Objectives

Previously, CRISPR-Cas9 modified phage exhibited superiority to vancomycin and fosfomycin therapeutics when treating *Staphyloccoccus aureus* LAC strain biofilms *in vitro* (Appendix A). Thus, we hypothesized that CRISPR-Cas9 could be used to optimize phage efficacy on *Staphylococcus aureus* strain ATCC 6538. Thus, the first aim of this study was to characterize CRISPR-Cas9 modified phage "#5φCas9" virus *in vitro*. Our objectives included identifying compatible delivery vehicles for this virus, investigation the release of this phage from such a delivery vehicle, and reconfirming bactericidal activity. We sought to analyze these

components utilizing Kirby-Bauer assays, antibiofilm plate assays, IVIS Lumina XRMS, and bacterial counts.

The second aim of this work was to develop an *in vivo* model of osteomyelitis. To aid our research, we desired that the model would be reliable, consistent, enable longitudinal tracking of infection, and would be challenging enough to warrant promising solutions to the therapeutic shortage for osteomyelitis, should our novel therapeutic(s) mitigate infection. Herein, we investigated two different osteomyelitis models. In model #1, our objectives were to develop osteomyelitis infection that did not: (i) limit rat mobility, (ii) was not naturally cleared by the host, and (iii) that could be tracked longitudinally. The objectives of model #2 largely centered on improvements of model #1. In model #2, our objectives included: (i) localizing infection in a consistent location, (ii) inducing an infection of consistent severity among various animals, and (iii) to have an efficient platform to test our therapeutics of interest. To characterize these models, we utilized IVIS Lumina XRMS imaging, histology, scanning electron microscopy, and bacterial counting.

The third aim of this work was to apply the CRISPR-Cas9 bacteriophage therapeutic in our model (#2) of osteomyelitis and investigate its ability to clear infection. Again, we utilized IVIS Lumina XRMS imaging, histology, scanning electron microscopy, and bacterial counting.

CHAPTER II

INTRODUCTION

Since penicillin was first introduced to the world in the 1940s, antibiotics have become a reliable "go-to" for health care professionals.[2] However, antibiotics have been losing their efficacy over time, due to the emerging population of antibiotic-resistant pathogens. This has in turn led to a deficit in reliable therapeutics for clinicians. Per a report published in 2013 by the Centers for Disease Control and Prevention (CDC), an estimated $20 billion in healthcare costs in the United States were due to bacterial antibiotic resistance, with costs estimated as high as $35 billion when lost productivity in the workforce was accounted for.[3] Thus, this is a significant problem our society currently faces.

Osteomyelitis

Overview

Osteomyelitis, or the infection of bone, is one disease whose severity has been exacerbated by the rise of these antibiotic resistant pathogens, as *Staphylococcus aureus (S.aureus)* is the most common cause of osteomyelitis.[4–6] In 2013, in the United States alone there were over 80,000 infections and 11,285 deaths due to these antibiotic-resistant strains *of S. aureus*.[3]

There are many ways to classify osteomyelitis infection, one of which categorizes infection into an acute or chronic state. Although both are essentially bacterial bone infections, they are very different in terms of pathology and therapeutic resistance and should thus be treated as separate diseases.[7] Acute osteomyelitis, typically recognized as the early stage of osteomyelitis, can generally be cleared with antibiotics if treated in a timely manner. In contrast, to treat chronic osteomyelitis, or infection that has persisted for longer than 6 weeks, long-term high dose administration of antibiotics with or without surgical intervention has traditionally been considered the minimum effective treatment.[7–9] Often, more than one antibiotic are necessary to eradicate infection.[10] However, even this treatment may not be vigorous enough, and patients may experience re-emergence of infection.[9]

Etiology

Osteomyelitis may be further categorized into three etiological groups: hematogenous, contiguous, or the result of contamination. In each of these cases, acute and chronic osteomyelitis can develop. Hematogenous osteomyelitis results from bacteria that has traveled through the blood stream to its bony host. Often, bacteria may then collect in bone capillaries. As a result, bacterial abscesses are found adjacent to the diaphysis in the middle of the bone.[11] Hematogenous osteomyelitis is especially prevalent in children, as bone growth may slow blood flow through the long bones, which allows bacteria in the blood to more readily colonize and grow.[11]

In cases of contiguous osteomyelitis, bacteria reach the bone from adjacent infections.[7] This is particularly detrimental for those with diabetes mellitus, in which the development of infections of the digits are common, as well as dermal abscesses, which can then lead to

osteomyelitis. As of 2015, a staggering 30.3 million people in the United States were estimated to have diabetes, and from the 1970s to the 2000s, the percentage of OM cases that were diabetes-related increased from 13% to 29%.[12,13] Thus, the diabetic population is particularly vulnerable to contiguous cases of osteomyelitis, and these patients are at a great disadvantage in terms of osteomyelitis infection outcome.

The final etiological category of osteomyelitis discussed herein, that which results from direct contaminations, is exactly as its name indicates. Sometimes, this may occur from compound fractures, in which the bone is directly exposed to the environment. Alternatively, this can be due to contaminated hardware, used for fracture fixation or joint repair. In orthopedics, these implant-associated infections can become a serious issue resulting in osteomyelitis, increased hospital bills, and hardware failure.[14]

Staphylococcus aureus

Overview

As mentioned previously, *S. aureus* is the most common cause of osteomyelitis. To develop therapeutics to combat this disease, the causative agent of the disease must first be understood. First discovered in the late 1880s, *S.aureus* is a gram positive bacteria with a diameter of about 1 μm.[15] Phenotypically, it appears as grape-like clusters.[15] *S. aureus* causes minor skin infections, as well as more serious conditions such as pneumonia, endocarditis, and osteomyelitis. It is also a bacterial strain that has managed to elude antibiotics over time.

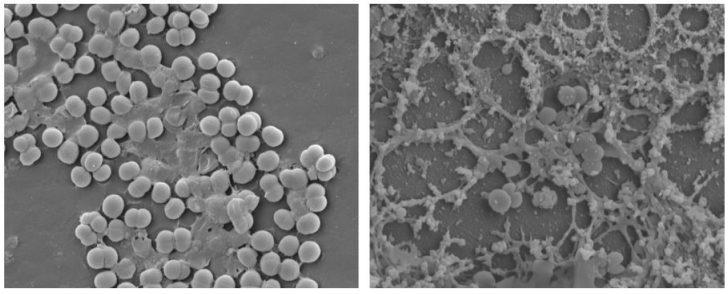

Figure 2.1 Scanning Electron Microscopy of Staphylococcus aureus

Figure 2.1

Impact & History of Antibiotic Resistance

In 1940, prior to antibiotics, *S.aureus* infections resulted in a mortality rate as high as 80%.[15] In 1940, penicillin was introduced to the health care industry. Within only two years, a penicillin-resistant *S.aureus* isolate was discovered. Similarly, when methicillin was introduced in 1959, methicillin-resistant *S. aureus* (MRSA) materialized.[2] To combat MRSA, the antibiotic vancomycin was developed. However, like the penicillin- and methicillin-resistant strains that emerged as new antibiotics were developed, a vancomycin-resistant strain of *S.aureus* (VRSA), materialized in 2002.[16] In February of 2015, the fourteenth case of VRSA was reported.[16] If this strain spreads, it would be quite detrimental to society as there are no currently no effective therapeutics for this strain.[3,16]

Phenotypic States of *Staphylococcus aureus* Contributing to Antibiotic Resistance

Two phenotypic states of *S. aureus* may be considered hallmarks of bacterial antibiotic resistance: small colony variants (SCVs) and biofilms.[17] An SCV refers to an *S. aureus* cell with markedly decreased metabolic activity compared to the wildtype.[17] The slower metabolic rate

may be attributed to auxotrophies, or to downregulated citric acid cycle activity, as seen in recent *in vitro* testing.[18] Due to this altered metabolic activity, SCVs are more resistant to antibiotics and may be more apt to form biofilms.[17,19] The mechanism by which *S. aureus* induces SCV formation is unknown, but the process is reversible.[19] A more recent study determined that SCV formation may be stimulated as part of the SOS response to oxidative stress, although this may not be the sole stimulant of SCV formation.[19] Exposure to antibiotics, such as gentamicin, may also promote SCV formation in human hosts.[17,18] In contrast to SCVs, a biofilm refers to a grouping of staphylococcal cells surrounded by a self-produced protective exopolysaccharide polymer.[7,18–20] The biofilm may contain SCVs or wildtype *S. aureus* cells. Once the biofilm is established, *S. aureus* may then eject groups of cells, in an effort to disperse its colonies to initiate the formation of additional biofilms.[20] Biofilms may form on skin, bones, and other tissues, as well as on implanted hardware.[20] Once bacteria enters this state, it is difficult for antibiotics to penetrate the glycocalyx matrix and thus clear infection.

Summary

The increase of antibiotic-resistant pathogens combined with the higher prevalence of comorbidities to osteomyelitis in our population highlight the importance of engineering new therapeutics for *S. aureus*, especially for chronic osteomyelitis cases.[21,22] Ideally, novel treatments would be noninvasive, highly specific, and less susceptible to bacterial resistance. The delivery vehicles for such therapeutics should be biocompatible and capable of delivering a sufficient amount of therapeutic over time. To develop an appropriate therapeutic agent, these factors must be considered, in addition to the pathogenesis of *S. aureus,* and the refinement of animal models to evaluate these various components of osteomyelitis treatment.

Current Therapeutics

Surgical Debridement

Surgical debridement, or the removal of infected and/or damaged tissues due to bacterial contamination, is often considered vital to successful treatment of chronic osteomyelitis.[8,23,24] Although health care professionals have tried to find alternatives to this procedure, it currently remains the cornerstone of chronic osteomyelitis treatment, and its superiority to sole antibiotic therapy has been emphasized by numerous studies.[24–26]

Antibiotics

For decades, the most common class of therapeutic agents for osteomyelitis have been antibiotics. However, bacteria have developed resistance to these drugs over time due in part to the ability of certain bacteria to alter their metabolism, which are referred to as "small colony variants" (SCVs).[17] Generally, antibiotics which act on the bacterial cell wall have greater efficacy on bacteria that are in the exponential phase, when they are growing quickly. Examples of such antibiotics include β-lactams, daptomycin, and fosfomycin.[17] Fosfomyin, a small drug (~138g/mol) which comprises its own class of antibiotics, is of particular interest as it has seen promising effects in recent literature.[27]

Fosfomycin induces bacterial lysis after entering the cytoplasm, by mimicking glucose-6-phosphate and glycerol-3-P, as native proteins GlpT and UhpT readily transport these sugar sources into the cell.[28] Once inside the bacterial cell, Fosfomycin serves as a replacement to typical phosphoenolpyruvate ("PEP"). Typically, PEP binds to a transferase ("MurA") which activates the enzyme (enolpyruvyl transferase), activating the cell wall synthesis pathway.[27,28] By serving as an analog of PEP, Fosfomycin irreversibly halts this pathway, and cell death occurs.[28]

Since this is a universal mechanism across gram positive and negative bacteria, Fosfomycin has broad-spectrum efficacy.

The use of Fosfomycin clinically is limited, most commonly to female UTI cases, dermal infection, and sepsis.[29–31] For UTI cases, oral administration at a dose of 3g every 2-3 days is recommended.[29] For soft tissue infection and/or sepsis, daily IV administration at doses ranging from 12-24g is recommended[27,32]

Another antibiotic family are the glycopeptides. One of the most significant antibiotics within this classification is vancomycin, which is considered to be a "last resort antibiotic" for multi-drug resistant or severe infection types. Unlike fosfomycin, it is not internalized by bacterial cells; rather, it exerts its killing action by acting on the exterior cell wall. The terminal end of PEP consists of a D-Ala-D-Ala chain, where vancomycin binds and deactivates the machinery necessary to maintain the cell wall structure.[33] Thus, the cell is lysed. In cases of biofilm, it could be difficult for vancomycin to work effectively.

Antibiotics may also act on protein biosynthesis, like Clindamycin. This drug would also see reduced bactericidal activity when faced with SCVs.[17] In some cases, these antibiotic types would not only be ineffective against SCVs but could induce or increase biofilm growth. Low doses of β-lactam antibiotics have been particularly noted to have this effect.[34] The function of the bacteria as a SCV, then, should be considered when deciding on an antibiotic for chronic osteomyelitis. rifampin, moxifloxacin, and vancomycin, among others, have effects on bacteria in this state.[17]

An alternative approach to antibiotic use in osteomyelitis patients may be to treat patients with combinations of the drugs, as this has been shown to be more effective than monotherapy

greater range of efficacy. For example, rifampin combined with either linezolid, vancomycin, cloxacillin, or ciproflaxin have all been explored.[35–37]

Bacteriophages

Bacteriophages are a specialized virus that have the ability to lyse bacterial hosts, making them a potential source for osteomyelitis treatment. Generally, they consist of a capsid head, in which DNA resides, a sheath, and tail fibers.[38,39] The bacterial host specificity of phage is determined by their tail fiber.[39] These tail fibers facilitate attachment to external bacterial cell wall binding proteins, such as OmpA or OmpC.[40] After attachment to the bacterial cell wall, phages use a protein "holin" and/or murine hydrolase to generate a hole through which they can insert their DNA in a screw-like manner.[41] Like most viruses, bacteriophages do not contain their own DNA synthesis machinery. They are dependent on hijacking bacterial host machinery, for progeny. Thus, after the pore in the cell membrane is created by holin, phage reproduces within the cell, until it lyses the host and seeks a new host. It should be noted that not all bacteriophages are virulent, or lytic; there are also lysogenic, or temperate phages. Temperate phages can integrate into their host genome, essentially serving as a parasite to their hosts. They can "live" within their host for multiple life cycles without inducing lysis.[42]

It has long been known that the viral family of bacteriophages ("phages") have high efficacy in lysing bacterium for which they are specific.[43,44] Other advantages of phages are that they multiply in response to the presence of bacterial hosts, allowing for increased "dosage" of treatment as needed.[45] However, several hurdles must be overcome before the positive qualities of phages may be utilized. Phages are generally specific for one strain of bacteria, and thus a wider range of bactericidal activity for polymicrobial infections, or infections in which the

bacterial agent is not identified, is desirable. To overcome this problem, phage "cocktails" containing multiple strains of phages have been developed.[46] Alternatively, the endoylsins produced by phages could be harvested, avoiding the need of directly placing phages into the human body. In a recent study utilizing the endolysin $CHAP_K$, delivered with lysostaphin, positive bacterial clearance was reported.[47] Additionally, phages must be delivered to the site of infection for efficacy.[44] Recent research has focused on engineering hydrogels, dry powders, nanoparticles, and coatings on implants for delivery of phages.[44,45,48,49]

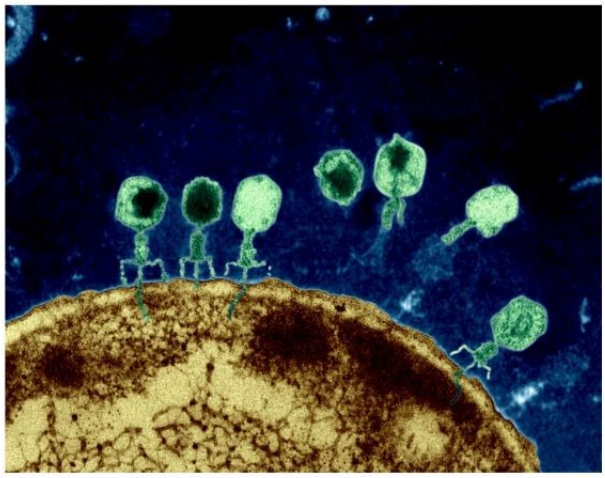

Figure 2.1 Example of Bacteriophage "Attack" on Bacteria

Bacteriophage, seen here in green, injects its DNA into susceptible bacterial host. This mechanism will result in additional bacteriophage proliferation, and eventual bacterial cell lysing. (Image from Eye of Science/Science Source)

Antimicrobial Peptides

Antimicrobial peptides, or "AMPs", have been gained popularity in recent years as therapeutics for osteomyelitis. The AMP Human β-defensin-3 (HBD-3) has been given particular

attention, and has been evaluated in mouse models of osteomyelitis, as mice naturally have a structural and functional homolog of HBD-3 called mouse β-defensin-14 (MBD-14).[50] Mice have also been treated directly with HBD-3, in a comparative study with vancomycin as a control treatment. In this particular study, a promising outcome was achieved in that there were no statistically significant differences between the two treatments.[51]

Magainin 2 is another antimicrobial peptide which may provide relief from the current therapeutic deficit in osteomyelitis treatment. Pexiganan acetate, a synthetic analog to magainin 2, has been explored in a rabbit implant model of osteomyelitis with promising results.[52]

Venoms from mammals may also serve as a source of AMPS. In one investigation, 14kDa and 65kDa proteins isolated from the venom of the *Naja Naja Oxiana* snake were found to have similar, and in some cases greater, bactericidal activity than several antibiotics. However, due to the novelty of this study, testing has been limited to *in vitro* methods and thus *in vivo* animal models will be needed to determine if this may be a promising therapeutic.[53] Bee venom may also be a useful source for AMPS. In an *ex vivo* study, calcium phosphate or PMMA cements were used to deliver analogs of bee venom halcitides (HAL-1 and HAL-2). In excised femoral heads, the AMPs exhibited significantly greater efficacy than Vancomycin.[53] These bee venom derived AMPs have also shown success in a rat model of osteomyelitis, when delivered in calcium phosphate. However, tests such as bacterial counts of bone homogenates are excluded, among others, and thus limit our knowledge of their efficacy.[54]

Ranalexin, isolated from the North American Bullfrog (*Rana catesbeiana)* has also exhibited bactericidal activity against MRSA. However, evaluation of this therapeutic has been

limited to dermal infection studies, delivered with lysostaphin. This warrants future research on the use of this AMP for osteomyelitis.[55]

Plant-based & Natural Remedies

Taking a holistic, natural approach to antimicrobial development has also been explored. Essential oils have long been hailed as having many health benefits, and more recently was shown to have antimicrobial properties, with a low likelihood of staphylococcal resistance. A few examples include: tea tree (*Melaleuca alternifolia),*[56] and *Gingko biloba.*[57]Tea tree oil has exhibited efficacy on *S.aureus* biofilms as well as planktonic cells at concentrations as low as 1%.[56] Recent studies on *Ginkgo biloba* extract, and one of *Ginkgo biloba*'s ginkgolic acids, "C15:1.," have shown biofilm formation inhibition. Interestingly, planktonic growth was not affected.[57]

Flavonoids are another natural source for potential antimicrobials. Curcumin, a natural component of the common spice turmeric, has been evaluated as a therapeutic in a rat implant model of osteomyelitis. A combination of this flavonoid and erythromycin proved to be more successful than curcumin or erythromycin monotherapy, indicating the synergistic effects curcumin may exhibit when administered with other antibiotics. No adverse effects were noted, as well.[58]

Enzymes

Another interesting area of current research revolves around the use of enzymes as therapeutics. One such enzyme is lysostaphin, a metalloendopeptidase which can lyse the cell wall of *S. aureus,* thus serving as a bacteriocin.[47,59,60] The attractiveness of lysostaphin to reseachers is heightened by the fact that it works synergistically with other therapeutics.37 In

particular, with AMPs.[55] Furthermore, in a recent study, a PEG-based hydrogel exhibited enzymatic activity over 14 days. [59] Endolysins, as mentioned above, are another feasible treatment for osteomyelitis. Isolated from bacteriophages, they can dismantle the bacterial cell well with their hydrolase activity.[47]

Quorum–sensing Inhibitors

Another aspect of *S.aureus* treatment falls under the umbrella of "quorum sensing inhibitors." The concept behind these therapies are that without the ability to communicate, the *S. aureus* cells will be more readily cleared from the body. Thus, this mode of treatment may be most effective combined with antibiotics or other bactericidal agents.[61] Some examples of substances explored for this purpose include: savirin (in mouse dermal ulcer studies),[62] and Hamamelitannin.[61]

Metals

A materials based outlook on potential therapeutics for osteomyelitis has also been considered. Largely, this focuses on optimizing metals used for orthopedic hardware. One novel metal formulation, stainless steel with a 4.5% copper alloy (317L-Cu), has been shown to exhibit antimicrobial properties while still maintaining biocompatibility *in vitro* and *in vivo*, making it a promising material choice for future implant devices.[63] It has also been found that this metal may increase the expression of the insulin-like growth factor-1 (IGF-1) in osteoblasts, unlike other commonly utilized metals such as 317L and Ti-6Al-4V.[63] A magnesium-copper (Mg-Cu) alloy (with 0.25 wt% Cu) may also provide desired antimicrobial activity, as supported by a recent *in vitro* and *in vivo* study. This study also demonstrated the ability of Cu content to adjust corrosion rate.[64]

Gold (Au), is an attractive yet pricey option for a metal-based therapeutic. As a nanoparticle, it has exhibited cytocompatibility, efficacy against planktonic and sessile bacteria, and bactericidal activity for MSSA and MRSA strains.[65] As a more tangible alternative, silver (Ag) has long been explored for both orthopedic implants and as a therapeutic. However, there are some conflicting reports of silver's (Ag) ability to serve as an antimicrobial in recent studies.[66] Ag may be more beneficial at higher doses, or in conjunction with other materials, or when utilized in a silver ion state.[66–68] In a study evaluating the delivery of Ag nanoparticles from a silk-fibroin hydrogel, it was determined that Ag had positive cytocompatibility and bactericidal activity at a concentration 0.5%, with adverse effects on osteocytes at any higher concentrations.[65] Alternatively, it's possible that the varied results may be attributed to the strains of *S. aureus* utilized.[66]

Miscellaneous

Based on their ability to differentiate into chondrocytes, osteocytes, and other relevant cell lineages, it has been postulated that mesenchymal stromal cells (MSCs) may serve as an effective therapeutic or synergistic agent in osteomyelitis treatment. However, in a recent study MSCs were found to exacerbate the severity of osteomyelitis.[69] Greater degrees of osteolysis spontaneous fracture, and upregulation of pro-inflammatory cytokines were evident in the MSC/infected treated group, versus the infected control subjects.[69]

Hyperbaric oxygen therapy has been proposed as a potential *S.aureus* infection treatment regimin, however in multiple *in vivo* studies it has been shown that this is an ineffective therapeutic.[70,71] It is has been demonstrated that it is faulty as an intermittent treatment, and as an supplement to antibiotic treatment.[71] Another intruiging therapy is the use of visible blue light,

which has been determined to be effective against MRSA strains at 470 nm.[72] It has been determined to heighten the efficacy of a variety of antibiotics, as well.[72]

Another method of inhibiting *S.aureus* virulence for effective osteomyelitis treatment is with the use of the NSAID diflunisal. This drug acts to inhibit one of the most well-studied loci of *S.aureus* virulence, and when combined with other drugs, may prove to be an effective treatment regimin.[5]

Another possible therapeutic is nitric oxide, which has exhibited efficacy against *S. aureus* in planktonic and biofilm forms. Specifically, it seems to exhibit synergistic efficacy when administered with antimicrobials.[73] Current research regarding this treatment typical revolves around delivery, and efficient levels of NO to exceed the MIC. In one recent study, by incorporating the precursor to NO, isosorbide mononitrate, into a novel hydrogel, efficient clearance of bacteria was achieved.[73]

Delivery Vehicles

Hydrogels

Commonly used by clinicians and researchers, hydrogels are a versatile and compatible delivery vehicle for therapeutics in cases of osteomyelitis. Hydrogels are a water-based material, constituting of synthetic or natural hydrophilic polymers in various combinations. Some materials that may be incorporated into the gel(s) include, but are not limited to: chitosan,[73] silk,[65] hydroxyapatite("HA"),[65] gelatin,[74,75] and keratin.[76]

Their release profiles vary, but there is typical an initial burst of therapeutics for about 7 days,[74,77] followed by a slow, low dose elution to follow. They then degrade completely and may be cleared by the body by 6 weeks, but again there is high variability per each unique clinical

case.[77] Hydrogels have been used as carriers for antibiotics,[23,74,77–80] nanoparticles,[49] microparticles,[80] bacteriophages,[43,44,49,81] proteins,[76] and other therapeutics.[59,69,73]

One of the positive qualities of hydrogels are the ability to have their properties tailored for one's own interests. Components of these gels that may be altered include: porosity, viscosity, elasticity, and the degree to which they swell. One of the most pertinent qualities of a delivery vehicle are their elution rates of one's drug of choice, and thus this is one area which has been researched extensively. To alter drug elution rates, the sensitivity of hydrogels to temperature,[23,79,80,82] pH,[82] or both can be altered to increase or decrease degradation rates, to optimize release profiles of therapeutics. [23,78,80]

Another way to modify drug elution rates is through changes in the composition of the gels. For example, altering gelatin concentration, which alters degradation rate.[74] More recently, silk fibroin obtained from *Bombyx mori* cocoon were used as a main component of a hydrogel. These silk fibers, dissolved in $CaCl_2$:CH_3CH_2OH:H_2O, are an attractive component in a hydrogel due to their tyrosine residues, which provide stabilization for Ag and Au additives.[65] Keratin has also been explored as an additive to hydrogels to obtain optimal mechanical, physical, and therapeutic qualities.[76] In one study, through an oxidative extraction process, a hydrogel consisting of "keratose" and ciprofloxacin achieved a release profile of 60% elution over 10 days, followed by a slow, sustained release for 3 weeks following initial injection.[76] The efficacy of the gel in inhibiting *Staphylococcal* growth, combined with the hypothesized electrostatic interactions enabling ciprofloxacin release to coincide with hydrogel degradation, make this formulation an intriguing delivery vehicle in future studies.[76]

A more unique way to control drug release may be through conformational changes. Recently, a layered hyaluronic acid methacrylate (HAMA) system was able to deliver triggered release of phages *in vivo.*[44] The success of the system is due to the outer HAMA layer, which is sensitive to an enzyme found in *S. aureus* called hyaluronidase (HAase). Upon contact, the HAMA layer degraded and released bacteriophages to treat *S.aureus* biofilms.[44] Another alteration of hydrogels which was been considered involves the utilization of a "gellan gum" conformation, in which the hydrogel took on a threefold double helical shape. This was used to deliver both dissolved vancomycin, and vancomycin encapsulated in PLGA nanoparticles.[83]

Cements

Traditionally, bone cements have been used by surgeons for placement of orthopedic hardware. In the past, these cements were largely non-degradable which impeded bone healing and led to additional surgical procedures. Recent modifications of bone cement have improved degradation rates and enabled them to become drug carriers. They may hold antibiotics, like teicoplanin,[78] vancomycin,[84–86] gentamicin,[87] or AMPs.[54,88] For greater antimicrobial properties and length of drug elution, new formulations of bone cements are being engineered. Some materials that have been considered are calcium sulfate hemihydrate, calcium phosphate,[54] and PMMA,[85–88] among others.[78,84] Some more recent cements have even used bioactive glass.[84] One interesting formulation included hydrophilized PMMA, due to a pluronic F68 additive, to effectively deliver vancomycin for up to 11 weeks.[85]

Micro- and Nano-particles

Recently, micro- and nano-particles have become a great area of interest for scientists. These particles are favorable because of their biocompatibility, use for local or systemic

delivery, and easy manipulation depending on their usage.[89] Micro- and nano-particles can vary by their size(s), what they are loaded with, what they are made of, how they are administered and how they are created.

They have been used to deliver antibiotics,[72,83,89–92] and bacteriophages,[49,93,94] among other drugs. Different materials that have been analyzed for favorable micro- and nano-particle synthesis include: PEG,[92] poly(ester-amide)-PEGs ("PEAE"),[89] Poly(N-isopropylacrylamide) ("PNIPAM"),[93] gold,[49,94] silver,[72] silk fibroin,[91] and PLGA.[83,90,92,95] Chitosan, gelatin, and a mixture of chitosan and gelatin cross-linked with genipin have also been used.[96] As gold micro- and nanoparticles are popular, recent research has focused on finding alternatives to circumvent their high price tags. Cockle shells may be able to serve this purpose.[97] Recent *in vitro* studies indicate a positive release kinetic profile of this material, which initially released about 85% of the vancomycin loaded into the nanoparticles within the first 15 hours followed by a slow release profile for a full 120 hours.[97] Another interesting development is the creation of raspberry-like gelatin microspheres. These microspheres have multiple compartments inside of a single microsphere, making them a desirable blend of nanoparticles and microspheres. Various biomolecules can be released from the microspheres by diffusion, erosion or degradation-controlled release. This shows promise for administering therapeutics such as vancomycin, dextran and other biomolecules.[75]

As mentioned previously, these particles may be used for local and systemic delivery of therapeutics. Hydrogels are a common way these particles have been delivered to the site of infection.[80,83] Given their size, however, oral ingestion seems to be a feasible way micro- and nanospheres may be introduced into the biological system. This would be desirable for modern

osteomyelitis treatments, as this would be less invasive than local treatments, and ensure the clearance of isolated colonies of bacteria. However, there is concern over this methodology, as stomach acid can hinder the effectiveness of phages and antibiotics. Thus, extra measures must be taken to deliver and protect microspheres from the harsh environment of the stomach if they are to be taken orally. Protection can involve encapsulation by a basic protectant such as calcium carbonate to counteract the acidic conditions.[48,98] Furthermore, the base of microspheres may be fine-tuned for those undergoing acidic conditions. Alginate, for example, has been proven to increase the survival of many bioactive substances in simulated stomach acid.[48,98] For greater protection of the phages, a combination of alginate with calcium carbonate may also be used as a buffer to the acid.[98]

Coatings/Films

Another effective local delivery system are coatings, or films, which can serve as either a preventative measure or an active treatment against contaminated implants. The number of substances used for these coatings are extensive. In recent studies, antibiotics,[45,99–104] phages,[45] and alternative microbials[105] released from films/coatings made of phosphatidylcholine,[99,102] hydroxypropylmethlycellulose (HPMC),[45] poly(D,L-lactide),[100,105] and hydrogels[101,106]have all been explored, among others.[107] Interestingly, silver may also be used as both an antimicrobial and delivery vehicle as a coating material. Or, silver can be combined with other materials.[68] Made of aluminum and silicon, zeolites are beneficial in this pairing because of their crystal-like porous structure.[68] In one study, zeolite alone decreased bacterial CFUs by approximately 3000 units. Through ion exchange, the silver-zeolite coating decreased the CFUs by an additional 1500 units compared to the zeolite.[68] Another metal silver has been paired with for a coating is

titanium, in order to limit the systemic silver ion side effects.[67] As mentioned previously, nanoparticles have a multitude of application potentials and coatings are no exception. In a recent study, silver nanoparticle coatings of a titanium orthopedic implant (316 L SS) were able to completely eradicate infection in an *in vivo* study spanning 42 days.[108] Thus, it may be possible to alter both the orthopedic hardware materials and nanoparticle coatings for optimal anti-infection properties. Poloxamer 407, also known as "F-127", is a hydrogel with many applications, but may also serve as a useful coating to prevent adhesion of bacteria to orthopedic hardware. In particular, for PMMA.[106]

Scaffolding

Bone scaffolds which serve as delivery vehicles for osteomyelitis treatment are desirable, as they could ideally offer support for a fracture and direct bone healing. Some scaffolds may be even be engineered to degrade, ideally at the rate of native bone regeneration.[109] A seemingly limitless amount of materials and therapeutics can be engineered for this purpose, making these scaffolds a great focus of current research. Scaffolds composed of combinations calcium sulfate,[95] PLGA,[95,109] polyurethane,[110] PLLDA,[111] β -tricalcium phosphate (β-TCP),[112] and other materials have been used to deliver a multitude of therapeutics, including: antibiotics,[95,109,111] proteins,[110] and others.

A recently engineered bone graft highlights the wide range of alterations that can be made to these scaffolds. In this study, calcium sulfate, hyaluronan,simvastatin, and PLGA microspheres loaded with vancomycin were used to create a hard "core," surrounded by a moldable protective shell. The goal of this design was to allow necessary antibiotic release upon implantation, followed by the release of an osteogenic agent (simvastatin) to promote bone

union.[95] Another novel approach includes the use of 3-D printing for scaffold production. In one study, a PDLLA cylinder was crafted of a series of 4 ring layers, for specific, alternating delivery of either levofloxacin or tobramycin.[111]

Miscellaneous

Other delivery vehicles which have been explored include, but are not limited to: pellets,[113,114] polyurethane foams,[5] and sponges.[37,115,116] Sponges have been specifically explored for military applications, when it may be difficult to maintain and implant alternative delivery vehicles mentioned herein.[37]

Animal Models

Animal models may provide the most promising outlet for advancing our understanding of *S. aureus,* and resulting osteomyelitis infections. *in vitro* models often have results vastly different than those of *in vivo* studies; for example, an antibiotic may demonstrate high efficacy *in vitro* but in an infected animal models, provide little or no remedy for infection.[17]

Small Animal Models

Mouse (Murine)

One unique aspect of murine models of osteomyelitis is the ability to evaluate the effect of diabetes on infectious pathophysiology. Scientists have successfully manipulated the genome of rats to induce both type I and type II diabetes in mice, unlike other animal models. Examples include the NOD/ShiLtJ mouse, which exhibits symptoms similar to type I diabetes.[117]

Post-traumatic

In post-traumatic models of osteomyelitis, researchers generate a bony defect which they then contaminate with bacteria before closing the surgical site. The bony defect may be generated with micromotors,[25] titanium burrs,[50] or needles.[5,118] Oftentimes, these models are utilized for evaluation of therapeutics,[5] diagnostic tools for osteomyelitis,[50] or investigation of pathophysiology.[118,119] Examples of therapeutics evaluated using this type of model include β-defensins, 41 antibiotics,[25] and NSAIDS.[5] As mentioned previously, surgical debridement is often necessary in cases of chronic osteomyelitis for clearing infected areas. Although the murine tibia is limited in size, one study successfully performed debridement 2 weeks after initial infection establishment, using a 20 gauge needle.[25] The aim of this work was to compare treatment outcomes of antibiotic treatment regimens with or without this invasive procedure. Ultimately, it was found that debridement significantly reduced bacterial counts.[25]

Implant

An alternative approach to modeling osteomyelitis involves the use of implant materials. They may serve as stabilization for obstructed limbs,[86,120,121] a method of introducing contamination to a bony site,[6,70,121] a delivery vehicle for osteomyelitis treatment,[102] or a location for future bacterial colonization.[86] A variety of materials have been explored for this purpose, including: pins, 4[70] stainless steel wires,[102,117,122,123] titanium rods,[51] sutures,[124] and fixation plates.[86,120,121]

In one unique study, a vicryl suture was used as the agent of bacterial contamination. A 27 gauge needle was first used to generate a hole within the proximal tibia. The vicryl suture, after soaking in *S.aureus* for 30 minutes, was then inserted into this defect. This model was used

to evaluation of a novel diagnostic tool, a MRI probe which targeted for overexpressed IL-13Rα2 receptors in OM.[124]In another compelling study, a K-wire was inserted through the femoral canal so 1 mm protruded into the joint space. It was here, where the implant extended into the surrounding soft tissues, that *S. aureus* was injected rather than inside the bony defect.[123] Later, this model was used to evaluate a dual-antibiotic (ciprofloxacin and rifampin) loaded sponge for military applications.[37] The outcomes of diabetic NOD/ShiLtJ mice in osteomyelitis has also been investigated based off of this model.[117,125] For translational work aimed at improving therapeutics for diabetic patients, this murine model was used to determine that PGE_1 administered with cephalosporin may improve recovery outcomes.[125] In another approach, the implant material served as a delivery vehicle for antimicrobials.[102] A phosphatidylcholine coating was applied to a k-wire, for release of loaded amikacin, C2DA, or both. After 1 week, all animals were euthanized and the femurs were evaluated for residual bacterial activity.[102]

For more traumatic surgeries, the femur may be utilized for placement of a fixation plate. In one study, contaminated titanium fracture fixation plates were placed onto the femur, and then an 0.44 mm osteotomy was created. In the control groups, complete bridging of the osteotomy gap was complete by 35 days. In contrast, the infected mice at 35 days exhibited dramatic bone damage and did not bridge the osteotomy gap. Increased levels of TGF-β and PDGF genes were noted in the control groups, which are indicators of the typical bone healing process. In contrast, these levels were markedly reduced in the infection groups.[121] In other models, a plate can be utilized without serving as the source of infection. In one such study, a fixation plate served to stabilize an 8 mm osteotomy. It was in this space that *S. aureus* was injected.[120] Later, debridement and lavage were performed.[120] Later, this model was used to analyze a novel

lysostaphin coating on titanium locking plates.[105] In a similar model, a radiolucent PEEK fracture fixation plate with a titanium coating was used to stabilize a 0.7 mm transverse osteotomy in the mid-diaphysis. Then, an *S.aureus* soaked collagen sheet was placed into the defect to establish infection. After 7 days, the surgical site was debrided and subjects received either systematic vancomycin or PMMA spacers with or without vancomycin. A significant finding of this study was that the implant fixation was undermined by 10-14 days following surgery, due to osteolysis around the titanium screws. Also, a biofilm formed on the screws and plate itself.[86]

Hematogeous

Hematogenous murine models of osteomyelitis are also feasible. Typically, *S. aureus* is injected into the lateral tail vein. Over the course of one experiment, it was noted that *S.aureus* initially invaded and proliferated not only in the bone but in several other organs. After 60 days, however, these organs were cleared and *S. aureus* was present only in the tibia. This was attributed to the tropism of the *S.aureus* strain used (6850) for bone. This demonstrates great potential for this strain of bacteria for hematogenous models, and emphasizes the significance of bacterial strain in infection studies.[126] This model was later used to evaluate the efficacy of antibiotics (Rifampicin, Gentamicin, and Cefuroxime). Only rifampin was successful in the acute osteomyelitis groups, whereas none of the antibiotics were successful in the chronic osteomyelitis groups. The bacterial resistance was attributed to the formation of antibiotic-resistant small colony variants (SCVs).[17] More recent work utilizing this model has found the SigB, a *S. aureus* regulator, plays an important role in murine hematogenous chronic osteomyelitis infection development.[127]

Rat

Rat models offer advantages in ease of care, cost, and less ethical complications seen in larger animals. Furthermore, rats tolerate long term antibiotic therapy, even when administered at high doses.[128] Their bones are also easily pulverized, enabling research groups to easily conduct bacteriology analysis.[128]Their immune systems have also been manipulated, which opens up the possibility of studying risk factors for osteomyelitis, and their impact on pathophysiology of the disease. [128,129]Thus, rats serve as good models for novel therapeutics, before moving onto more expensive and taxing animal models. Rat models became popular following the publication of Zak et al. (details below).[36,129] Since then, an abundance of models have emerged.

Post-traumatic

The first rat osteomyelitis models largely relied on sclerosing agents to induce infection in post-traumatic tibial models. As mentioned previously, the model published by Zak et al. led to the popularization of rats as an animal for osteomyelitis research. In this model, a 5% sodium morrhuate solution placed into the metaphysis of the tibia, followed by an injection of *S.aureus* suspension.[36] In 1985, Rissing et al. investigated which was preferable for traumatic injury and infection establishment: the use of a 22-gauge needle or drill. In both cases, the protocol described by Zak et al was used.[10,36] It was determined that the drill protocol yielded a higher rate of infection versus the needle protocol, at rates of 81% and 51% respectively. [36] Rissing et al. further optimized their protocol by comparing two sclerosing agents, arachidonic acid and sodium morrhuate. Arachidonic acid was chosen as a sclerosing agent by this group because it is one of the fatty acids found in sodium morrhuate, and was thought to play a role in bone resorption and the inflammatory response. The Rissing drill protocol, mentioned above, was

used.[10]It was determined that arachidonic acid was able to generate infection at much lower doses than sodium morrhuate, as the effects of a 5 μL of 5% sodium morrhuate treatment was paralleled by an almost 1000-fold smaller dose of arachidonic acid. A surprising finding was that in the control group, given *S.aureus* and saline, there was still a relatively high rate of infection.[130]

Sclerosing agents introduce an unwanted variable into osteomyelitis studies, and sodium morrhuate has a toxic effect on *S. aureus.*[10] Thus, after Rissing et al.'s findings that infection could be established without sodium morrhuate or arachidonic acid, modern models have avoided the use of these sclerosing agents. One of the first groups to exclude sclerosing agents modified Rissing et al.'s drill protocol, and utilized fibrin glue as a facilitator of infection development.[10,128] *S.aureus*, in theory, was expected to adhere to the glue and thus establish a localized infection without spreading systemically. Infection was noted in more than 90% of tibias, as indicated by roentgenograms and histology.[128] In another study, agar beads were used to introduce *S.aureus* to the proximal tibia, where acute osteomyelitis then developed.[131]

Femoral models with no additives have also been explored. In one study, a syringe needle was placed directly into the distal femur, where *S.aureus* was injected and bone wax was used to seal the defect. After two weeks, this surgical site was accessed again and cleared with PBS. A novel bone cement was then placed into the femoral cavity and evaluated as a potential therapeutic.[85] A similar model was utilized to evaluate AMP treatment, delivered in calcium sulfate cement, for acute osteomyelitis.[54]

Implant

Perhaps the greatest use of rats in osteomyelitis studies are for implant-based models, and related research. A wide variety of implant materials have been explored, including: nails,[66] screws,[132] titanium/Kirschner wires,[35,58,91,133–136] hollow needles,[136] and fixation plates.[20,26,69,95,110,129,137–140]

A popular non-fractured implant model of osteomyelitis was published by Lucke et al., in which acute osteomyelitis was localized in the tibia.[133] In this model, *S.aureus* was injected into the medullary canal followed by insertion of a 0.8 mm k-wire, serving as a permanent implant. All animals were sacrificed after 28 days.[133] This model has since been used to evaluate boric acid therapy, systemically and locally.[134] This therapy was evaluated 21 days after bacterial inoculation, at which time the k-wire was removed. Results indicated the potential of boric acid as a synergistic agent, potentially with vancomycin, but not a stand-alone therapeutic.[134] In a similar model, it was found that this same methodology of *S.aureus* injection and k-wire placement within the tibia could generate chronic osteomyelitis after 4 weeks.[135] At this time, systemic teicoplanin treatment with or without extracorporeal shockwave therapy was then evaluated.[135] Other therapeutics investigated using a wire implant model of osteomyelitis include silk fibroin nanoparticles loaded with vancomycin,[91] and efficacy of erythromycin given with or without the flavonoid curcumin.[58] Femoral wire-based implant models of osteomyelitis also exist. Such models have been used to compare moxifloxacin to vancomycin treatment(s) 7 days after initial infection establishment.[136]

Similar to k-wires, stainless steel tubing may also be used as an implant for infection development. In one study, this tubing was used over more commonly used wires in order to induce a greater volume of biofilm. The tubing was pre-soaked in *S.aureus,* inserted into the

femur, and then a supplementary *S.aureus* suspension was injected into the space. At days 6 and 45 post-initial infection, respectively, signs of acute and chronic osteomyelitis were confirmed.[141]

Although not as common as wires, screws[132] and nails[66] have also been used to simulate implant-related osteomyelitis in rats. In one study, a polyetheretherketone (PEEK) screw coated in titanium was used as the agent to introduce bacteria into the tibia. The animals were monitored for up to 28 days, in which μCT was used to evaluate bone formation and resorption.[132] To observe osseointegration and antimicrobials of a novel nail, a similar model was used. A unicortical hole 8 mm in depth was first drilled into the proximal lateral tibial metaphysis, followed by *S.aureus* injection and nail placement. It was found that the HA and HA-Ag coated screws had excellent osseointegration and biocompatibility, but exhibited no anti-infection properties.[66]

Fracture/Segmental Defect

Typically, in models inducing fracture, wire or fixation plate implants are utilized. The groundwork for many of these fracture models can be derived from a study by Bonnarens and Einhorn.[142] In this model, a portable apparatus, similar to a guillotine, was used to drop a weight onto the femur and create transverse fractures. Prior to fracture, a Steinmann pin was placed into intramedullary canal of the femur, exiting through the great trochanter process. The pin was then bent and a 3mm "handle" was buried into the muscle. Although this model did not induce infection, it provided a starting point for osteomyelitis researchers.[142] In one modification, the femur was accessed distally for reaming rather than at the femoral condyles. Bacterial suspension was inoculated into this canal with an 18-gauge polypropylene catheter, which was left for 2

minutes following injection of the bacteria. Then, a pin was inserted and the drop apparatus used. This model was used for analysis of ceftriaxone treatment.[143] The pin may also be placed after fracture occurs. In one study, a k-wire was placed starting at the proximal fragment, through the distal fragment, until it was partially seated into the epiphysis. This antegrade k-wire placement resulted in a favorable, consistent infection rate (90-100%) with a small dose of *S.aureus* over a period of 3 weeks.[144] A modified Bonnarens and Einhorn model has also been used to study the effectiveness of chitosan films loaded with the antibiotic Ciprofloxacin, for osteomyelitis treatment. Fixation and bacterial contamination were performed after fixation, and followed by placement of films before closing the surgical site.[104]

Other fracture models utilize fixation plates, and avoid the use of a drop apparatus. Instead, fracture is surgically induced. Oftentimes, an osteotomy is generated. In a majority of these studies, a defect 6mm in width is used.[26,95,110,137–140]In other cases, *S.aureus* has been introduced through fibrin hydrogels[69] or onto the implant itself.[129]

One of the first publications describing this fixation plate, osteotomy, and osteomyelitis rat model was Chen et al., in which a polyacetyl plate and kirshner wires were the fixation plate utilized.[137] . It was determined that a 10^4 dose of *S.aureus* resulted in osteolysis and loss of stability over 2 weeks. After optimization of the model in pilot studies, debridement and the antibiotic ceftriaxone were evaluated as a therapeutic regimen. This model has been adapted to fit the aims of multiple research projects in recent years. In one study, a novel bone graft composed of calcium sulfate, hyaluran, and PLGA microspheres, formulated into a hard "core," with a moldable outer shell, was evaluated. With this graft, vancomycin was delivered from the PLGA microspheres and the osteogenic agent simvastatin was utilized to stimulate bony union.[95]

Engineered polyurethane scaffolds, loaded with vancomycin, D-amino acids, and other treatments have also been evaluated using this model.[110,139]

Other investigations include: biofilm formation in diabetic rats,[129] whether osteogenic protein-1 (OP-1) could induce bone formation in the presence of *S. aureus,*[137] and debridement optimization.[26,140]

Although less common, tibial fracture models also exist. In one unique study, an open tibial fracture model, akin to a Gustilo type III wound, was developed. To induce infection, a 1 cm longitudinal (linear) trough was first created in the tibial medullary cavity by drilling first into the anterior cortex, in a proximal to distal motion. After the trough was created, a cautery device was used to damage the endosteal blood supply. *S. aureus* was then placed into the trough, followed by curettage and lavage. This model successfully established acute osteomyelitis.[145]

Hematogenous

Although rare, a hematogenous rat model of osteomyelitis exists. In this model, a medial parapatellar arthrotomy was created, and then a cannulated needle was used to clear the medullary canal. Then, a k-wire was inserted into the medullary canal. After surgery, a catheter inserted into the tail vein was used to deliver *S.aureus* into the circulatory system of the rat. From this study, it was determined that a high dose of *S.aureus* (10^7 CFU) was necessary. Furthermore, it was determined that after 14 days the k-wire addition significantly increased the rate of infection.[11]

Rabbit

Rabbits are another animal model commonly used for osteomyelitis studies. They are a good solution for those who need an animal model larger than the more common rodents (mice & rats), but are not ready for the economic burden and greater responsibility associated with large animal models. They are also a great choice for pilot studies on implant devices, or implant coatings, as designing these products for rodents is limited or faulty due to their smaller size.[146] Some products designed for humans can even be used on rabbits with no modifications.[146] A downside to rabbit models are their ruminant gastrointestinal system, which has made the ability of a rabbit model to evaluate antibiotic treatments questionable.[147] Additionally, they are known to undergo respiratory depression during experimentation when put under anesthesia.[148]

Post-traumatic

As with murine and rat models described herein, there exist post-traumatic models of osteomyelitis in the rabbit, centered around the use of sclerosing agents.[114] In one tibial model using this protocol, hallmarks of chronic OM were noted at 4 weeks.[114] At this time, the rabbits either underwent debridement and placement of novel bioactive glass implants, or debridement supplemented with daily intravenous injections of Teicoplanin for 4 weeks.[114] This model has also been used to evaluate a nano-hydroxyapatite /polyamide-66 (nHP66) nanoscaffold with varied amounts of oxidized titanium and silver ions, in order to maximize antibacterial material properties.[67] A similar protocol was adopted for evaluation of fibrin gel scaffolding placed in the tibia, with or without mesenchymal stem cells and vancomycin alginate beads. It was found that bacterial numbers were significantly lower in groups with the vancomycin alginate beads than those without.[149] These post-traumatic models using sodium morrhuate are also ideal for

mimicking blast wound trauma seen in the battlefield, and resulting bone infection. This is because sodium morrhuate induces necrosis of bones like blast wound trauma. In one such study, several strains of bacteria were evaluated, in monocultures or delivered in combination with one another.[150] In femur models adopting this protocol, some cases of unexpected death have been reported.[111,151] However, one study was able to successfully evaluate a novel 3-D printed scaffold laced with antibiotics, placed at 3 weeks following debridement.[111] Thus, this model could be used for future work.

Other post- traumatic models exclude the use of sclerosing agents. Interestingly, many studies that fall within this category used the radius as their site of bacterial inoculation.[78,113,152–154]. A 1 cm segment was removed, where *S. aureus* could then be directly injected into the medullary canal. Then, the excised segment was replaced.[152,153] This model has since been adapted for use in a femoral model, to evaluate Teicoplanin-encapsulate nanoparticles.[78] It has also been employed to evaluate calcium sulfate pellets, with or without debridement/tobramycin. Infection was allowed to develop for four weeks, and then treatment groups were assigned and implemented, with observation for an additional 4 weeks.[113] Calcium sulfate pellets loaded with Daptomycin and coated with deacetylated chitosan have also been investigated with this model.[154]For a greater degree of severity, a unicortical defect as large as 5mm has been reported. Again, to induce infection *S. aureus* was injected at the damaged site. In this study, the damaged bone fragment was not replaced.[46]Other femoral models avoid the creation of unicortical defects. In one investigation, femoral trepanation was first performed, so a suspension of *S. aureus* could be inoculated into the knee cavity through a parapatellar injection. Following surgery, animals

were euthanized at 1,2,3,9, and 14 days for evaluation of bacterial load in bone marrow over time. Signs of acute osteomyelitis were noted.[155]

Implant

Due to a larger working space, rabbits enable a larger variety of implant-use than previously described murine and rat models. Implants that have been reported in literature include but are not limited to: nails,[64,148,156] screws,[63] wires,[77,99] cylindrical/cylindrically shaped materials,[52,103] and plates.[52,79,146,157]

By generated a 4 mm defect in the tibia, injected *S.aureus* in this space and then placing a titanium nail, one study established an acute osteomyelitis model. Interestingly, different calcium-binding fluorophores were administered at 14, 28, and 41 days to enable bone formation evaluation at various times.[148] Another unique nail-based study generated a bifocal osteotomy in the tibia, to evaluate internal versus external fixation in osteomyelitis. This is of particular interest, as most animal models described herein only utilize a single osteotomy. After this break was created, the tibial fragment was infused in a MRSA culture and replaced into the leg where an IM nail was used for stabilization. Four days later, surgical debridement was performed and the nails were removed. Rabbits were then placed into one of two groups, sterile nail fixation or bilateral external fixation with a homemade device. Following these procedures, rabbits were also given vancomycin intramuscularly twice a day, until euthanasia (4 days later, for a total of 8 days of observation).[156]

Chronic models have also been reported. In one such study, sodium morrhuate was used to induce infection in the tibia over a period of 4 weeks. At this time, debridement was performed and either two novel Mg-Cu alloy based nails were placed or two pure titanium IM

nails.[64] Screws models, similar to nail models due to implant likeness, have also been reported. For bacterial contamination, the screw of interest was exposed to both *S. aureus* and *E. Coli* for 6 minutes prior to implantation. A 2.5 mm hole was created in the femur, where the screw(s) of interest were placed and their ability to mitigate infection was then evaluated.[63]

Although uncommon, PMMA cylinders have also been used as an implant. A 8.5mm long defect was drilled parallel to the axis connecting the medial and lateral condyles of the femur, and irrigated thoroughly. Then, contaminated PMMA cylinder were pressed into the defect space. To prevent soft tissue infection, the face of the cylinder that was exposed was cleaned thoroughly. Four days after this initial surgery, the cylinders were removed and infected soft tissues surrounding the bony defect underwent debridement. The rabbits then received either sterile or polyelectrolyte-film-coated titanium implants, for 4 or 7 additional days.[103] A similarly shaped implant of porous tantalum or a titanium alloy control, 36 mm long with a 2.7mm diameter and hexagonal cross-section, was used in a tibial study simulating amputees. Briefly, a bicortical hole was created towards the proximal tibia where one of two implants was then placed. The ends of a 24-gauge cerclage wire, placed along the anterior cortex and through the medial end of the implant, were twisted together on the medial side after proper placement was achieved. A 2mm skin puncture was then created proximal to the incision, where the implant exited the skin. Following surgery, some groups received a topical AMP treatment.[52]

Fracture/ Segmental Defects

Segmental defect models have also been developed. In one work, biofilm-coated stainless steel fixation plates, attached with 4 screws on the midshaft of the femur, were used to successfully induce osteomyelitis. A 1mm fracture was created after placement of the plate,

between the second and third screws. In 21 days, some noted symptoms included: implant failure, callus formation away from the fracture site, swelling, pus, and tissue damage.[157] In another project, a 1 cm segment of bone was removed from the radius. Then, a k-wire was placed through the medullary cavity of the excised bone and the entire construct was placed into bacterial culture, and replaced into the dead space. 3 weeks after this surgery, the site was debrided, the k-wire was replaced, and a novel biodegradable hydrogel delivering gentamicin was utilized.[77] This model was later used to analyze phosphatidylcholine coated wires with or without 25% vancomycin, which were inserted through the excised bony segment and placed back into the medullary canal.[99] Other notable research centers around the use of the humerus for OM. In one effort, custom-designed intramedullary nails and a 7 hole locking compression plate was secured to the bone. At the central screw hole, an osteotomy was performed. Here, *S. aureus* was then injected into the defect.[146] Later, this model was used to evaluate a thermoresponse hydrogel delivering gentamicin at the implant site.[79]

Large Animal Models

For initial studies of novel therapeutics, small animal models are often preferable due to their lower costs, ease of handling, and quicker data generation. After these preliminary studies, however, many scientists find it beneficial to reconfirm their findings in large animal models. This is because large animals more closely resemble humans in many aspects, such as in bone density, weight, and immune system functions. Large animal models are also particularly useful for the study of implants versus small animal models, as small animals have difficulty withstanding the use of some orthopedic implants.[107] The similarity in bone size between large animals and humans also makes it easier to evaluate orthopedic hardware, as little or no

adjustments need to be made to prepare commercially available materials used for humans for animal research. For example, the diameter of the goat tibia is compatible with currently used interlocking nails.[158] Additionally, for surgical protocols which necessitate multiple procedures, large animal models are preferable. It has been found that large animals are more likely to withstand the stressors associated with multiple procedures, such as debridement or hardware removal, versus smaller animals. Large animal models are needed in the translational pipeline, as a necessary step in the advancement of technologies and therapeutics from research labs to the clinic.

Pig (porcine)

A benefit of porcine models is their pulmonary intravascular macrophages, which inhibit bacteremia and allow hematogenous inoculation of bacteria.[159] Although humans do not have these macrophages, it is well documented that bacteria may reach sites of osteomyelitis through the blood stream, so it is important to study this mode of transmission. In other animal models, reproducible models of hematogenous OM have been limited. The intravascular macrophages of pigs allow them to live longer following hematogenous inoculation, in contrast to other animal models, in which the animals would have to be euthanized due to systemic infection. Another benefit of using a pig model is that pigs are omnivores, unlike the herbavoric small animal models often used (such as the rabbit). This diet change can alter the response of an animal to antibiotics, making pigs a good candidate for oral and/or systemic antibiotic treatment evaluation.[147] Furthermore, although the bone material of humans overall most closely resembles dogs, pigs are next in line. Notably, fracture stress is higher in dogs when compared to pigs. In a recent study, human bones were found to withstand an average of 1.21 N/mm^2 fracture stress,

whereas pigs were found to withstand approximately 2.40 N/mm^2 and dogs 6.12 N/mm2. Studies on fractures, and related stress bearing, may thus be more closely translated for human applications in a pig model versus canine models.[160] One disadvantage of pigs is their rate of bone growth, which is considerably faster than that of a human.[147] Additionally, the porcine tibia and fibula are shorter than those of a human. Therefore, it is not advised to test implants using a porcine model, if other large animal models are feasible. [147]

Post-traumatic

For simulation of gunshot wounds, one porcine post-traumatic OM model fired a 200mg steel fragment into the right tibial metaphysis. After this procedure, *S. aureus* was inoculated into the defect site on a strip of sterile bovine collagen. Experimentally, pigs received Benzylpenicillin and Flucloxacillin through intramuscular injection every 6 hours for 7 days. After 14 days, animals were euthanized. It was found that systemic antibiotic administration could successfully eradicate infection. All control animals exhibited signs of localized, acute osteomyelitis.[9]

Implant

An implant associated tibial osteomyelitis model has also been established in pigs, utilizing the k-wire fixation methodology seen in other animal models. Two different ages of pigs were evaluated, 3 months and 8 months. Briefly, fluoroscopic guidance was utilized to clear out the medullary cavity of the tibia with a k-wire (4mm). After the cavity was sufficiently cleared, the wire was removed. Afterwards, bacterial inoculum was placed at this site and a k- was placed into the medullary cavity for stabilization. Although animals were only observed for 5 days, signs of localized, acute osteomyelitis were noted.[147] From this same study, Tøttrup et al.

conducted a pharmacokinetic study of Cefuroxime in the 8 month old pigs. Controlled infection was reported in 90% of their subjects, with evidence of acute osteomyelitis. It was also found that Cefuroxime penetration was incomplete by day five. This may implicate the need for prolonged administration of antibiotics to patients with acute osteomyelitis, to ensure complete treatment of infected sites.[147,161]

Hematogenous

Hematogenous osteomyelitis model have also been explored pigs. In one study, a catheter was inserted into the left ear vein of juvenile pigs. Depending on assigned groups, the pigs then received a one-time inoculation of 10^8 CFU *S. aureus*, or twice at this initial surgery and 12h post surgery.[162] After initial inoculation, it was found that infection was successfully induced in the long bones and lungs of the pig model, without affecting the vertebrae. After 48h, the pulmonary bacterial load decreased, and a bacteremia test was negative. This was largely attributed to the pulmonary intravascular macrophages of the pig, which can effectively phagocytize S. aureus.[159,162] Animals were euthanized at 6h,12h,24h, or 48h, but even at such short time points signs of acute osteomyelitis were evident. Overall, this model is promising for juvenile osteomyelitis research. In the long bones of the pigs above, infection started from the deep metaphysis and then spread to the capillary loops near the growth plate. Additionally, no vertebral lesions developed. These are common characteristics of juvenile osteomyelitis.[162,163] This model has received considerable revision over the years. In one study, the use of the brachial artery rather than the ear vein resulted in 62.5% (5/8) of subjects euthanized for lameness.[164] The use of the right femoral artery was also explored, in conjunction with the evaluation of several strains of Staphylococcus aureus. From this research, it was determined the

right femoral artery was superior to other previously tested modes of bacterial inoculation in porcine hematogenous models.[165,166]Thus, in a subsequent study, Nielsen et al. used the right femoral artery for a study of osteomyelitis detection diagnostics ^{111}In-leukocytes, ^{18}F-FDG, ^{11}C-methionine, ^{11}C-PK11195 and ^{68}Ga-citrate. However, 38% of subjects had to be prematurely euthanized due to lameness.[167] Overall, the current hematogenous porcine models fail to be reliable due to high mortality rates, but remains a promising area for future animal model development, due to the porcine immune system.[162]

Dog (canine)

Canine animal models serve as a very positive animal model for orthopedic research. In a recent study, it was determined that canine bones most closely resembled human bones versus all other animal samples tested. Bone composition, density, and other orthopedic properties were evaluated.[160] Furthermore, like other large animal models, dogs can undergo multiple procedures. This makes them ideal for studies utilizing debridement or other interventional procedures.[24] Despite all of these desirable attributes for an animal model, few canine models exist. This is most likely due to the ethical complications that are associated with the use of animals commonly adopted as household pets. Furthermore, it may be difficult to control the breed differences across a population of dogs, even among mutts.

The first published canine model was in 1976, by Deysine et al.[168] Unique to this study was the use of the nutrient artery of the tibia as the inoculation site of radiopaque barium sulfate (used for radiograph enhancement) and *S.aureus,* somewhat mimicking hematogenous OM. Although some signs of acute osteomyelitis were apparent, undesirable outcomes such as septic infection and spontaneous fracture occurred.[168]

Fitzgerald et al. established one of the first canine post-traumatic models. In this study, a defect created in the proximal tibial metaphysis was inoculated with bacteria, then filled with polymethylmethlyacrylate (PMMA) cement. Later, the PMMA was removed and replaced with gentamicin impregnated PMMA, which allowed 90% of subjects to overcome infection.[87] Almost 10 years later, in 1994, the model proposed by Fitzgerald et al. was used for the evaluation of other gentamicin delivery *in vivo.* Parenteral gentamicin therapy every 8 h for 4 weeks, polymethylmethacrylate (PMMA) polylactide implant coated with gentamicin, and polyglycolide (PLGA) implant coated with gentamicin, were all tested. Debridement was performed at 4 weeks post initial surgery, and after antibiotic treatment subjects were observed for another additional 6 weeks (up to 10 weeks total). There was no statistical difference between the animals treated with PMMA or PLGA, but both were statistically significant versus the parenternal gentamicin treatment.[24] Later, the model fabricated by Fitzgerald et. al was modified for femoral usage. First, a defect was drilled into the femur, inoculated with bacteria, and then one of several permanent implant materials was installed. Implant materials included: stainless steel and cobalt-chromium alloys, polyethylene, prepolymerized PMMA, and PMMA polymerized *in vivo.* As expected, the introduction of foreign materials at a site of bacterial inoculation increased the rate of bacterial proliferation.[169]

Work deviating from these models, and simulating open fracture, also exist. In one such project, a captive bolt device delivered 6800 N of force to the proximal tibia. Then, intramedullary nails were used to fix the site of fracture. *S.aureus* was then injected into the medullary cavity, and allowed to flow freely into the surrounding soft tissue. A muscle flap was then surgically created on some of the subjects. It was found that the use of the transpositional

muscle flap increased vascular endothelial growth factor (VEGF) mRNA expression versus the fracture only group at 2 hours post-surgery, indicating that the type of closure used in surgery should be carefully selected. The use of muscle flaps was determined to have the potential to facilitate healing, largely believed to be due to increased blood supply at the site of injury.[170]

Goat (caprine)

Caprine, or goat, osteomyelitis models have not been widely utilized across research groups. This is likely due to increased costs leading to limited sample sizes, and difficulty in managing the animals without prior experience. However, their larger bone sizes more closely mimic the human long bones, versus those of small animal models. The diameter of the goat tibia is compatible with many currently available fixation devices used on humans, such as interlocking nails. This provides an easier translation of research findings for human applications, as well as enabling scientists to avoid the increased economic burden associated with custom-made, novel devices designed specifically for animals.[158] At this time, the only caprine OM models that fell within the constraints of the review's consideration were tibial models.

Other studies focused on post-traumatic models. In one study, a 3 mm diameter unicortical hole was developed in the proximal diaphysis of the tibia. Like other previously mentioned post-traumatic models, sodium morrhuate and *S. aureus* were then placed into this space. The Later, the area of infection was debrided. Radiographic and histologic evidence was collected to indicate signs of chronic and acute osteomyelitis in 100% of subjects throughout the 12-16 week study.[171] A similar caprine defect model was published the same month as this model, but a 12mm unicortical defect was created in the metaphysis of the tibia, followed by

bacterial inoculation. The larger defect size resulted in the omission of any sclerosing agents, while still inducing OM.[172]

To compare the infection rate of fractures with external fixation (a modified Hoffman device, with two 5mm cortical pins on each side of the fracture) versus intramedullary locking nails, with or without reaming, one study developed two separate surgical protocols. For simulation of external fixation, a chevron osteotomy was created along the tibia followed by generation of 4 mm drill holes. For intramedullary nail placement, a medial parapatellar incision at the knee was performed, followed by use of a 6mm drill bit for access into the medullary canal. After fixation, *S. aureus* was introduced to the fracture site on an absorbable gelatin sponge. After 14 days, all animals were euthanized. Bacterial growth in the group with reaming and IM nailing was significantly greater than the groups with an external fixation device or no reaming and IM nailing.[158] IM nails were further analyzed in a more recent study, in which a tibial mid-diaphysial osteotomy was performed with intramedullary nail fixation. Micro-CT images indicated the successful development of chronic osteomyelitis. However, infected soft tissue conflicts and a small sample size of 2 make the results of this study questionable.[173] Future investigations will need to be conducted for more thorough conclusions on IM nails.

Sheep (ovine)

Sheep are a desirable model of long bone osteomyelitis, as their bones are similar in size to those of humans. Additionally, sheep and humans share a similar rate of osteogenesis. Sheep femoral bone has also been shown to closely mimic the torsional stiffness of human bone.[174] However, it should be noted that sheep bone is denser and has fewer Haversian canals than human bone. [174] Sheep models, like all large animal models, do come with the burden of

increased research costs. It should be noted that goat and sheep animal models have very similar characteristics; largely, these two could be interchanged depending on availability and costs to research groups.

Kaarsemaker et al. pioneered the use of sheep for osteomyelitis models in 1997. A 4.2 mm drill hole was created in the medial proximal cortex of the tibia, and then a sclerosing agent (1 mL of 3% tetradecyl sodium sulphate solution) was put into the defect. Then, *S.aureus* soaked in gelatin sponge strips were packed into the medullary cavity. In the first round of surgery, 7/12 (58%) of subjects experienced fatal sepsis. Medically necessary intervention was then taken, with administration of the antibiotic Steptoprocpen (containing streptomycin and penicillin) an hour after surgery. It was determined that this allowed localized infection to develop, while preventing the previously observed fatal sepsis.7 In a similar femoral model, the use of sclerosing agents was avoided. A hole was drilled into the medial femoral condyle, where novel scaffold materials were packed. In both the control and experimental groups, no bacteria were isolated from blood samples, indicating localized infection which provides evidence that sclerosing agents are not necessary in post-traumatic ovine models.[109]

Other efforts are directed towards implants, and segmental defects. In 2002, an ovine tibial chronic osteomyelitis model using a midshaft chevron osteotomy, followed by bacterial inoculation and then intramedullary (IM) nail placement was published. It was determined that IM nail fixation may not be appropriate in all models, as it may stimulate virulence and thus interfere with the efficacy of antibiotic treatment. The use of external fixation was suggested for future studies.[175]

Another research group seemingly took this advice when designing their model, in which a titanium locking compression plate was used to stabilize an osteotomy. Another novelty in this protocol was the introduction of *S. aureus* using a catheter at the site of the osteotomy.[14] The reproducibility of this model was further validated in a following study evaluating a novel N,N-dodecyl,methyl- polyethylenimine (PEI) coating on locking compression plates. This coating was found to prevent the formation of biofilms, and stimulate bone growth in the tibial defect. Furthermore, 100% of the animals used as controls successfully developed osteomyelitis. This indicates the reliability of this model.[107] Another ovine-based study utilizing orthopedic plates modeled open fracture type IIIB.[176] To contaminate the stainless steel plates, *S. aureus* was first allowed to reach a biofilm state *in vitro*. Then, it was attached to a polyetheretherketone (PEEK) membrane, and placed on the stainless steel plate. 100% of sheep treated with the contaminated plates developed infection. The variance of results depending on the state of bacteria, planktonic or biofilm, at the time of inoculation was emphasized in this work .[176]

Miscellaneous Models

Some exotic small animals have also been considered for osteomyelitis animal models, but have not received much interest. In 1984, the use of a guinea pig as a model of femoral post traumatic osteomyelitis was published. After exposing the lateral side of the right femur, the bone was cut with a scalpel saw and split at the diaphysis using a small forceps, then the site was closed with sutures. Depending on experimental group, the guinea pigs then either received no bacteria, *S. aureus* alone, or *S. aureus* and pin fixation. The stainless steel wire was 1.4 mm in diameter, and was inserted from the fracture in the proximal direction, before exiting the femur through an incision in the dermis of the trochanter region. After repositioning the fracture, the

wire was then pushed into the distal part of the diaphysis. In infected rodents, a needle leading to the site of injury was used to inoculate S. aureus.[177]

Another non-traditional animal considered for femoral OM models are hamsters. An osteotomy was created, which was then left to heal on its own or fixed with a 0.9 mm K-wire. The pin was inserted retrograde, from the site of bony defect to the knee. To establish infection, *S. aureus* was placed in the muscle next to the site of surgery. Unique to this study, unlike many others, was that no wound care was performed. The site of incision was healed within 5 days, without sutures, and animals were observed for 1-2 weeks total.[178]

Another animal that has been used, but is not commonly chosen for research projects, are chicken. To establish an acute hematogenous model, *S. aureus* was inoculated into a wing vein. Abscesses developed as early as 24 hours, and were most often found in the metaphysis of the long bones. Within 48h, many subjects exhibited signs of lameness. Only 23/29 developed osteomyelitis.[179]

CHAPTER III

METHODS

in vitro Work

Bacterial Strain(s) and Culture

For all bacterial work herein, a modified *Staphylococcus aureus* strain ATCC 6538 ("Rosenbach") , originally isolated from a human lesion, was used. As a well characterized biofilm strain, this enabled us to generate a challenging infection see in other literature. Unless otherwise stated, all bacterial work done within this study was performed utilizing Brain Heart Infusion ("BHI") based media and agar (BD Diagnostics, #211059). For propagation of bacterial culture, a single colony was picked and placed into a sterile culture tube filled with 4 mL of BHI medium. This tube was then cultured for 24h at 37℃ and 150 RPM. For enumeration of bacterial colonies, 100 µL of bacteria was spread onto a BHI agar plate and incubated for 24 h statically at 37℃.

Chromosomal Integration of GFP into ATCC 6538

Staphylococcus aureus strain ATCC 6538 was genetically modified to contain chromosomally integrated green fluorescence protein ("GFP"), as previously described.[180] Extended details can be found in appendix C. Briefly, plasmid pTH100 harboring GFP was isolated from purchased DH5α *E. coli* (addgene, #84458) using QIAprep Spin MiniPrep kit (Qiagen). Isolated pTH100 plasmid was then introduced to competent *S. aureus* strain RN 4220 by electroporation (Harvard Apparatus, BTX:ECM360) and plated onto an agar plate with

chloramphenicol, then incubated overnight at 30°C for recovery. Under UV light (Cole Palmer UVP-21, #EW-09817-02), the largest and most visibly fluorescent colonies were picked and cultured for 24h. Plasmid pTH100 was then isolated from RN4220-pTH100 culture using QIAprep Spin MiniPrep kit (Qiagen), and introduced to *S. aureus* ATCC 6538 by electroporation (Harvard Apparatus, BTX:ECM360). Resulting bacterial culture was placed onto an agar plate with chloramphenicol, then incubated overnight at 30°C for recovery. Under UV light (Cole Palmer UVP UVP-21, #EW-09817-02), the largest and most visibly fluorescent colonies were picked and cultured for recovery. A series of two heat shock events were then performed in BHI culture medium at 45℃, for 48h each.

After the second heat shock, individual bacterial colonies recovered overnight in BHI culture at 200 RPM and 30°C. Cultures were diluted by 1:1000, cultured approximately 4 hours, then again diluted at 1:1000 and grown for 16 hours. This was performed for approximately 3-5 dilution cycles, to ensure sufficient chromosomal crossover. The final bacterial culture was plated onto agar plates containing anhydrotetracylcine, and incubated overnight at 37°C. Single colonies were plated in duplicate on chloramphenicol and BHI agar. *S.aureus* colonies that grew on the BHI agar, but not the chloramphenicol plates, were then selected for future use. A plate reader (SpectraMax M5) was then used to identify the resulting bacterial strain with highest fluorescence signal. The final strain of interest was continuously diluted and plated over a period of 1 week to ensure stable integration of pTH100 into *S. aureus* ATCC 6538 (Fig.4.1, left). In later studies, bacteria isolated from *Ex Vivo* rat tissue samples were found to emit fluorescence under UV lamp (Cole Palmer UVP-21, #EW-09817-02) (Fig.4.1, right).

Preparation of Alginate Hydrogels

All alginate gels were initially prepared at a 3% concentration, in anticipation of diluting the gel to 2% formulations after loading them with desired therapeutics. A 3% alginate mixture (w/v) was made with alginic acid powder (Sigma, #W201501) and αMEM media (Gibco, #12561-056), and left overnight, undisturbed, at room temperature to fully dissolve. This solution was pipetted into 1mL syringes, and sterilized using 2µm syringe filters (Pall, #4187). Desired therapeutics were then sterilely placed into this same syringe, with the dissolved alginate. The cross-linker, calcium sulfate, was then generated at a concentration of 0.21 g CaSO4 / mL distilled H_2O and autoclaved at 121℃ for 30 minutes. Volume of desired cross linker was determined by dividing the total volume of alginate/ αMEM, in µL, by 25. This volume of calcium sulfate was then loaded into a new, sterile 1mL syringe. By attaching the two syringes (dissolved alginate with therapeutics in one syringe, and cross linker in the other) with a connector, and mixing vigorously for approximately one minute, the gel was formed with therapeutics distributed homogenously. The prepared syringe was then placed into a sterile container, and kept in the refrigerator or on ice until use.

Kirby-Bauer Analysis of Phage and 2% Alginate Hydrogel Compatibility

To analyze the bactericidal activity of desired therapeutics within the alginate gels, a Kirby-Bauer assay was performed.[90] Phage in PBS, empty 2% alginate gels, or phage loaded within the 2% alginate hydrogel were applied at volumes of: 5, 10, 15, or 20 µL onto BHI agar plates covered with ATCC-6538-GFP. The applied solutions were allowed to set undisturbed for approximately 10 minutes at room temperature, and were then incubated at 37℃ for 24h.

Anti-biofilm Efficacy of Selected Therapeutics

The ability of our selected therapeutics to mitigate biofilm infection was investigated as previously described, with minor modifications.[59] A single colony of ATCC 6538-GFP was picked and placed into 4 mL of BHI culture medium, and placed into 37°C at 150RPM for 24h. The bacteria was then centrifuged to form a pellet, and re-suspended in PBS. 250 µL of this culture was put into 750 µL of PBS, and diluted by a factor of either 0, 10^3, or 10^5. Biofilms were grown by placing 20 µL of each designated bacterial culture (dilution factor 0, 10^3, or 10^5) into individual wells of a tissue culture coated 48-well plate, and supplemented with 500 µL 1% glucose(Sigma, #G7021) BHI (w/v) media. The biofilm was then placed into a 37°C incubator to grow statically for 24 h. All media was removed, and the biofilms were then gently washed with 500 µL PBS. 75 µL of 2% alginate hydrogels loaded with fosfomycin, phage, or phage and fosfomycin ("dual") were then placed on top of the biofilms. Additionally, two different controls were considered: empty 2% alginate hydrogels, and no treatment (only 1% glucose/BHI media applied). 400 µL 1% glucose BHI media was then placed on top of these hydrogels, and the 48 well plate was incubated statically at 37 °C for 24 hours. All media was then removed, and the 48 well plate was placed on ice for transportation to IVIS Lumina XRMS. Each well plate was imaged at 480-520 nm, then placed back on ice. Each well plate then underwent vigorous washing with 1mL PBS, which was then collected for subsequent plating for enumeration of bacteria.

Optimization of Ultimate Bacterial Load on Orthopedic Screws

A single colony of ATCC-6538-GFP was picked and placed into sterile culture tube with 4 mL BHI media. This bacteria was grown at 37°C at 150RPM for 24 hours. This culture was then centrifuged at 4000 RPM for 2 minutes, and re-suspended in PBS. Four different 1.5mL,

sterile tubes were then generated consisting of: 250µL of this culture, and 750µL of PBS. 200 µL of this culture/PBS solution was then placed into each individual well within a 96 well plate. Sterilized aluminum sheet metal was then placed over the wells of the plate, carefully. Sterile orthopedic screws were then placed through the aluminum foil gently using forceps, so that the head of the screw remained above the foil whereas the shaft of the screw was covered by the bacterial culture. To remove the screw from this setup, forceps tightly grasped the head of the screw and the aluminum foil was removed from around the screw. The screw was then placed into a clean, new 96 well plate to dry. To quantify the ultimate bacterial load, the dried screws were then placed into 1mL of PBS, vortexed to ensure homogeneity of the solution, and serially diluted as necessary. 100µL of the sample of interest was then spread onto BHI agar plates, and incubated for 24h at 37°C for bacterial counting. Throughout this process, three variables were analyzed: (i) the bacterial load in each well, (ii) the dry time, and (iii) the time the screws remained within the culture. Effect of soaking time

To analyze the effects of soaking time, screws were placed in 200µL culture diluted 10 fold (~$1.0x10^8$ CFU in each well) for 5, 10, or 20 minutes. All screws were then dried for 5 minutes before bacterial counting procedures were performed.

Effect of Dry Time

To analyze the effect of drying time, screws were placed into 200µL of culture diluted 10-fold (~_$1.0x10^8$ __CFU/well) for 5 min. Screws were then carefully moved to a fresh 96 well plate, and dried for either 0, 5, or 10 minutes before bacterial counts were performed.

Investigation of Various Osteomyelitis Model(s)

All procedures were performed in accordance with the Institutional Care and Use Committee of Mississippi State University, under IACUC protocol 17-097. Female, 13-week old (190-260g) Sprague Dawley Rats (Charles River) were used throughout the course of these studies. Upon arrival, all animals were quarantined for 3 days, during which time they were initially weighed, observed for any gross anatomical abnormalities, and allowed to acclimate to the animal facility. Rats were housed individually with 12h light/dark cycles and were provided food and water *ad libitum* prior to testing, and again after buprenorphine was cleared from their system.

Aseptic, Pilot Model Considerations

Prior to the introduction of bacteria into any model, aseptic pilot studies were performed to confirm efficient stability and bone healing to manipulated femurs. The first model-type we considered was pin fixation, due to the large prevalence of literature describing this model.[133,135,142,178] The second model type we considered was a segmental defect, secured with a fixation plate. This model type was appealing as it would allow the additional consideration of bone healing with infection treatment. In both aseptic models, inadequate femoral stabilization resulted in adverse events of: early euthanasia, limping, swelling, and up to 15% weight loss(See appendix A). Thus, these models were abandoned in pursuit of implant-based models utilizing orthopedic screws (Osteomyelitis Models #1 and #2, described below). Future work could utilize either a pin model or segmental defect model, given necessary modifications to the surgical protocol.

Implant-based Models of Osteomyelitis: Overview

Two implant-based models of osteomyelitis were considered in the course of these studies. In model #1, *S.aureus* ATCC 6538-GFP was delivered to the femur by PBS injection into a bicoritcal defect (McMaster Carr, #65), followed by placement of an orthopedic screw (Antrin Miniature Specialties Inc., #00-90, 303 stainless steel, Ø=0.047, ¼ length).At 14 days, phage was delivered to the site of infection by poloxamer 407 hydrogel. Control animals were sacrificed on day 14, as well.

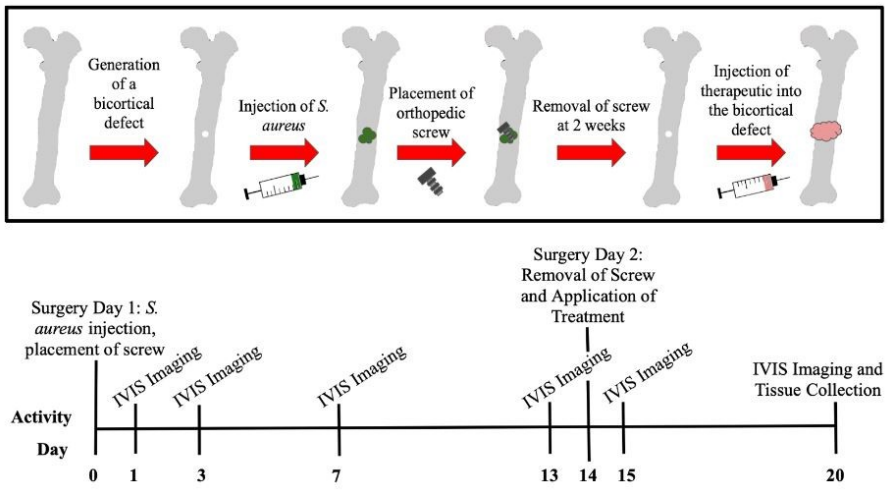

Figure 2.1 Overview of Model 1

In model #1, *S.aureus* was injected into a bicortical defect, followed by placement of an orthopedic screw. At day 14, treatment(s) were applied and at day 20 (a 6 day treatment period) tissues were collected for further analyses.

Due to inconsistencies in bacterial localization, and undesired severity of infection, modifications were made to model #1 to create model #2. In model #2 of osteomyelitis, *S.aureus* was delivered to the bicortical defect (McMaster Carr, #65), on a pre- contaminated orthopedic screw(Antrin Miniature Specialties Inc., #00-90, 303 stainless steel, Ø=0.047, ¼ length). The

screw was soaked in approximately 200µL of 10^8 CFU/mL ATCC 6538-GFP for ~5 minutes, and dried for ~5 minutes prior to implantation Due to inconsistencies with gel synthesis, and poor maintenance of gelatinous form at the time of injection, poloxamer 407 was not used for model #2. Instead, a more standard 2% alginate gel was utilized to deliver therapeutics at day 7.

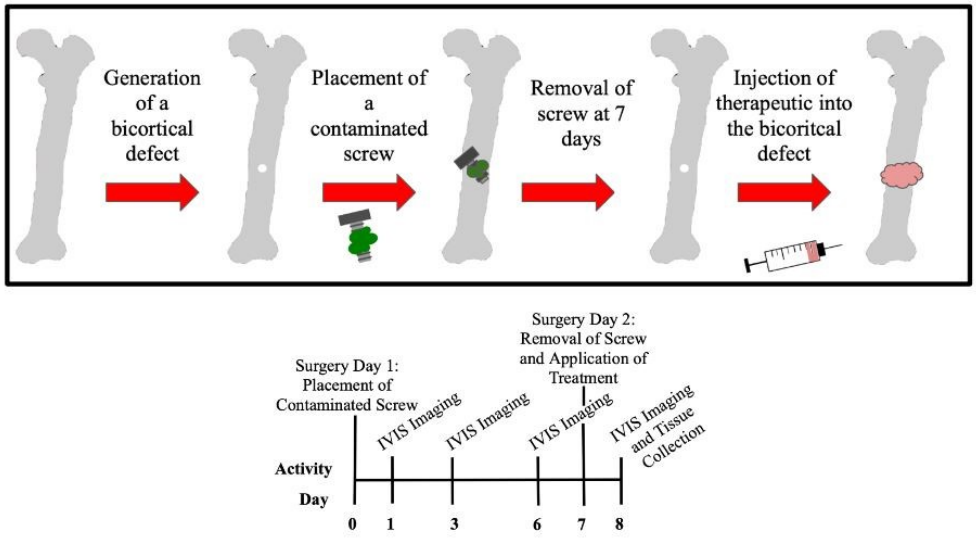

Figure 2.1 Overview of Model #2

In model #2, *S.aureus* was injected into a bicortical defect, followed by placement of an orthopedic screw. At day 7, treatment(s) were applied and at day 8 (a 24h treatment period) tissues were collected for further analyses.

Implant-based Models of Osteomyelitis: Procedures

General Surgical Procedure(s) for Infection Establishment

For all surgical procedures, rats were anesthetized with isoflurane at an initial concentration of 2-3%, then kept at 1-2% for maintenance. Rats were administered slow release buprenorphine (1.0-1.2 mg/kg BW) pre-operatively for pain relief. Fur from the left hind leg and surrounding areas was removed with electric clippers, followed by application of depilatory

cream. An ear tag was also applied. Then, subjects were transferred to the surgical table, where the hind limbs were cleaned with alcohol and chlorhexidine and sterilely draped. After preparation of the site of surgery, the skin was incised with an anterior approach, from the level of mid-diaphysis to the patella, along the lower half of the femur. The muscle tissue was separated using blunt dissection along the muscle bundle divisions on the anterolateral side of the femur. Approximately 2 mm from the distal epiphysis, a bicortical defect was created with a pneumatic power drill (Conmed Hall #PRO6150), and a #65, uncoated drill bit (McMaster Carr), to create a defect approximately 0.035" inches in diameter.

Infection Procedure for Osteomyelitis Model #1: S.aureus Delivery by Injection

In osteomyelitis model #1, a 10µL PBS solution containing approximately 10^6 CFU of ATCC 6538-GFP was injected into the bicortical defect, and allowed to sit for 2 minutes undisturbed. Then, a sterile #00-90 stainless steel orthopedic screw (Antrin Miniature Specialties) was fastened to the defect using a 0.070" slotted screwdriver (McMaster Carr). Then, the superficial fascia lata (and subcutaneous tissues, if needed) and skin were closed with monocryl sutures.

Infection Procedure for Osteomyelitis Model #2: S.aureus Delivery by Orthopedic Screw

In osteomyelitis model #2, A #00-90 stainless steel screw (Antrin Miniature Specialties) was pre-contaminated with approximately 10^3 CFU of ATCC 6538-GFP as described within the *in vitro* methods above (see: "Optimization of Ultimate Bacterial Load on Orthopedic Screws"). It was then fastened into the defect using a 0.070" slotted screwdriver (McMaster Carr). Then, the superficial fascia lata (and subcutaneous tissues, if needed) and skin were closed with monocryl sutures.

General Surgical Procedures for Treatment Application

On this assigned treatment day, all rats were anesthetized and the leg was cleaned for surgery as described above. The surgical site was re-opened along the previous incision line. All residual suture material was carefully removed, and in some cases, placed within PBS for future bacterial counting analyses. Again, the muscle tissue was separated using blunt dissection along the muscle bundle divisions on the anterolateral side of the femur. If pus was evident, it was removed. However, no debridement was performed. The orthopedic screw was removed using 0.070" slotted screwdriver (McMaster Carr), and collected for bacterial counting. Approximately 100μL of assigned therapeutic was then placed into the bicortical defect, which was able to fill the defect and the underlying, ventral surrounding soft tissue(s). Then, the superficial fascia lata (and subcutaneous tissues, if needed) and skin were closed with monocryl sutures. All animals were randomly assigned treatment groups and surgeons to minimize any additional variables. The radiance numerical data obtained for IVIS Lumina XRMS 24 prior to treatment was used to ascertain that there was an even distribution of infection severity among treatment groups.

Treatment Procedure for Osteomyelitis Model #1: S.aureus Delivery by Injection

In model #1, all animals were sacrificed (n=6) or given bacteriophage therapy (~MOI=5, n=5) in 30% (w/v) Poloxamer 407 ("P407") hydrogel on day 14. All phage treated animals were sacrificed on day 20. All screws were collected on day 14. Soft tissues and bones were collected for bacterial counts, SEM, and/or histological analyses on day 14 for the control group, and day 20 for the phage treated groups.

Treatment Procedure for Osteomyelitis Model #2: S.aureus Delivery by Orthopedic Screw

In model #2, all rats were treated on day 7 and sacrificed on day 8. The treatment groups (n=6) were as follows: (i) fosfomycin (3mg) (ii) phage (~MOI=5), (iii) dual (3mg fosfmycin + ~MOI=5 phage) delivered in 100µL of 2% alginate hydrogels. All animals assigned to the control group (n=5) received 100µL empty 2% alginate hydrogel. All screws, soft tissues, and bones were collected for bacterial counts, SEM, and/or histological analyses.

IVIS Imaging

Throughout the course of *in vivo* studies, radiographs with fluorescent overlays were collected using the IVIS Lumina XRMS Series III system (Cole Palmer). In model 1, imaging was performed on days 1, 7, 13, and 15. In model 2, images were collected on days 1, 3, 6, and 8. For imaging, rats were anesthetized with 2% isoflurane, and maintained at 1-2% isoflurane for approximately 10-20 minutes, for the duration of the imaging process. For imaging, rats were placed in the right lateral recumbent position. For fluorescent imaging, images were read at 480-520 nm. A circular region of interest (ROI) was collected from the IVIS system, from which an average radiance value per area covered ([p/s/cm≤/sr]) was automatically calculated and recorded. All images were normalized to day 1.

ex vivo Work

Bacterial Counts of Screws, Soft Tissue, and Bone

Screws

Screws were collected on the day of treatment application (in model 1=day 14, in model 2=day 7). Screws were removed from the femur and immediately placed into 1 mL PBS. During

all processing procedures, the samples were kept on ice or at 2-4℃. All screws were vortexed at 2000 RPM for 2 minutes, serially diluted 100-1000 fold, plated for enumeration.

Soft Tissue

Soft tissue samples were collected on day 20 for model 1, and on day 8 for model 2, immediately following animal sacrifice and tissue collection. During all processing procedures, the samples were kept on ice or at 2-4℃. Soft tissue samples were collected generously; all soft tissue immediately surrounded the femur was collected for analysis. This tissue was placed directly into 10mL PBS, cut into fine pieces using sterile scissors, then vortexed at 2000 RPM for 2 minutes. The sample was weighed, then serially diluted in PBS for subsequent bacterial plating.

Bone

Bone samples were collected on day 20 for model 1, and on day 8 for model 2, immediately following animal sacrifice and tissue collection. After careful acetabular and patellar disarticulation, and soft tissue removal, the femur was placed into 10mL PBS. During all processing procedures, the femur samples were kept on ice or 2-4℃. Each femur was initially broken using sterile bone rongeurs. Then, a homogenizer (Cole Palmer, LabGEN7) was used to thoroughly mince the samples. All samples were initially homogenized on a low setting (2-3) for approximately 2 minutes, and then at high (8-9) for 1 minute. Between samples, the homogenizer was cleaned with Ethanol and distilled H_2O. All samples were then weighed, vortexed, and serially diluted in PBS for bacterial plating.

Histology

In model #1, the entire, intact femur and surrounding soft tissues were histological processed on day 20. In model #2, the excised femur was broken along the screw line using bone rongeurs, at which point the distal portion was collected for histological analysis. All samples were initially placed into 10% formalin for 48h at room temperature. For bone samples, decalcification was performed for 2 days in Kristensen's solution, then rinsed and placed into 10% formalin. Tissues were routinely processed, embedded in paraffin, sectioned at 5µm, and stained with hematoxylin and eosin ("H&E") or Saffarin-O/Gram ("Saf-O").

Scanning Electron Microscopy

Screw Preparation

Screw samples for microscopy were collected on treatment surgery day (model 1=day 14, and model 2=day 7). Screws were removed carefully from the infected femur and placed directly into 1 mL of 0.1M sodium cacodylate, ½ karnovsky's (2.5% glutaraldehyde, 2% paraformaldehyde) fixative for 24 hours. Prior to imaging, all samples were placed onto stubs with carbon tape. All screw samples required additional support, and thus a permanent adhesive glue was positioned underneath the screw, on top of the carbon tape. These samples were then sputter coated (Quorom Tech Model # SC7640) at a plasma current of 30mA, and 3.5 kV, for approximately 3-5 minutes with Platinum. All samples were then imaged using FESEM (Carl Zeiss AG-SUPRA 40).

Bone Preparation

On day 20 (model #1) or day 8 (model #2), animals were sacrificed and the femurs were collected for SEM imaging. In model 2, only the portion of the femur proximal to the screw line

was analyzed. To prepare the samples for imaging, they were first broken into 1-3mm pieces using bone rongeurs. All samples were immediately placed into 5mLs of 0.1M sodium cacodylate, ½ karnovsky's (2.5% glutaraldehyde, 2% paraformaldehyde) fixative for 24 hours. Prior to imaging, all samples were placed onto stubs with carbon tape. These samples were then sputter coated (Quorum Tech Model # SC7640) at a plasma current of 30mA, and 3.5 kV, for approximately 3-5 minutes with Platinum. All samples were then imaged using FESEM (Carl Zeiss AG-SUPRA 40).

CHAPTER IV

RESULTS

in vitro Work

Chromosomal Integration of GFP into ATCC 6538

Integration of GFP into ATCC-6538 was successful, as indicated by IVIS Lumina XR Series III micro-plate reader (SpectraMax M5), and *Ex Vivo* culturing of the selected strain. This strain enabled phenotypic characterization of our model throughout the course of infection progression and regression (Fig.4.3, Fig.4.4).

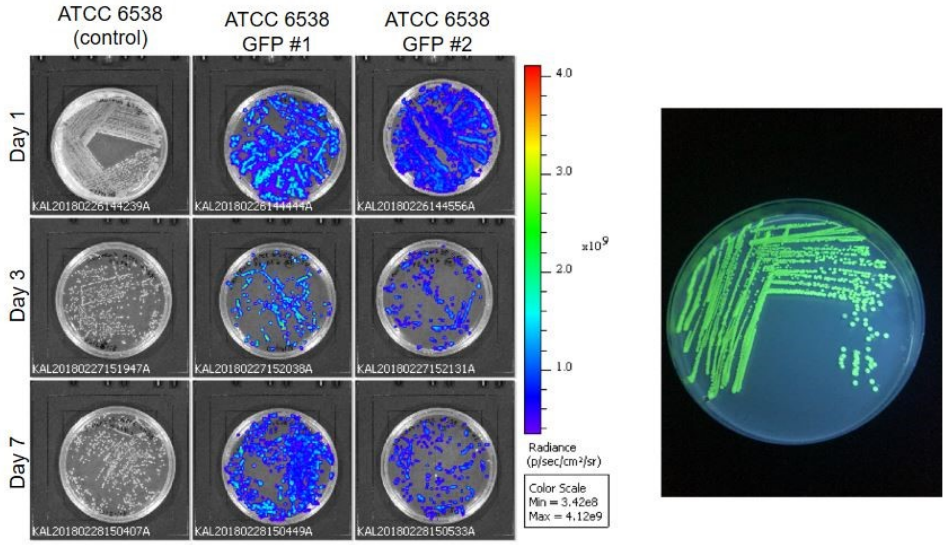

Figure 4.1 Chromosomal Integration of GFP into ATCC 6538

(Left) GFP is successfully integrated into ATCC 6538 in two strains. Ultimately, strain #1 was selected as it held a higher intensity of signal versus strain 2, as confirmed in plate reader (SpectraMax M5). Over the span of 7 days, the signal remained consistent per CFU present. (Right) GFP continues to be expressed within the ATCC 6538-GFP strain cultured *ex vivo.*

Kirby-Bauer Analysis of 2% Alginate Hydrogels

Kirby-Bauer analysis was used to assess whether bacteriophage therapy was compatible with 2% alginate hydrogels. This preliminary work indicated that bacteriophage therapy still exhibited bactericidal activity within the gels, as indicated by the clear region within this agar plate (Left, far right bottom).

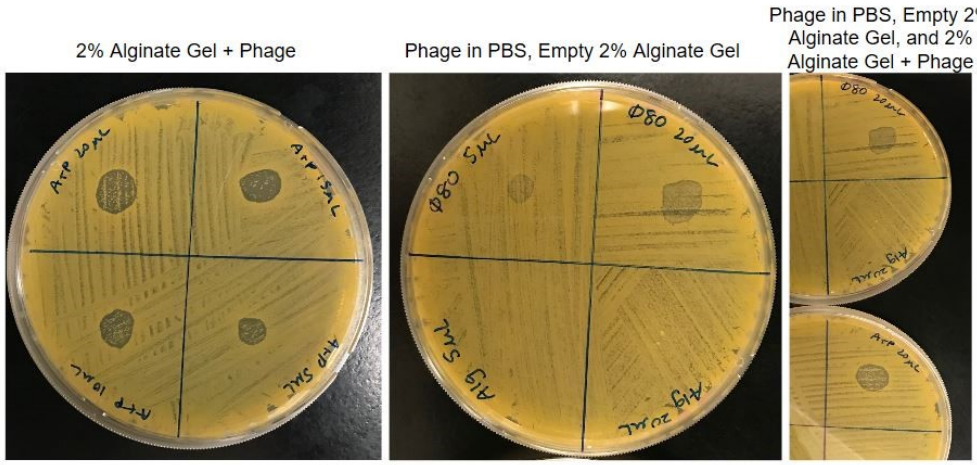

Figure 4.2 Kirby-Bauer Analysis of 2% Alginate Hydrogels

(Left) Phage loaded in 2% alginate gels has bactericidal activity, as indicated by the clear region of therapeutic placement. From top left, clockwise: 20µL, 15 µL, 5 µL, 10µL. (Center) From top left, clockwise: 5 µL phage, 20 µL phage, 20 µL empty 2% alginate gel, 5 µL empty 2% alginate gel. Alginate hydrogels appear to have no bactericidal activity, as expected. Phage therapeutic displays some bactericidal activity. (Right) From top to bottom: 20µL of phage, empty 2% alginate hydrogel, and phage +2% alginate hydrogels plated on bacterial lawns indicate that alginate and phage are compatible.

Anti-biofilm Efficacy of Selected Therapeutics

Utilizing IVIS Lumina XRMS and bacterial counts, the efficacy of our therapeutics at 6, 12, and 24h was assessed.

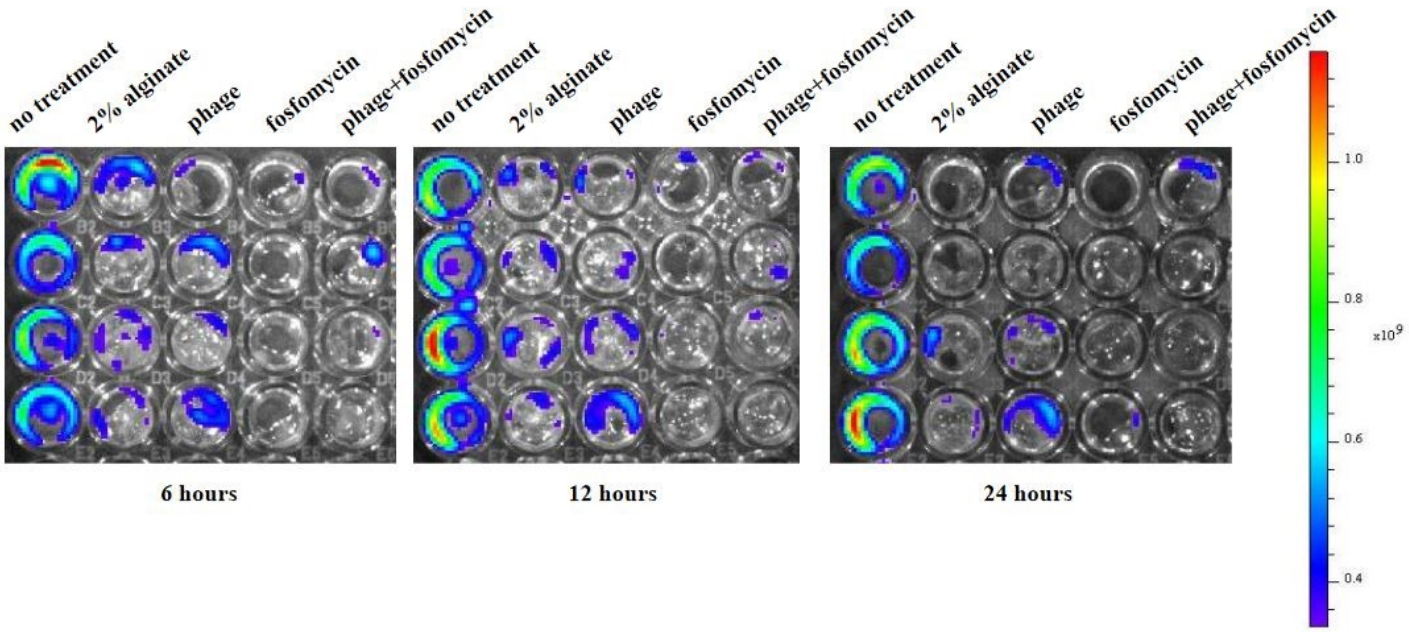

Figure 4.3 Antibiofilm Plate Assay

(From left to right) Biofilm plates with applied treatments at 6, 12, or 24 hours, where cool colors indicate lower levels of *S.aureus*, and warm colors indicate a higher prevalence of *S.aureus*.

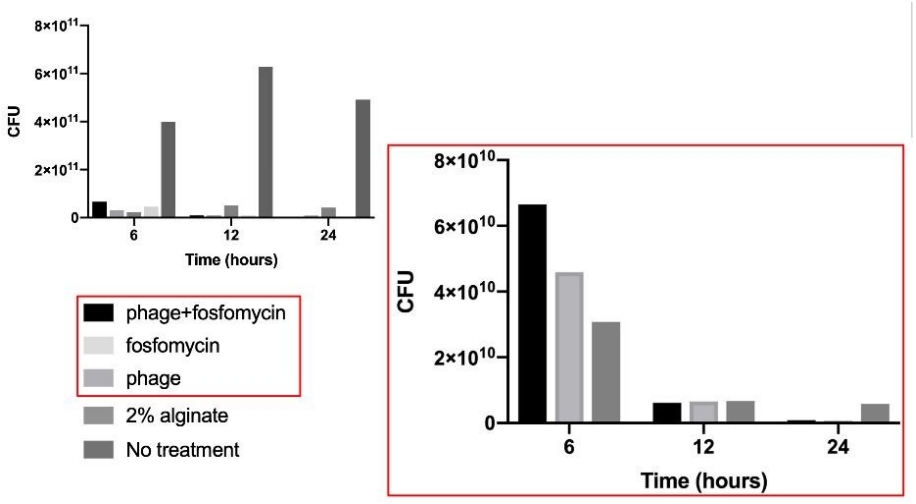

Figure 4.3 (continued) Antibiofilm Assay: Bacterial Counts

(Top left) Bacterial counts collected at 6, 12, and 24h reveal that our selected therapeutics did have efficacy on cultured biofilms, relative to the untreated control.

Optimization of Ultimate Bacterial Load on Orthopedic Screws

Based on bacterial counts, the amount of soaking time is positively related to the ultimate bacterial load on the screws. At 5, 10, and 20 minutes the average load(s) are $9.9x10^3$, $3.6x10^4$, and $8.3x10^4$, respectively.

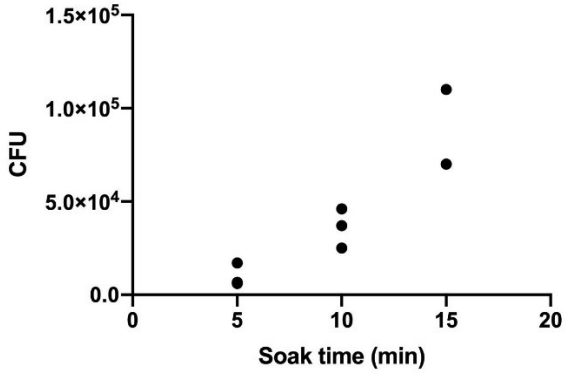

Figure 4.3 Effect of Soaking Time on Screw Bacterial Load

Soaking time appears to be positively correlated to bacterial load.

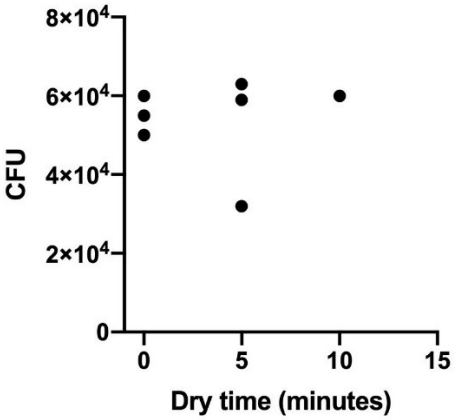

Figure 4.3 Effect of Drying Time on Screw Bacterial Load

Dry time (0-10 minutes) does not appear to have a large effect on *S.aureus* viability.

Osteomyelitis Model #1 (Delivery of *S.aureus* by Injection) Results

in vivo Results

Clinical Signs of Osteomyelitis

On day 14 (treatment day) all rats presented with pus along the femoral surgical site. In several rats, the area surrounding the femur remained swollen throughout the course of infection (mild-moderate). Porphyrin staining of the eyes and nose was common.

IVIS Imaging

IVIS imaging of rats from model #1 indicate that both the location (Fig.4.3) and the severity of infection (compare Rat A,B, and C on day 1 of Fig.4.3) varied among subjects. The average signal at days 1, 7, and 13 were: $5.16x10^8$, $1.18x10^8$, and $1.66x10^8$ [p/s/cm≤sr], respectively. Pre-treatment (day 13) signal ranged from: $8.46x10^7$-$1.60x10^8$ [p/s/cm≤sr].

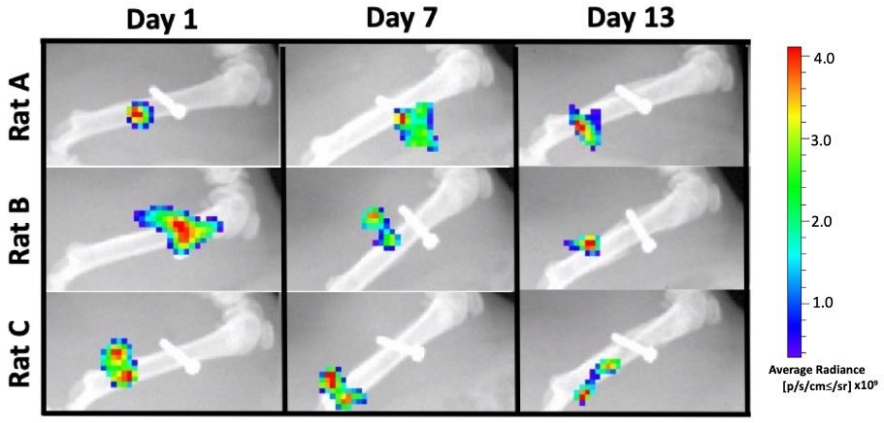

.

Figure 4.4 Model 1 Representative IVIS Images at Day 1, 7, and 13

Presence of bacteria, indicated by the presence of color, in representative rats A, B, and C is observed at days 1, 7, and 13. In this model, we see inconsistent localization of bacteria, with a magnitude of 10^9 photons, as indicated by the scale bar.

Ex vivo Results

Bacterial Counting

Bacterial counts performed on day 14 on orthopedic screws ranged from $9.55x10^3$-$2.32x10^5$CFU. The average recovered bacteria on these screws was $5.25x10^4$ CFU. The average soft tissue counts for control groups, collected on day 14, was $2.41x10^6$. The average soft tissue bacterial counts for phage treated groups, collected on day 20, was $2.75x10^6$. No statistical differences existed between these two groups (p=0.8562). The average recovered bacterial counts from bones were: $9.09x10^5$ in control groups (collected at day 14), and $2.06x10^6$ in the phage treated group (collected at day 20). The bone bacterial counts were found to be significantly different, and higher, than those of the control group (p=0.0476).

Soft Tissue

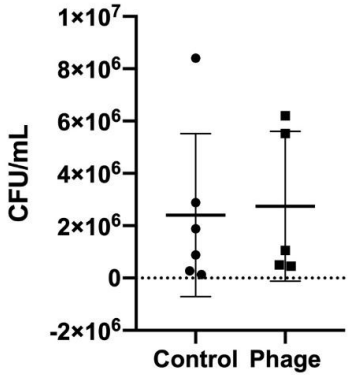

Figure 4.5 Figure 4.4 at Day 20

No statistical differences exist between the control and phage treated groups (p=0.8562, unpaired t-test). We note inconsistent bacterial counts among groups, indicated by the range of data points visualized above.

Bone

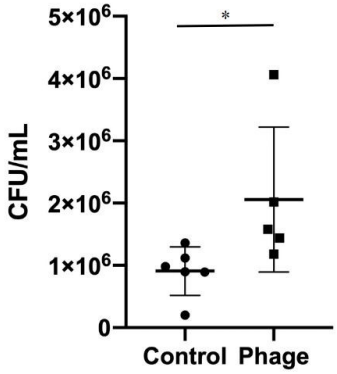

Figure 4.6 Figure 4.5 at Day 20.

Control and phage treated groups are statistically different (p=0.0476, unpaired t-test).

Histology

Histological analysis included H&E stains of infected and uninfected bone, and Saf-O/gram stains of infected bone samples. Histology results indicate successful establishment of osteomyelitis, with "hallmark" symptoms such as necrotic bone (Fig.4.6A-B), inflammation (Fig.4.6C), and evidence of gram positive bacteria (Fig. 4.6E-F).

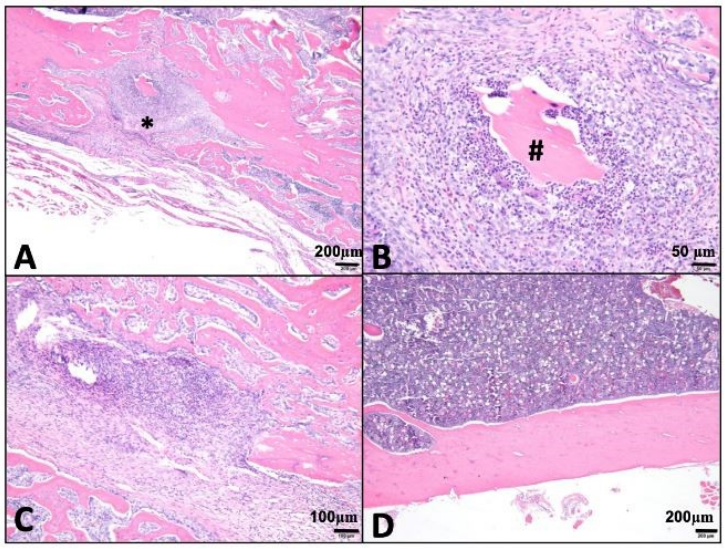

Figure 4.7 Figure 4.7

(A-C): Infected samples; (D): Uninfected control samples. (A).Within the *S.aureus* infected bone there are multifocal areas of inflammation with bone necrosis (*) surrounding by marked medullary and cortical bone proliferation. (B, C): Higher magnification of areas of inflammation demonstrate abundant neutrophils with fewer macrophages and reactive fibroblasts. In (B) the area of inflammation surrounds a piece of necrotic bone (*). (D): Normal control bone with normal cortical thickness and medullary bone marrow.

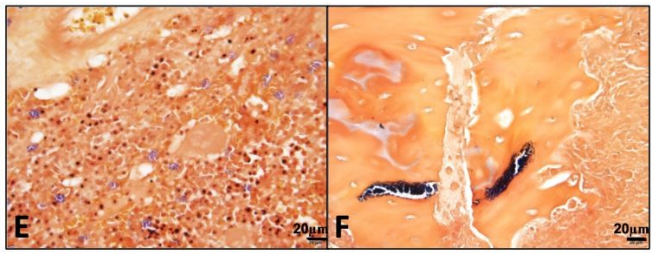

Figure 4.7 Model #1 Histology: Saf-O/Gram Strains

(E-F) Clusters of gram positive bacteria within marrow and areas of remodeling. Some bacteria appear to be within macrophages.

Scanning Electron Microscopy

Scanning electron microscopy (SEM) of excised screws and control bones at day 14 further support the successful establishment of osteomyelitis in our rat model. We see clusters of gram positive bacteria within the threading of excised orthopedic screws as well as residual glycocalyx fibers (Fig.4.7A-B). Processed bone tissues also show evidence of *S.aureus* deep in bone canniculi (Fig.4.7C-D).

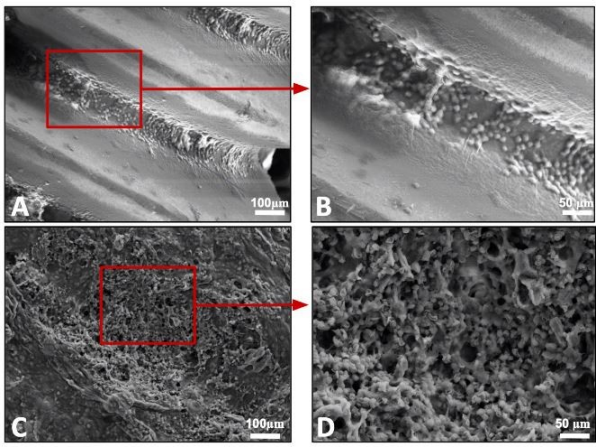

Figure 4.8 Model #1: SEM at Day 14

(A-B) Gram positive bacteria and glycocalyx formation are seen within the ridges of a screw excised at day 13 at various magnifications. (C-D) Robust biofilm formation and gram positive bacteria growth is apparent in internal cortical bone samples from infected tissues.

Osteomyelitis Model #2 (Delivery of *S.aureus* by Orthopedic Screw) Results

in vivo Results

Clinical Signs of Osteomyelitis

On day 7 (treatment day) a few rats presented with pus along the femoral surgical site. Only mild swelling and porphyrin staining of the eyes and nose were noted.

IVIS Imaging

IVIS images collected from model #2 reveal consistent localization of bacteria along the screw line, as anticipated (seen by the rainbow colors in Fig. 4.8). Furthermore, the severity of infection remained similar across different animals: on day 6 (pretreatment) signals ranged from $4.24x10^7$-$1.48x10^8$.The average signal at day 6 (pre-treatment) was $9.11x10^7$ [p/s/cm≤sr].

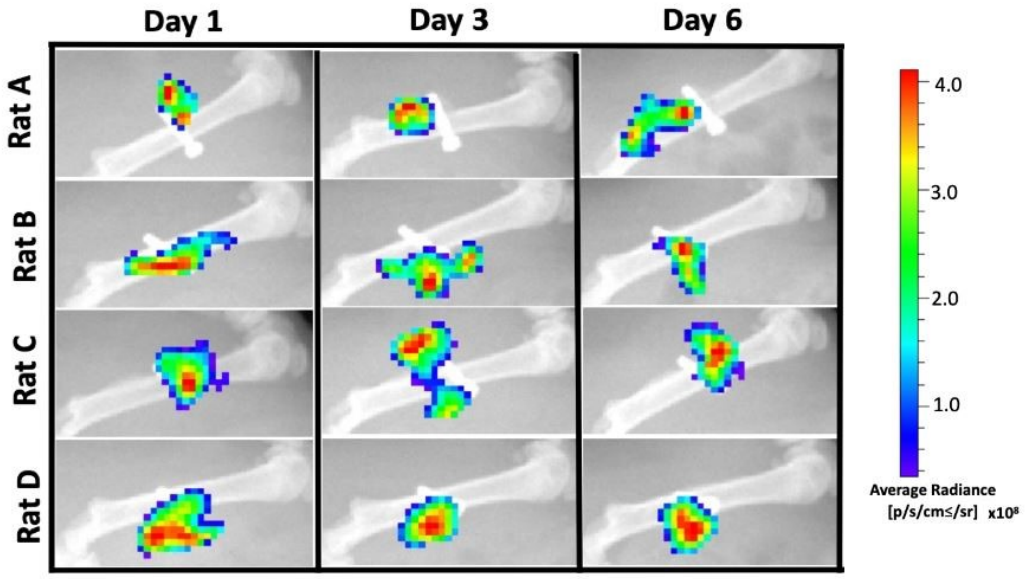

Figure 4.9 Model #2 Representative IVIS Images at Day 1, 3, and 6

In Rats A, B, C and D, the location of S. aureus is predictable (at the screw) and consistently maintained in this location as infection develops. We also note an ultimate lower bacteria load versus Model 1, as indicated by the photon magnitude of 10^8 within the scale bar.

Ex vivo Results

Bacterial Counting

Using Sidak's multiple comparisons tests, significant differences were determined between four groups: (i) control v. fosfomycin (p=0.0083), (ii) control v. dual therapy

(p=0.0105), (iii) fosfomycin v. phage (0.0139), and (iv) phage v. dual (p=0.0178). The average bacterial counts (CFU/mL) per bone tissue treatment group were as follows: (i) control: $1.15x10^4$, (ii) fosfomycin: $3.91x10^3$, (iii) phage: $1.06x10^4$ and (iv) dual: $3.49x10^3$. Soft tissue bacterial counts were not significantly different (One way ordinary ANOVA p=0.131). The average bacterial counts (CFU/mL) per soft tissue treatment group were as follows: (i) control: $9.07x10^4$, (ii) fosfomycin: $2.28x10^4$, (iii) phage: $2.13x10^4$ and (iv) dual: $4.32x10^4$.

Soft Tissue

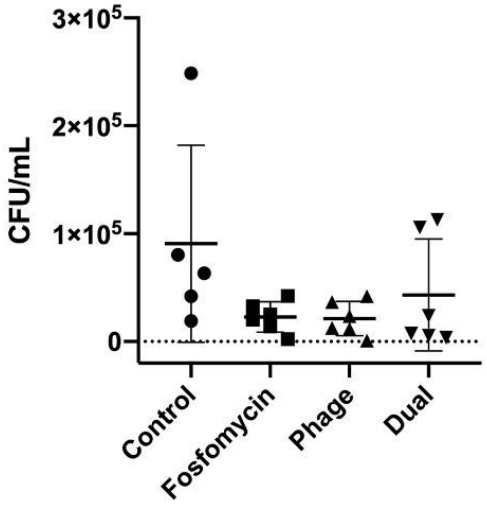

Figure 4.10 Figure 4.9 at Day 8

No statistical differences exist between soft tissue bacterial counts within model 2. (One way ordinary ANOVA p=0.131).

Bone

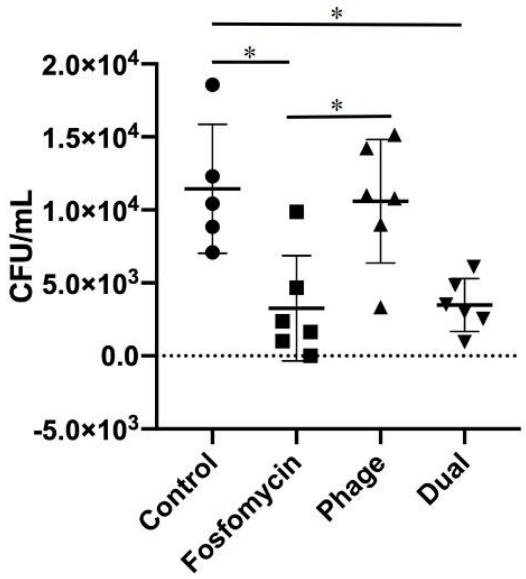

Figure 4.11 Figure 4.10 at Day 8

Significant differences were determined between four groups: (i) control v. Fosfomycin (p=0.0083), (ii) Control v. dual (p=0.0105, n=6), (iii) Fosfomycin v. phage (0.0139), and (iv) phage v. dual (p=0.0178).

Scanning Electron Microscopy

Scanning electron microscopy reveals evidence of successful osteomyelitis establishment in model #2. Screws collected at day 7 reveal thick layers of *S.aureus* within the ridges of orthopedic screws (Fig.4.12). On pieces of bone subjected to SEM, gram positive cocci are visible sporadically among the cortical bone (Fig.4.12), with evidence of biofilm slime (Fig.4.12, right).

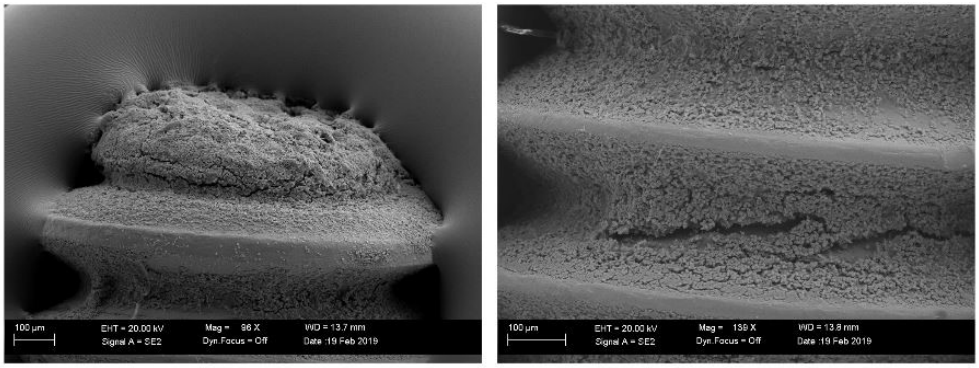

Figure 4.12 SEM of Screws Collected at Day 7

(Left) Gram positive cocci, and potential underlying biofilm, is evident on the distal portion of the orthopedic screw excised at day 7. (Right) Bacteria fills the threading of the orthopedic screws excised at day 7.

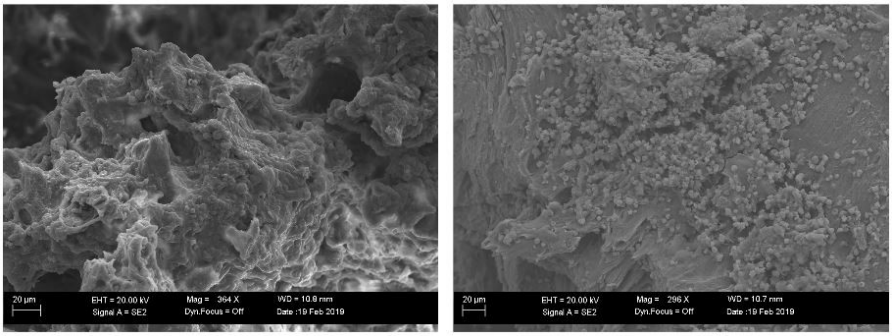

Figure 4.13 SEM of Bone Tissue Excised on Day 8

Bacteria are found within the various surfaces of cortical bone. (Right) Indications of biofilm, in which *S.aureus* is presumably suspended within, is apparent.

Model #1 and Model #2: Comparison of Average Bacterial Counts in Soft Tissue and Bone

As mentioned previously, model #2 was generated in response to shortcomings found within model #1. Model #1 was induced with ~10^6CFU bacteria, whereas model #2 was induced

with ~10^3 CFU bacteria on the orthopedic screw. In table 4.2, we see that these initial bacterial loads are reflected in final bacterial counts.

Table 4.2 Comparison of Average Bacterial Counts Between Model #1 and #2

		Model #1	Model #2
Soft Tissue Counts	Control	$2.41x10^6$	$9.07x10^4$
	Phage	$2.75x10^6$	$2.13x10^4$
Bone Counts	Control	$9.09x10^5$	$1.15x10^4$
	Phage	$2.06x10^6$	$1.06x10^4$

In the table above, we see evidence that model #2 successful generated a less severe infection than model#1, based off of average bacterial counts from phage and control samples.

CHAPTER V

DISCUSSION

Infections induced by antibiotic resistant strains of bacteria are increasing in prevalence throughout the world, resulting in tremendous economic turmoil and negative outcomes for patients, with no immediate end in sight. This has created a great need to identify and commercialize novel therapeutics, to overcome the ongoing insufficiency of bacterial killing offered by traditional antibiotics. Bacteriophages may be suitable to fill this niche, as they exhibit bactericidal activity, are highly specific, non-toxic, and are readily cleared from the body. Largely, the use of these antimicrobials has been limited thus far due to the public opinion towards voluntarily taking viruses, and because of the specificity exhibited by each bacteriophage, which can hinder the ability of clinicians to rapidly treat infection. With CRISPR-Cas9 modification, it may be possible to extend the specificity of bacteriophage therapeutics to a variety of pathogens, thus enhancing the appeal and utility for clinical application. Bacteriophage therapeutics would also circumvent the current antimicrobial crises, as risk for bacterial modification is low with exposure to these viruses over time. Within this study, we thus aimed to lay the groundwork for future CRISPR-Cas9 bacteriophage use, motivated by preliminary *in vitro* work on *S.aureus* LAC biofilms (Appendix A, FigureA.1).

in vitro Investigations

Cytation5: Preliminary Work (Appendix A)

Largely, this work was motivated by preliminary work treating biofilms with antiobiotics (vancomycin or fosfomycin) or bacteriophage (appendix A), which were then imaged using the Cytation5 software system. With this system, bacterial presence (green) indicated poor therapeutic action. Black panels were ideal results, indicating full bacterial clearance. Surprisingly, preliminary results indicated that fosfomycin was more effective at nearly a tenth lower dose (128 μg/mL) than vancomycin (1024 μg/mL) on biofilm lawns. This difference in bactericidal efficacy may be due to the glycocalyx surrounding the developed biofilm, and the previously mentioned mechanisms of each drug. Vancomycin, with its larger size, may have a more difficult time reaching the live, underlying later of *Staphylococcus aureus* within biofilm than the smaller Fosfomycin molecule. Also, the extracellular matrix of biofilms is sustained by a protective layer of dead *staphylococcal* cells. Vancomycin may be attaching to these cells, and is thus not reaching the live cells. Fosfomycin, on the other hand, would not act on these dead cells and thus have greater efficacy in disrupting biofilms. Within this work, we also note that a phage MOI of 10 is ideal for bacterial clearance.

Bacteriophage Therapy: Advantages and Disadvantages

As previously discussed, CRISPR-Cas9 modified bacteriophage was utilized within the study. This therapeutic had two mechanisms of action: (i) “traditional” bacteriophage lysing, and (ii) CRISPR-Cas9 “cutting” mechanism of bacterial cell wall. Phage are not known to be susceptible to bacterial resistance efforts, are highly specific, readily available in the environment around us, and have been used with great success in the country of Georgia. In cases of biofilm, phage may also prove superior to traditional antibiotics because it will not bind

to the dead *Staphylococcal* cells surrounding the underlying, live layer of bacteria and thus become ineffective. As seen in this study, a potential disadvantage of this therapeutic is delivery and optimal dosing of this therapeutic. In the current clinical scenario, there is not a library of phage readily available for use, as seen in the country of Georgia. For effective treatment of polymicrobial infections, or patients in critical care, it would be essential to have quick and easy access to a variety of bacteriophage(s). Bacteriophage therapeutics would need to be mass produced and carefully maintained to ensure virus vitality.

Integration of GFP into ATCC 6538-GFP: Implications and Advantages

Integration of GFP into *S.aureus* ATCC 6538 was successful (Fig.4.1), enabling the longitudinal analysis of bacterial growth for future *in vitro* and *in vivo* investigations. The genetic incorporation of this fluorescent protein into our bacterial genome was performed in an effort to address some of the downsides of conventional bioluminescent bacterial strains. Our strain may allow longitudinal analyses superior to conventional bioluminescent imaging ("BLI"), as our strain can hypothetically be imaged indefinitely. Conventional BLI bacterial strains have the capabilities to lose their luminescent signal over time, limiting time course studies and *in vivo* studies seeking long-term analyses.

There are some disadvantages to the use of a GFP-tagged bacterial strain. BLI is generally detectable at a lower level than GFP, which would be useful in less severe infection models. In one study, only 50 luciferase-tagged cells were needed for BLI detection, versus nearly 5x10^5 GFP-tagged cells.[181] Furthermore, researchers have to be careful not to introduce auto fluorescent materials within their studies when utilizing GFP-tagged bacteria. Some common materials which can fluoresce are collagen, certain hydrogels, cell culture medium, and genipen.[181] There is also the potential of GFP to emit a signal after cell death. Furthermore,

within this work we were not able to establish a direct standard curve correlation CFU to emitted signal. In other work, BLI signal has been successfully correlated to CFU.[182]

Kirby-Bauer Assays

Phage therapeutics were successfully loaded into alginate hydrogels, and were found to exhibited no adverse effects on the therapeutics, as supported by Kirby-Bauer assays (Fig.4.2), which was consistent with reports of other studies utilized hydrogel delivery vehicles for bacteriophage therapeutics.[44]

Antibiofilm Assays

Currently, there exist no commercially available release profile for assays for fosfomycin or bacteriophage therapeutics. In an effort to: (i) characterize the release profile of 2% alginate gels loaded with fosfomycin, phage, or fosfoymcin + phage and (ii) confirm the efficacy of these therapeutics on ATCC 6538-GFP biofilm, a previously described antibiofilm assay was modified.[59] IVIS Lumina XRMS data output confirmed the efficacy of therapeutics against biofilm (Fig. 4.3). Subsequent bacterial counts from these assays were successfully utilized to generate graphs of both signal intensity changes over time(Fig.4.3), and bacterial counts over time (Fig.4.3), which indicated that our selected therapeutics were successful in mitigating infection, relative to the untreated control. Through optimization of: bacterial culture magnitude, soaking time, and drying, we demonstrate the ability to consistently deliver CFU on orthopedic screws. For future studies, this data may be utilized to induce infections of various magnitudes.

Antiseptic Model #1 and Model #2

In this study, two different antiseptic models were considered. In model #1, a Kirschner wire was used. Unfortunately, we saw rotation about the wire itself, which resulted in poor health

and spontaneous fracture within our rats. For ethical reasons, we decided to try another model. In aseptic model #2, a fixation plate was used. The plate consisted of a variety of parts we had created by a small company in Tupelo, MS. Again, this method of stabilization did not work, and spontaneous fracture and imcomplete healing of the defect was noted. We believe that this model, like aseptic model #1, did not allow adequate stabilization. It is possible the designed components of the fixation plate were not manufactured properly.

in vitro and *ex vivo* Investigations of Osteomyelitis Model #1 (Delivery of *S.aureus* by Injection into the Bicortical Defect)

Within this work, we investigated two different osteomyelitis models. In model #1, infection was induced by injection of *S.aureus* into a bicortical defect. In this model, there was a two week infection period, and a 6 day treatment period. Successful establishment of infection was confirmed by multiple platforms. On surgery days, pus was evident in all subjects. IVIS Lumina XRMS imaging (Fig.4.3) allowed successful, longitudinal tracking of infection over time. However, IVIS results indicated inconsistent localization of bacteria in this model, and evidence of unintended soft tissue infection. Histological analyses revealed typical hallmarks of infection, such as: necrotic bone, abundant neutrophils, inflammation, and gram positive bacteria (Fig4.6). Scanning Electron microscopy revealed gram positive bacteria within the ridges of excised orthopedic screws and on pieces of bone (Fig.4.7). Within SEM images, evidence of residual glycocalyx is also apparent. Finally, bacterial counts were performed to quantify the bacteria present on orthopedic screws on day 14, and the effect of phage therapy on soft tissue and bone samples 6 days after treatment (Fig.4.9,4.10). Interestingly, the only significant differences we extrapolated from the bacterial counts were between the phage-treated and control bone samples. The bacterial counts of the phage treatment group were determined to be

significantly greater than the control group (p=0.0476). We attribute these results to a variety of factors. First, the 6 day treatment period was not ideal, given the single, 100 µL treatment applied. Realistically, this treatment may have been cleared from the body in 24h. Furthermore, this was a very robust infection. It is possible that the infection would have continued to increase in severity given any treatment under these conditions. Furthermore, some literature reports the capacity of *S.aureus* to respond to mechanical and chemical stimuli aggressively when it is an insufficient dose to induce cell death, resulting in greater biofilm formation or generation of SCVs.[17–19,183] *in vivo* and *ex vivo* Investigations of Osteomyelitis Model #2 (Delivery of *S.aureus* to the Bone by Orthopedic Screw)

Due to inconsistent localization of infection, variance in bacterial counts, and the inability of our therapeutics to lower infection over a span of 6 days, model #1 was abandoned in pursuit of model #2. In model #2, several key protocol changes were made to address the issues seen in model #1: (i) a lower initial dose of bacteria was introduced to animals, (ii) the infection period was reduced from 14 days to 7 days, (iii) the treatment period was limited to 24h, (iv)bacteria was delivered to the femur by orthopedic screw, and (v) the use of a 2% alginate hydrogel instead of poloxamer 407.

Ultimately, we believe these to be positive decisions, based on the outcomes of IVIS Lumina XR images, histology, SEM, and bacterial counting. IVIS images revealed consistent infections localized along the screw line (Fig.4.8). SEM revealed that despite the changes we made to our *in vivo* protocol, gram positive bacteria were still easily detected among the excised orthopedic screw and *ex vivo* bone tissue, indicating infection establishment (Fig.4.11,4.12).

Significant differences were found in several of the bone bacterial count groups: (i) control v. fosfomycin (p=0.0083), (ii) control v. dual therapy (p=0.0105), (iii) fosfomycin v.

phage (0.0139), and (iv) phage v. dual (p=0.0178). Soft tissue bacterial counts were not significantly different (One way ordinary ANOVA p=0.131). However, a trend suggests that there was an effect of treatment on ultimate soft tissue bacterial load, albeit variation among samples. This may be due to the differing immune systems of each subject, surgeon error (dropping screw during placement or removal), or variation in cultured screws.

Although fosfomycin treatment was successful in lowering bacterial load versus the control and phage groups, it should be noted that it was administered at a much higher dose than typical. In humans, an oral dose falls around 3g and intravenous doses fall around 12-16g, and up to 20g for life threatening infections.[184] In our rats, we administered ~3mg per rat. Comparatively, the phage therapeutic was administered at a low dose (~MOI=5). Given a higher phage dose, it is possible that the efficacy of fosfomycin could be matched.

Infected Models #1 and #2: Summary and Discussion

Animal Choice

Within our animal studies, rats were used. Rats are a good selection for initial screening of novel therapeutics, but do not ultimately closely simulate the clinical scenario. Rodents are capable of withstanding, comfortably, high doses of *Staphylococcus aureus.* In model#1, ~$1x10^6$ CFU bacteria were introduced into the defect, and in model #2 ~10^3 CFU were introduced into the defect. In humans, fewer *Staphylococcal* cells are needed to induce infection of the bone. What may contribute to the greater tolerance seen in rats is the lack of a *S.aureus* virulence receptor, which is found in humans. For this reason, rabbits may be a more viable choice for future osteomyelitis studies, as they are still a "small" animal, but have these virulence receptors.[153]

Similarities and Differences to Clinical Scenarios

In this work, ATCC 6538-GFP was utilized. This strain was originally isolated from human lesions. This strain also generates biofilms, one of the most common reasons for orthopedic hardware failure and/or persistent, chronic infections in humans. For this reason, we claim that the bacteria used in the work herein mimics the clinical reality.

In both models, the orthopedic screw was removed, which is standard for most revision surgeries involving contaminated orthopedic hardware (when the stability of the limb has not been compromised). For our research purposes, this was necessary to allow delivery of the therapeutics. It also enabled us to do bacterial counting assays on the screw themselves. In the true clinical scenario, a sterilized, new screw would typically replace the older, contamined screw. We did not do this; we did not want our therapeutics forced out of the infected defect space. Furthermore, by not replacing the screw in the "treatment period," the use of this model can be extended to analyzing scaffolding, such as: cements, fibrous networks, and more rigid or semi-permanent materials.

In model #2, the model used for the full animal study, bacteria was introduced through contaminated orthopedic screw(s). Although this is possible in the clinical scenario, it is not the most common cause of osteomyelitis. In the modern world, orthopedic hardware is more readily sterilized than ever before and thus we see less of this type of infection.

Currently, the majority of osteomyelitis cases are found within the immunocompromised communities.[185,186] Within this study, our rats were healthy prior to bacterial introduction, and were not immune-compromised in any way. To more accurately depict the true nature of osteomyelitis, and treatment difficulties, animals with diabetes or cardiac diseases would be more suitable for translation of results to the true clinical scenario. In diabetic patients, for

example, there is oftentimes limited vascularization. This can lead to necrotic extremities, which are a common place for infection to begin.[186] Furthermore, these patients have a more limited capacity to fight infection.[186] The rate of osteomyelitis is 4 times higher in the diabetic population than non-compromised, healthy individuals.[186]

As mentioned previously, typical chronic infection is characterized by a 6 week period of persistent infection. Within this study, our infection period lasted only one week. We were limited by many factors which made accomplishing the "typical" human chronic infection impossible. A longer infection period results in additional time and economic constraints. Furthermore, to induce such an infection, we would have to administer a much lower dose of bacteria or continuously introduce antibiotics into the rat system. However, rats can rapidly clear small doses of *S.aureus,* making this difficult. Administering antibiotics consistently would have introduced another variable into our study, and potentially altered the effects of future therapeutics. Furthermore, we did not want to induce an infection so severe it would be impossible to treat.

Another difference between our model and the clinical scenario is that we did not induce debridement, a gold standard for osteomyelitis treatment. Future studies may want to incorporate this into the surgical protocol.

Therapeutic Regimen

Within this study, a single 100 μL dose of selected therapeutics were applied to the infection site, and animals were sacrificed after 24 hours. Typical osteomyelitis treatment involves up to 3 months of continuous antibiotic administration, highlighting the true bold nature of our therapeutic regimen. Although our regimen does not simulate the clinical scenario, or

allow for full infection mitigation, it does offer insight on the potential of our therapeutics to clear infection.

In this study, bacteriophage was administered at a low dose (~3-5 MOI). In preliminary work (appendix A), we noted that an MOI of 10 was needed to effectively clear infection. In this work, we were limited in the amount of phage we could deliver in a single, 2% alginate gel loaded 100 µL treatment, and thus could not deliver an MOI > ~3-5. It should also be noted that the *in vitro* conditions allowed optimal localization of therapeutic on top of biofilms. *in vivo* work allows the bacteria to "hide" within the bony host, motivating an MOI of greater than 10 to match *in vitro* efficacy (appendix A).

Fosfomycin was administered, in contrast, at an extremely high dose (~3mg per treatment). In humans, this high of a dose is not recommended or typical used. Within the rat system, however, higher levels of antibiotic can be tolerated. Surprisingly, this extremely high dose was also unable to clear infection.

In this study, the dual treatment utilized the same doses as phage and antibiotic monotherapy. Both therapeutics were administered at the same time. Ideally, a pilot study would be dedicated to optimizing the timing and dose of these two therapeutics when used in combination with one another. Additionally, it should be noted that the combination of these two therapeutics within 2% alginate hydrogels resulted in the most rigid gels, when compared to the controls or monotherapy. It is possible this altered the release of these therapeutics *in vivo.*

In model #2, we note that phage appears to have more efficacy in soft tissues than in bone. This may be due to insufficient delivery of phage to the infected, bony defect site: our therapeutics were allowed to "pool" into the soft tissue below the femur, as the defect size has limited volume for therapeutic injection (~6-10uL). Alternatively, it could be an issue of phage

locomotion within the bone. Future studies are warranted to determine whether phage is more apt for soft tissue infections versus osteomyelitis.

In conclusion, our therapeutic regimen offered temporary bacterial reduction but future work will require sustained, greater doses of therapeutics to truly alleviate infection. Greater doses of phage are needed to see true bactericidal activity.

Applications

Within current literature, there is great discussion of "the race to the surface" between native cells and bacterial cells for implant material(s). Currently published osteomyelitis models do not generally allow for the study of this phenomenon. Although it is inconsistent and severe infection, model #1 could be used to simulate this process in future work.

As discussed above, model #2 does have its downsides, as any typical animal model would. However, it has the potential to be a rapid platform for testing novel therapeutics and delivery vehicles. This model has many key advantages (discussed in more detail above): (i) a rapid testing period, (ii) longitudinal tracking of infection, (iii) low costs, relative to other models and (iv) a severe infection, which would only reveal infection reduction for strongly bactericidal agents.

Limitations

Within the majority of this work, *Staphylococcus aureus* and CRISPR-Cas9 modified bacteriophage virus were utilized. Naturally, there exist variations between both living systems over time. It is difficult to perfectly replicate the load of bacteria or virus day to day, which may have had minor effects on procedures performed over multiple days.

The IVIS Lumina XRMS system was useful for tracking infection localization, and changes over time, but was limited in its ability to provide quantification of bacterial load. The generation of a standard curve, correlating CFU to signal output was pursued, but could ultimately never be generated. The IVIS system measures signal strength "relatively;" meaning, only the highest region of fluorescence will be displayed upon analysis. It is likely there is more bacteria surround the femur, but its signal was 1-2 log difference than the most apparent area of bacterial proliferation.[187] Furthermore, it was not possible to image rats in precisely the same manner each trial, resulting in images that may be misleading, depending on rat orientation. See appendix E for more information on IVIS system image normalization, and numerical data collection.

in vivo testing also has its limitations. Rats vary in size and naturally have different gut flora and immune systems, which could alter their responses to infection[188] Animal research can be expensive, time consuming, and the biology of animals are never identical. Furthermore, we would ideally test both male and female rats. Within this study, our work was limited to only female Sprague Dawley rats. Additionally, our results are limited by the relatively small number of animals per treatment group in this study (n=5-6). Given a larger n, there is potential for more significant differences in bone and soft tissue bacterial counts per treatment group.

Future Work

On-going work aims to increase the power of our results from model 2, by increasing our sample size. This work will serve as a platform for future CRISPR-Cas9 osteomyelitis studies.

For future studies, novel biomaterials should be considered for therapeutic delivery of osteomyelitis therapeutics. Within this work, we were unable to sustain the release of our therapeutics from poloxamer 407 or 2% alginate hydrogels, and thus effectively clear infection.

In the future, we hope to explore treatment regimens lasting longer than 24h, enabling a larger dose of phage treatment. With a longer treatment regimen, it may also be possible to assess additional parameters of infection mitigation. Pull out testing could characterize bone strength of experimental groups, and offer insight into the osseo-integration of the orthopedic screw with the native bone.

Additional changes that could be performed for future studies are lower initial bacterial doses, the use of immunocompromised rodents, and the inclusion of surgical debridement.

.

CHAPTER VI

CONCLUSION

Within this work, we have successfully developed a model of implant-related osteomyelitis. Our model is straight forward, enables longitudinal monitoring of infection (hypothetically indefinitely), and mimics the clinical reality of contaminated implant materials. It enables rapid testing of novel delivery vehicles, screw coatings, scaffolding, and antimicrobials. It is a challenging model; biofilm is particularly difficult to penetrate, and the bone architecture provides a space for pathogens to evade antimicrobials. However, the ability of novel therapeutics to minimize infection in this model would, for these reasons, point future researchers towards a truly promising therapeutic option.

In this work, we provided evidence for the potential use of bacteriophage therapeutics for infection mitigation. Phage therapy has many positive qualities over conventional antibiotics; for one, they can be genetically engineered to kill a wide range of positive and negative gram bacteria.[189] They can be made quite readily *in vitro,* and at a low cost. There are also no known side effects of administration of bacteriophage therapeutics; they are highly specific, non-toxic, and are readily cleared from the body. CRISPR-Cas9 gene editing software is a largely "untapped resource" for bacteriophage improvement, and should be considered for future research efforts. Given these promising assets, we believe bacteriophage therapeutics warrant further examination as a potential therapeutic for not only osteomyelitis, but for infections induced by antibiotic resistant bacterial strains.

REFERENCES

1. Hannan, C. M. & Attinger, C. E. Special considerations in the management of osteomyelitis defects (diabetes, the ischemic or dysvascular bed, and irradiation). *Semin. Plast. Surg.* **23**, 132–140 (2009).

2. Deurenberg, R. H. & Stobberingh, E. E. The evolution of Staphylococcus aureus. *Infection, Genetics and Evolution* (2008). doi:10.1016/j.meegid.2008.07.007

3. Tom Frieden. Antibiotic Resistance Threats. *Cdc* (2013). doi:CS239559-B

4. Li, D. *et al.* Quantitative mouse model of implant-associated osteomyelitis and the kinetics of microbial growth, osteolysis, and humoral immunity. *J. Orthop. Res.* (2008). doi:10.1002/jor.20452

5. Hendrix, A. S. *et al.* Repurposing the nonsteroidal anti-inflammatory drug diflunisal as an osteoprotective, antivirulence therapy for Staphylococcus aureus osteomyelitis. *Antimicrob. Agents Chemother.* (2016). doi:10.1128/AAC.00834-16

6. Jørgensen, N. P. *et al.* Rifampicin-containing combinations are superior to combinations of vancomycin, linezolid and daptomycin against Staphylococcus aureus biofilm infection in vivo and in vitro. *Pathog. Dis.* (2016). doi:10.1093/femspd/ftw019

7. Sanders, J. & Mauffrey, C. Long Bone Osteomyelitis in Adults: Fundamental Concepts and Current Techniques. *Orthopedics* (2013). doi:10.3928/01477447-20130426-07

8. Kaarsemaker, S., Walenkamp, G. H. I. M. & Anthony, A. E. J. New model for chronic osteomyelitis with Staphylococcus aureus in sheep. *Clin. Orthop. Relat. Res.* (1997). doi:10.1097/00003086-199706000-00033

9. Hill, P. F. & Watkins, P. E. The prevention of experimental osteomyelitis in a model of gunshot fracture in the pig. *Eur. J. Orthop. Surg. Traumatol.* (2001). doi:10.1007/BF01686897

10. Rissing, J. P., Buxton, T. B., Weinstein, R. S. & Shockley, R. K. Model of experimental chronic osteomyelitis in rats. *Infect. Immun.* (1985).

11. Shiels, S. M., Bedigrew, K. M. & Wenke, J. C. Development of a hematogenous implant-related infection in a rat model. *BMC Musculoskelet. Disord.* (2015). doi:10.1186/s12891-015-0699-7

12. Kremers, H. M. *et al.* Trends in the Epidemiology of Osteomyelitis. *J. Bone Jt. Surgery-American Vol.* (2015). doi:10.2106/JBJS.N.01350

13. Center for Disease Control. *National Diabetes Statistics Report, 2014*. *National Diabetes Statistics Report* (2014). doi:10.1017/CBO9780511804007.003

14. Stewart, S. *et al.* Vancomycin-modified implant surface inhibits biofilm formation and supports bone-healing in an infected osteotomy model in sheep: A proof-of-concept study. *J. Bone Jt. Surg. - Ser. A* (2012). doi:10.2106/JBJS.K.00886

15. Monteiro, J. M. *et al.* Cell shape dynamics during the staphylococcal cell cycle. *Nat. Commun.* (2015). doi:10.1038/ncomms9055

16. Saheed, M. & Rothman, R. Update on Emerging Infections: News From the Centers for Disease Control and Prevention. *Ann. Emerg. Med.* **67**, 386–387 (2016).

17. Tuchscherr, L. *et al.* Staphylococcus aureus develops increased resistance to antibiotics by forming dynamic small colony variants during chronic osteomyelitis. *J. Antimicrob. Chemother.* (2016). doi:10.1093/jac/dkv371

18. Kriegeskorte, A. *et al.* Staphylococcus aureus small colony variants show common metabolic features in central metabolism irrespective of the underlying auxotrophism. *Front. Cell. Infect. Microbiol.* (2014). doi:10.3389/fcimb.2014.00141

19. Painter, K. L. *et al.* Staphylococcus aureus adapts to oxidative stress by producing H2O2-resistant small-colony variants via the SOS response. *Infect. Immun.* (2015). doi:10.1128/IAI.03016-14

20. Gil, C. *et al.* Biofilm matrix exoproteins induce a protective immune response against Staphylococcus aureus biofilm infection. *Infect. Immun.* (2014). doi:10.1128/IAI.01419-13

21. Dantes, R. *et al.* National burden of invasive methicillin-resistant Staphylococcus aureus infections, United States, 2011. *JAMA Intern. Med.* (2013). doi:10.1001/jamainternmed.2013.10423

22. Klein, E. Y., Sun, L., Smith, D. L. & Laxminarayan, R. The changing epidemiology of methicillin-resistant Staphylococcus aureus in the United States: A national observational study. *Am. J. Epidemiol.* (2013). doi:10.1093/aje/kws273

23. Aparna, R. S. L., Prasad, R. G. S. V & Nirmal, N. P. An Injectable In-Situ Conducting Thermosensitive Gel for Controlled Delivery of Vancomycin in Osteomyelitis Treatment and Bone Regeneration. *SCIENCE OF ADVANCED MATERIALS* **8**, 1470–1477

24. Garvin, K. L. *et al.* Polylactide/polyglycolide antibiotic implants in the treatment of osteomyelitis: A canine model. *J. Bone Jt. Surg. Am. Vol.* **76**, 1500–1506 (1994).

25. Wagner, J. M. *et al.* Surgical debridement is superior to sole antibiotic therapy in a novel murine posttraumatic osteomyelitis model. *PLoS One* (2016). doi:10.1371/journal.pone.0149389

26. Penn-Barwell, J. G., Murray, C. K. & Wenke, J. C. Early antibiotics and debridement independently reduce infection in an open fracture model. *Bone Joint J.* (2012). doi:10.1302/0301-620X.94B1.27026

27. Dijkmans, A. C. *et al.* Fosfomycin: Pharmacological, Clinical and Future Perspectives. *Antibiotics* (2017). doi:10.3390/antibiotics6040024

28. Takahata, S. *et al.* Molecular mechanisms of fosfomycin resistance in clinical isolates of Escherichia coli. *Int. J. Antimicrob. Agents* (2010). doi:10.1016/j.ijantimicag.2009.11.011

29. Matthews, P. C. *et al.* Oral fosfomycin for treatment of urinary tract infection: A retrospective cohort study. *BMC Infect. Dis.* (2016). doi:10.1186/s12879-016-1888-1

30. Seija, V. *et al.* Sepsis caused by new delhi metallo-β-lactamase (blaNDM-1) and qnrD-producing Morganella morganii, treated successfully with fosfomycin and meropenem: Case report and literature review. *Int. J. Infect. Dis.* (2015). doi:10.1016/j.ijid.2014.09.010

31. Liao, Y. *et al.* Retrospective analysis of fosfomycin combinational therapy for sepsis caused by carbapenem-resistant Klebsiella pneumoniae. *Exp. Ther. Med.* (2017). doi:10.3892/etm.2017.4046

32. Wenzler, E., Ellis-Grosse, E. J. & Rodvolda, K. A. Pharmacokinetics, Safety, and Tolerability of Single-Dose Intravenous (ZTI-01) and Oral Fosfomycin in Healthy Volunteers. *Antimicrob. Agents Chemother.* (2017). doi:10.1128/AAC.00775-17

33. Wang, F., Zhou, H., Olademehin, O. P., Kim, S. J. & Tao, P. Insights into key interactions between vancomycin and bacterial cell wall structures. *ACS Omega* (2018). doi:10.1021/acsomega.7b01483

34. Ng, M. *et al.* Induction of MRSA biofilm by low-dose ??-lactam antibiotics: Specificity, prevalence and dose-response effects. *Dose-Response* (2014). doi:10.2203/dose-response.13-021.Kaplan

35. Vergidis, P. *et al.* Treatment with linezolid or vancomycin in combination with rifampin is effective in an animal model of methicillin-resistant Staphylococcus aureus foreign body osteomyelitis. *Antimicrob. Agents Chemother.* (2011). doi:10.1128/AAC.00740-10

36. Zak, O. *et al.* Experimental staphylococcal osteomyelitis in rats: therapy with rifampin and cloxacillin alone or in combination. *Curr. Chemother. Immunother. Am. Soc. Microbiol. Washington, DC* 973–974 (1982).

37. Wells, C. M. *et al.* Ciprofloxacin and Rifampin Dual Antibiotic-Loaded Biopolymer Chitosan Sponge for Bacterial Inhibition. in *Military Medicine* (2018). doi:10.1093/milmed/usx150

38. Yap, M. L. & Rossmann, M. G. Structure and function of bacteriophage T4. *Future Microbiology* (2014). doi:10.2217/fmb.14.91

39. Riede, I., Degen, M. & Henning, U. The receptor specificity of bacteriophages can be determined by a tail fiber modifying protein. *EMBO J.* (2018). doi:10.1002/j.1460-2075.1985.tb03936.x

40. Rakhuba, D. V., Kolomiets, E. I., Szwajcer Dey, E. & Novik, G. I. Bacteriophage receptors, mechanisms of phage adsorption and penetration into host cell. *Polish Journal of Microbiology* (2010). doi:10.1016/j.micres.2015.01.008.1.94

41. Young, R. Bacteriophage lysis: mechanism and regulation. *Microbiol. Rev.* (1992).

42. Ul Haq, I., Chaudhry, W. N., Akhtar, M. N., Andleeb, S. & Qadri, I. Bacteriophages and their implications on future biotechnology: A review. *Virology Journal* (2012). doi:10.1186/1743-422X-9-9

43. Balcão, V. M. *et al.* Structural and functional stabilization of phage particles in carbohydrate matrices for bacterial biosensing. *Enzyme Microb. Technol.* (2013). doi:10.1016/j.enzmictec.2013.03.001

44. Bean, J. E. *et al.* Triggered Release of Bacteriophage K from Agarose/Hyaluronan Hydrogel Matrixes by Staphylococcus aureus Virulence Factors. *CHEMISTRY OF MATERIALS* **26**, 7201–7208

45. Kaur, S., Harjai, K. & Chhibber, S. Bacteriophage mediated killing of Staphylococcus aureus in vitro on orthopaedic K wires in presence of linezolid prevents implant colonization. *PLoS One* (2014). doi:10.1371/journal.pone.0090411

46. Kishor, C. *et al.* Phage therapy of staphylococcal chronic osteomyelitis in experimental animal model. *Indian J. Med. Res.* (2016). doi:10.4103/0971-5916.178615

47. Hathaway, H. *et al.* Thermally triggered release of the bacteriophage endolysin CHAPKand the bacteriocin lysostaphin for the control of methicillin resistant Staphylococcus aureus (MRSA). *J. Control. Release* (2017). doi:10.1016/j.jconrel.2016.11.030

48. Tang, Z., Huang, X., Sabour, P. M., Chambers, J. R. & Wang, Q. Preparation and characterization of dry powder bacteriophage K for intestinal delivery through oral administration. *LWT - Food Sci. Technol.* (2015). doi:10.1016/j.lwt.2014.08.012

49. Souza, G. R. *et al.* Bottom-up assembly of hydrogels from bacteriophage and Au nanoparticles: The effect of Cis- and trans-acting factors. *PLoS One* (2008). doi:10.1371/journal.pone.0002242

50. Zhu, C. *et al.* The potential role of increasing the release of mouse β-defensin-14 in the treatment of osteomyelitis in mice: A primary study. *PLoS One* (2014). doi:10.1371/journal.pone.0086874

51. Zhu, C., Bao, N. R., Chen, S. & Zhao, J. N. The mechanism of human β-defensin 3 in MRSA-induced infection of implant drug-resistant bacteria biofilm in the mouse tibial bone marrow. *Exp. Ther. Med.* (2017). doi:10.3892/etm.2017.4112

52. Rosenbaum Chou, T. G., Petti, C. A., Szakacs, J. & Bloebaum, R. D. Evaluating antimicrobials and implant materials for infection prevention around transcutaneous osseointegrated implants in a rabbit model. *J. Biomed. Mater. Res. - Part A* (2010). doi:10.1002/jbm.a.32413

53. Mehrdar, M. T., Madani, R., Hajihosseini, R. & Bidhendi, S. M. Antibacterial activity of isolated immunodominant proteins of Naja Naja (Oxiana) Venom. *Iran. J. Pharm. Res.* (2017).

54. Melicherčík, P. *et al.* Testing the efficacy of antimicrobial peptides in the topical treatment of induced osteomyelitis in rats. *Folia Microbiol. (Praha).* (2018). doi:10.1007/s12223-017-0540-9

55. Desbois, A. P., Gemmell, C. G. & Coote, P. J. In vivo efficacy of the antimicrobial peptide ranalexin in combination with the endopeptidase lysostaphin against wound and systemic meticillin-resistant Staphylococcus aureus (MRSA) infections. *Int. J. Antimicrob. Agents* (2010). doi:10.1016/j.ijantimicag.2010.01.016

56. Kwieciński, J., Eick, S. & Wójcik, K. Effects of tea tree (Melaleuca alternifolia) oil on Staphylococcus aureus in biofilms and stationary growth phase. *Int. J. Antimicrob. Agents* **33**, 343–347 (2009).

57. Lee, J. H., Kim, Y. G., Ryu, S. Y., Cho, M. H. & Lee, J. Ginkgolic acids and Ginkg o biloba extract inhibit Escherichia coli O157: H7 and Staphylococcus aureus biofilm formation. *Int. J. Food Microbiol.* (2014). doi:10.1016/j.ijfoodmicro.2013.12.030

58. Zhou, Z. *et al.* Combination of Erythromycin and Curcumin Alleviates Staphylococcus aureus Induced Osteomyelitis in Rats. *Front. Cell. Infect. Microbiol.* (2017). doi:10.3389/fcimb.2017.00379

59. Johnson, C. T. *et al.* Hydrogel delivery of lysostaphin eliminates orthopedic implant infection by *Staphylococcus aureus* and supports fracture healing. *Proc. Natl. Acad. Sci.* (2018). doi:10.1073/pnas.1801013115

60. Wu, J. A., Kusuma, C., Mond, J. J. & Kokai-Kun, J. F. Lysostaphin Disrupts Staphylococcus aureus and Staphylococcus epidermidis Biofilms on Artificial Surfaces. *Antimicrob. Agents Chemother.* (2003). doi:10.1128/AAC.47.11.3407-3414.2003

61. Brackman, G. *et al.* The Quorum Sensing Inhibitor Hamamelitannin Increases Antibiotic Susceptibility of Staphylococcus aureus Biofilms by Affecting Peptidoglycan Biosynthesis and eDNA Release. *Sci. Rep.* (2016). doi:10.1038/srep20321

62. Sully, E. K. *et al.* Selective Chemical Inhibition of agr Quorum Sensing in Staphylococcus aureus Promotes Host Defense with Minimal Impact on Resistance. *PLoS Pathog.* (2014). doi:10.1371/journal.ppat.1004174

63. Chai, H. *et al.* Antibacterial effect of 317L stainless steel contained copper in prevention of implant-related infection in vitro and in vivo. *J. Mater. Sci. Mater. Med.* (2011). doi:10.1007/s10856-011-4427-z

64. Li, Y. *et al.* Biodegradable Mg-Cu alloy implants with antibacterial activity for the treatment of osteomyelitis: In vitro and in vivo evaluations. *Biomaterials* (2016). doi:10.1016/j.biomaterials.2016.08.031

65. Ribeiro, M. *et al.* Original Article: Antibacterial silk fibroin/nanohydroxyapatite hydrogels with silver and gold nanoparticles for bone regeneration. *Nanomedicine Nanotechnology, Biol. Med.* **13**, 231–239 (2017).

66. Harrasser, N. *et al.* A new model of implant-related osteomyelitis in the metaphysis of rat tibiae. *BMC Musculoskelet. Disord.* (2016). doi:10.1186/s12891-016-1005-z

67. Lu, M. *et al.* An effective treatment of experimental osteomyelitis using the antimicrobial titanium/silver-containing nHP66 (nano-hydroxyapatite/polyamide-66) nanoscaffold biomaterials. *SCIENTIFIC REPORTS* **6**,

68. Wang, J. *et al.* Antibacterial and anti-adhesive zeolite coatings on titanium alloy surface. *Microporous Mesoporous Mater.* (2011). doi:10.1016/j.micromeso.2011.04.005

69. Seebach, E. *et al.* Mesenchymal stromal cell implantation for stimulation of long bone healing aggravates Staphylococcus aureus induced osteomyelitis. *Acta Biomater.* (2015). doi:10.1016/j.actbio.2015.03.019

70. Shandley, S. *et al.* Hyperbaric oxygen therapy in a mouse model of implant-associated osteomyelitis. *J. Orthop. Res.* (2012). doi:10.1002/jor.21522

71. Jørgensen, N. *et al.* Hyperbaric Oxygen Therapy is Ineffective as an Adjuvant to Daptomycin with Rifampicin Treatment in a Murine Model of Staphylococcus aureus in Implant-Associated Osteomyelitis. *Microorganisms* (2017). doi:10.3390/microorganisms5020021

72. Akram, F. E., El-Tayeb, T., Abou-Aisha, K. & El-Azizi, M. A combination of silver nanoparticles and visible blue light enhances the antibacterial efficacy of ineffective antibiotics against methicillin-resistant Staphylococcus aureus (MRSA). *Ann. Clin. Microbiol. Antimicrob.* (2016). doi:10.1186/s12941-016-0164-y

73. Hasan, S., Thomas, N., Thierry, B. & Prestidge, C. A. Controlled and Localized Nitric Oxide Precursor Delivery From Chitosan Gels to Staphylococcus aureus Biofilms. *J. Pharm. Sci.* (2017). doi:10.1016/j.xphs.2017.08.006

74. Changez, M., Burugapalli, K., Koul, V. & Choudhary, V. The effect of composition of poly(acrylic acid)-gelatin hydrogel on gentamicin sulphate release: In vitro. *Biomaterials* (2003). doi:10.1016/S0142-9612(02)00364-2

75. Diba, M. *et al.* Nanostructured raspberry-like gelatin microspheres for local delivery of multiple biomolecules. *Acta Biomater.* (2017). doi:10.1016/j.actbio.2017.05.059

76. Saul, J. M., Ellenburg, M. D., De Guzman, R. C. & Dyke, M. Van. Keratin hydrogels support the sustained release of bioactive ciprofloxacin. *J. Biomed. Mater. Res. - Part A* (2011). doi:10.1002/jbm.a.33147

77. Overstreet, D., McLaren, A., Calara, F., Vernon, B. & McLemore, R. Local Gentamicin Delivery From Resorbable Viscous Hydrogels Is Therapeutically Effective. *Clin. Orthop. Relat. Res.* (2015). doi:10.1007/s11999-014-3935-9

78. Peng, K. T. *et al.* Treatment of osteomyelitis with teicoplanin-encapsulated biodegradable thermosensitive hydrogel nanoparticles. *Biomaterials* (2010). doi:10.1016/j.biomaterials.2010.03.027

79. Ter Boo, G. J. A. *et al.* Local application of a gentamicin-loaded thermo-responsive hydrogel allows for fracture healing upon clearance of a high Staphylococcus aureus load in a rabbit model. *Eur. Cells Mater.* (2018). doi:10.22203/eCM.v035a11

80. Mahmoudian, M. & Ganji, F. Vancomycin-loaded HPMC microparticles embedded within injectable thermosensitive chitosan hydrogels. *Prog. Biomater.* **6**, 49–56 (2017).

81. Johnson, C., Dinjaski, N., Prieto, M. & García, A. Bacteriophage Encapsulation in Poly(Ethylene Glycol) Hydrogels Significantly Reduces Bacteria Numbers in an Implant-Associated Infection Model of Bone Repair. *Igarss 2014* (2014). doi:10.1007/s13398-014-0173-7.2

82. Dong, L. chang & Hoffman, A. S. A novel approach for preparation of pH-sensitive hydrogels for enteric drug delivery. *J. Control. Release* (1991). doi:10.1016/0168-3659(91)90072-L

83. Posadowska, U., Brzychczy-Wloch, M. & Pamula, E. Injectable gellan gum-based nanoparticles-loaded system for the local delivery of vancomycin in osteomyelitis treatment. *J. Mater. Sci. Mater. Med.* (2016). doi:10.1007/s10856-015-5604-2

84. Ding, H. *et al.* A novel injectable borate bioactive glass cement as an antibiotic delivery vehicle for treating osteomyelitis. *PLoS One* (2014). doi:10.1371/journal.pone.0085472

85. Oh, E. J., Oh, S. H., Lee, I. S., Kwon, O. S. & Lee, J. H. Antibiotic-eluting hydrophilized PMMA bone cement with prolonged bactericidal effect for the treatment of osteomyelitis. *J. Biomater. Appl.* (2015). doi:10.1177/0885328216629823

86. J.A., I., E.M., S., S.L., K. & H.A., A. A novel murine model of established Staphylococcal bone infection in the presence of a fracture fixation plate to study therapies utilizing antibiotic-laden spacers after revision surgery. *Bone* (2015). doi:10.1016/j.bone.2014.11.019

87. Fitzgerald, R. H. Experimental osteomyelitis: description of a canine model and the role of depot administration of antibiotics in the prevention and treatment of sepsis. *J. Bone Joint Surg. Am.* (1983).

88. Melicherčík, P., Nešuta, O. & Čeřovský, V. Antimicrobial peptides for topical treatment of osteomyelitis and implant-related infections: Study in the spongy bone. *Pharmaceuticals* (2018). doi:10.3390/ph11010020

89. Szczeblinska, J., Fijalkowski, K., Kohn, J. & El Fray, M. Antibiotic loaded microspheres as antimicrobial delivery systems for medical applications. *Mater. Sci. Eng. C* (2017). doi:10.1016/j.msec.2017.03.215

90. Posadowska, U., Brzychczy-Włoch, M. & Pamuła, E. Gentamicin loaded PLGA nanoparticles as local drug delivery system for the osteomyelitis treatment. *Acta Bioeng. Biomech.* (2015). doi:10.5277/ABB-00188-2014-02

91. Hassani Besheli, N. *et al.* Sustainable Release of Vancomycin from Silk Fibroin Nanoparticles for Treating Severe Bone Infection in Rat Tibia Osteomyelitis Model. *ACS Appl. Mater. Interfaces* (2017). doi:10.1021/acsami.6b14912

92. Dorati, R. *et al.* An experimental design approach to the preparation of pegylated polylactide-co-glicolide gentamicin loaded microparticles for local antibiotic delivery. *Mater. Sci. Eng. C* (2016). doi:10.1016/j.msec.2015.09.053

93. Hathaway, H. *et al.* Poly(N-isopropylacrylamide-co-allylamine) (PNIPAM-co-ALA) nanospheres for the thermally triggered release of Bacteriophage K. *Eur. J. Pharm. Biopharm.* (2015). doi:10.1016/j.ejpb.2015.09.013

94. Rastogi, L., Kora, A. J. & Arunachalam, J. Highly stable, protein capped gold nanoparticles as effective drug delivery vehicles for amino-glycosidic antibiotics. *Mater. Sci. Eng. C* (2012). doi:10.1016/j.msec.2012.04.044

95. Brown, M. E. *et al.* Testing of a bioactive, moldable bone graft substitute in an infected, critically sized segmental defect model. *J. Biomed. Mater. Res. - Part B Appl. Biomater.* (2018). doi:10.1002/jbm.b.34001

96. Del Gaudio, C. *et al.* Natural polymeric microspheres for modulated drug delivery. *Mater. Sci. Eng. C* (2017). doi:10.1016/j.msec.2017.02.051

97. Saidykhan, L., Bakar, M. Z. B. A., Rukayadi, Y., Kura, A. U. & Latifah, S. Y. Development of nanoantibiotic delivery system using cockle shell-derived aragonite nanoparticles for treatment of osteomyelitis. *Int. J. Nanomedicine* (2016). doi:10.2147/IJN.S95885

98. Ma, Y. *et al.* Enhanced alginate microspheres as means of oral delivery of bacteriophage for reducing staphylococcus aureus intestinal carriage. *Food Hydrocoll.* (2012). doi:10.1016/j.foodhyd.2010.11.017

99. Jennings, J. A. *et al.* Antibiotic-loaded phosphatidylcholine inhibits staphylococcal bone infection. *World J. Orthop.* (2016). doi:10.5312/wjo.v7.i8.467

100. Lucke, M. *et al.* Gentamicin coating of metallic implants reduces implant-related osteomyelitis in rats. *Bone* (2003). doi:10.1016/S8756-3282(03)00050-4

101. Giavaresi, G. *et al.* Efficacy of antibacterial-loaded coating in an in vivo model of acutely highly contaminated implant. *Int. Orthop.* (2014). doi:10.1007/s00264-013-2237-2

102. Harris, M. A., Beenken, K. E., Smeltzer, M. S., Haggard, W. O. & Jennings, J. A. Phosphatidylcholine Coatings Deliver Local Antimicrobials and Reduce Infection in a Murine Model: A Preliminary Study. *Clin. Orthop. Relat. Res.* (2017). doi:10.1007/s11999-016-5211-7

103. Moskowitz, J. S. *et al.* The effectiveness of the controlled release of gentamicin from polyelectrolyte multilayers in the treatment of Staphylococcus aureus infection in a rabbit bone model. *Biomaterials* (2010). doi:10.1016/j.biomaterials.2010.04.011

104. Paiva Costa, L. *et al.* Effectiveness of Chitosan Films Impregnated With Ciprofloxacin for the Prophylaxis of Osteomyelitis in Open Fractures: An Experimental Study in Rats. *Arch. Trauma Res.* (2016). doi:10.5812/atr.36952

105. Windolf, C. D. *et al.* Lysostaphin-coated titan-implants preventing localized osteitis by staphylococcus aureus in a mouse model. *PLoS One* (2014). doi:10.1371/journal.pone.0115940

106. Veyries, M. L., Faurisson, F., Joly-Guillou, M. L. & Rouveix, B. Control of staphylococcal adhesion to polymethylmethacrylate and enhancement of susceptibility to antibiotics by poloxamer 407. *Antimicrob. Agents Chemother.* (2000). doi:10.1128/AAC.44.4.1093-1096.2000

107. Schaer, T. P., Stewart, S., Hsu, B. B. & Klibanov, A. M. Hydrophobic polycationic coatings that inhibit biofilms and support bone healing during infection. *Biomaterials* (2012). doi:10.1016/j.biomaterials.2011.10.038

108. Nandi, S. K., Shivaram, A., Bose, S. & Bandyopadhyay, A. Silver nanoparticle deposited implants to treat osteomyelitis. *J. Biomed. Mater. Res. - Part B Appl. Biomater.* (2018). doi:10.1002/jbm.b.33910

109. McLaren, J. S. *et al.* A biodegradable antibiotic-impregnated scaffold to prevent osteomyelitis in a contaminated in vivo bone defect model. *Eur. Cells Mater.* (2014). doi:10.22203/eCM.v027a24

110. Sanchez, C. J. *et al.* Effects of local delivery of d-amino acids from biofilm-dispersive scaffolds on infection in contaminated rat segmental defects. *Biomaterials* (2013). doi:10.1016/j.biomaterials.2013.06.026

111. Wu, W., Ye, C., Zheng, Q., Wu, G. & Cheng, Z. A therapeutic delivery system for chronic osteomyelitis via a multi-drug implant based on three-dimensional printing technology. *J. Biomater. Appl.* (2016). doi:10.1177/0885328216640660

112. Zhou, J., Zhou, X. G., Wang, J. W., Zhou, H. & Dong, J. Treatment of osteomyelitis defects by a vancomycin-loaded gelatin/β-tricalcium phosphate composite scaffold. *Bone Joint Res.* (2018). doi:10.1302/2046-3758.71.BJR-2017-0129.R2

113. Nelson, C. L. *et al.* The treatment of experimental osteomyelitis by surgical debridement and the implantation of calcium sulfate tobramycin pellets. *J. Orthop. Res.* (2002). doi:10.1016/S0736-0266(01)00133-4

114. Zhang, X. *et al.* Teicoplanin-loaded borate bioactive glass implants for treating chronic bone infection in a rabbit tibia osteomyelitis model. *Biomaterials* (2010). doi:10.1016/j.biomaterials.2010.04.005

115. Schindeler, A. *et al.* Local delivery of the cationic steroid antibiotic CSA-90 enables osseous union in a rat open fracture model of Staphylococcus aureus infection. *J. Bone Jt. Surg. - Am. Vol.* (2015). doi:10.2106/JBJS.N.00840

116. Parker, A. C. *et al.* Characterization of local delivery with amphotericin B and vancomycin from modified chitosan sponges and functional biofilm prevention evaluation. *J. Orthop. Res.* (2015). doi:10.1002/jor.22760

117. Lovati, A. B. *et al.* Diabetic Mouse Model of Orthopaedic Implant-Related Staphylococcus Aureus Infection. *PLoS One* **8**, e67628 (2013).

118. Cassat, J. E. *et al.* A secreted bacterial protease tailors the staphylococcus aureus virulence repertoire to modulate bone remodeling during osteomyelitis. *Cell Host Microbe* (2013). doi:10.1016/j.chom.2013.05.003

119. Chen, X. Q. *et al.* CHI3L1 regulation of inflammation and the effects on osteogenesis in a Staphylococcus aureus-induced murine model of osteomyelitis. *FEBS J.* (2017). doi:10.1111/febs.14082

120. Windolf, C. D. *et al.* Implant-associated localized osteitis in murine femur fracture by biofilm forming Staphylococcus aureus: A novel experimental model. *J. Orthop. Res.* (2013). doi:10.1002/jor.22446

121. Rochford, E. T. J. *et al.* Monitoring immune responses in a mouse model of fracture fixation with and without Staphylococcus aureus osteomyelitis. *Bone* (2016). doi:10.1016/j.bone.2015.10.014

122. Nishitani, K. *et al.* Quantifying the natural history of biofilm formation in vivo during the establishment of chronic implant-associated Staphylococcus aureus osteomyelitis in mice to identify critical pathogen and host factors. *J. Orthop. Res.* **33**, 1311–1319 (2015).

123. Bernthal, N. M. *et al.* A mouse model of post-arthroplasty Staphylococcus aureus joint infection to evaluate in vivo the efficacy of antimicrobial implant coatings. *PLoS One* (2010). doi:10.1371/journal.pone.0012580

124. Xiao, L. *et al.* Detecting Chronic Post-Traumatic Osteomyelitis of Mouse Tibia via an IL-13Rα2 Targeted Metallofullerene Magnetic Resonance Imaging Probe. *Bioconjug. Chem.* (2017). doi:10.1021/acs.bioconjchem.6b00708

125. Lovati, A. B. *et al.* Does PGE1 vasodilator prevent orthopaedic implant-related infection in diabetes? Preliminary results in a mouse model. *PLoS One* (2014). doi:10.1371/journal.pone.0094758

126. Horst, S. A. *et al.* A novel mouse model of staphylococcus aureus chronic osteomyelitis that closely mimics the human infection: An integrated view of disease pathogenesis. *Am. J. Pathol.* (2012). doi:10.1016/j.ajpath.2012.07.005

127. Tuchscherr, L., Geraci, J. & Loeffler, B. Staphylococcus aureus Regulator Sigma B is Important to Develop Chronic Infections in Hematogenous Murine Osteomyelitis Model. *PATHOGENS* **6**,

128. Spagnolo, N. *et al.* Chronic staphylococcal osteomyelitis: A new experimental rat model. *Infect. Immun.* (1993).

129. Brown, N. L. *et al.* Bioburden after Staphylococcus aureus inoculation in type 1 diabetic rats undergoing internal fixation. *Plast. Reconstr. Surg.* (2014). doi:10.1097/PRS.0000000000000434

130. Rissing, J. P., Buxton, T. B., Fisher, J., Harris, R. & Shockley, R. K. Arachidonic acid facilitates experimental chronic osteomyelitis in rats. *Infect. Immun.* **49**, 141–144 (1985).

131. Fukushima, N., Yokoyama, K., Sasahara, T., Dobashi, Y. & Itoman, M. Establishment of rat model of acute staphylococcal osteomyelitis: Relationship between inoculation dose and development of osteomyelitis. *Arch. Orthop. Trauma Surg.* (2005). doi:10.1007/s00402-004-0785-z

132. Stadelmann, V. A. *et al.* In vivo MicroCT monitoring of osteomyelitis in a rat model. *Biomed Res. Int.* (2015). doi:10.1155/2015/587857

133. Lucke, M. *et al.* A New Model of Implant-Related Osteomyelitis in Rats. *J. Biomed. Mater. Res. - Part B Appl. Biomater.* (2003). doi:10.1002/jbm.b.10051

134. Güzel, Y. *et al.* The Efficacy of Boric Acid Used to Treat Experimental Osteomyelitis Caused by Methicillin-Resistant Staphylococcus aureus: an In Vivo Study. *Biol. Trace Elem. Res.* (2016). doi:10.1007/s12011-016-0662-y

135. Inanmaz, M. E. *et al.* Extracorporeal shockwave increases the effectiveness of systemic antibiotic treatment in implant-related chronic osteomyelitis: Experimental study in a rat model. *J. Orthop. Res.* (2014). doi:10.1002/jor.22604

136. Kalteis, T. *et al.* Moxifloxacin superior to vancomycin for treatment of bone infections - A study in rats. *Acta Orthop.* (2006). doi:10.1080/17453670610046082

137. Chen, X., Kidder, L. S. & Lew, W. D. Osteogenic protein-1 induced bone formation in an infected segmental defect in the rat femur. *J. Orthop. Res.* (2002). doi:10.1016/S0736-0266(01)00060-2

138. Chen, X. *et al.* Characterization of a chronic infection in an internally-stabilized segmental defect in the rat femur. *J. Orthop. Res.* (2005). doi:10.1016/j.orthres.2005.01.009

139. Li, B., Brown, K. V., Wenke, J. C. & Guelcher, S. A. Sustained release of vancomycin from polyurethane scaffolds inhibits infection of bone wounds in a rat femoral segmental defect model. *J. Control. Release* (2010). doi:10.1016/j.jconrel.2010.04.002

140. Penn-Barwell, J. G., Rand, B. C. C., Brown, K. V. & Wenke, J. C. A versatile model of open-fracture infection: a contaminated segmental rat femur defect. *Bone Jt. Res.* (2014). doi:10.1302/2046-3758.36.2000293

141. Lei, M. G., Gupta, R. K. & Lee, C. Y. Proteomics of Staphylococcus aureus biofilm matrix in a rat model of orthopedic implant-associated infection. *PLoS One* (2017). doi:10.1371/journal.pone.0187981

142. Bonnarens, F. & Einhorn, T. A. Production of a standard closed fracture in laboratory animal bone. *J Orthop Res* **2**, 97–101 (1984).

143. Robinson, D. A., Bechtold, J. E., Carlson, C. S., Evans, R. B. & Conzemius, M. G. Development of a fracture osteomyelitis model in the rat femur. *J. Orthop. Res.* (2011). doi:10.1002/jor.21188

144. Lindsey, B. A., Clovis, N. B., Smith, E. S., Salihu, S. & Hubbard, D. F. An animal model for open femur fracture and osteomyelitis: Part I. *J. Orthop. Res.* (2010). doi:10.1002/jor.20960

145. Buxton, T. B. *et al.* Low-dose infectivity of Staphylococcus aureus (SMH strain) in traumatized rat tibiae provides a model for studying early events in contaminated bone injuries. *Comp. Med.* (2005).

146. Arens, D. *et al.* A rabbit humerus model of plating and nailing osteosynthesis with and without staphylococcus aureus osteomyelitis. *Eur. Cells Mater.* (2015). doi:10.22203/eCM.v030a11

147. Jensen, L. K. *et al.* Novel porcine model of implant-associated osteomyelitis: A comprehensive analysis of local, regional, and systemic response. *J. Orthop. Res.* (2017). doi:10.1002/jor.23505

148. Odekerken, J. C. E., Arts, J. J. C., Surtel, D. A. M., Walenkamp, G. H. I. M. & Welting, T. J. M. A rabbit osteomyelitis model for the longitudinal assessment of early post-operative implant infections. *J. Orthop. Surg. Res.* (2013). doi:10.1186/1749-799X-8-38

149. Xing, J. *et al.* Anti-Infection Tissue Engineering Construct Treating Osteomyelitis in Rabbit Tibia. *Tissue Eng. Part A* (2013). doi:10.1089/ten.tea.2012.0262

150. Yin, L.-Y., Manring, M. M. & Calhoun, J. H. A Rabbit Osteomyelitis Model to Simulate Multibacterial War Wound Infections. *Mil. Med.* (2013). doi:10.7205/MILMED-D-12-00550

151. Schulz, S., Steinhart, H. & Mutters, R. Chronic osteomyelitis in a new rabbit model. *J. Investig. Surg.* (2001). doi:10.1080/08941930152024246

152. Evans, R. P., Nelson, C. L. & Harrison, B. H. The effect of wound environment on the incidence of acute osteomyelitis. *Clin. Orthop. Relat. Res.* (1993). doi:10.1097/01.blo.0000183276.33237.24

153. Smeltzer, M. S. *et al.* Characterization of a rabbit model of staphylococcal osteomyelitis. *J. Orthop. Res.* (1997). doi:10.1002/jor.1100150314

154. Beenken, K. E. *et al.* Chitosan coating to enhance the therapeutic efficacy of calcium sulfate-based antibiotic therapy in the treatment of chronic osteomyelitis. *J. Biomater. Appl.* (2014). doi:10.1177/0885328214535452

155. Gaudin, A. *et al.* A new experimental model of acute osteomyelitis due to methicillin-resistant Staphylococcus aureus in rabbit. *Lett. Appl. Microbiol.* (2011). doi:10.1111/j.1472-765X.2010.02992.x

156. Hamel, A., Caillon, J., Jacqueline, C., Rogez, J.-M. & Potel, G. Internal device decreases antibiotic's efficacy on experimental osteomyelitis. *J. Child. Orthop.* **2**, 239–243 (2008).

157. Zhang, X. *et al.* A rabbit model of implant-related osteomyelitis inoculated with biofilm after open femoral fracture. *Exp. Ther. Med.* (2017). doi:10.3892/etm.2017.5138

158. Curtis, M. J., Brown, P. R., Dick, J. D. & Jinnah, R. H. Contaminated fractures of the tibia: A comparison of treatment modalities in an animal model. *J. Orthop. Res.* (1995). doi:10.1002/jor.1100130217

159. Dehring, D. J. *et al.* Comparison of live bacteria infusions in a porcine model of acute respiratory failure. *J. Surg. Res.* (1983). doi:10.1016/0022-4804(83)90054-9

160. Aerssens, J., Boonen, S., Lowet, G. & Dequeker, J. Interspecies differences in bone composition, density, and quality: Potential implications for in vivo bone research. *Endocrinology* (1998). doi:10.1210/endo.139.2.5751

161. Tøttrup, M. *et al.* Effects of Implant-Associated Osteomyelitis on Cefuroxime Bone Pharmacokinetics: Assessment in a Porcine Model. *J. Bone Jt. Surgery, Am. Vol.* **98**, 363–369 (2016).

162. Jensen, H. E. *et al.* A non-traumatic Staphylococcus aureus osteomyelitis model in pigs. *In Vivo (Brooklyn).* (2010). doi:10.1016/0377-8401(94)00694-5

163. Dahl, L. B., Hoyland, A. L., Dramsdahl, H. & Kaaresen, P. I. Acute osteomyelitis in children: A population-based retrospective study 1965 to 1994. *Scand. J. Infect. Dis.* (1998). doi:10.1080/00365549850161124

164. Johansen, L. K. *et al.* A porcine model of acute, haematogenous, localized osteomyelitis due to Staphylococcus aureus: A pathomorphological study. *APMIS* (2011). doi:10.1111/j.1600-0463.2010.02700.x

165. Johansen, L. K. *et al.* Pathology and Biofilm Formation in a Porcine Model of Staphylococcal Osteomyelitis. *J. Comp. Pathol.* (2012). doi:10.1016/j.jcpa.2012.01.018

166. Johansen, L. K. *et al.* A new technique for modeling of hematogenous osteomyelitis in pigs: Inoculation into femoral artery. *J. Investig. Surg.* (2013). doi:10.3109/08941939.2012.718043

167. Nielsen, O. L. *et al.* Comparison of autologous (111)In-leukocytes, (18)F-FDG, (11)C-methionine, (11)C-PK11195 and (68)Ga-citrate for diagnostic nuclear imaging in a juvenile porcine haematogenous staphylococcus aureus osteomyelitis model. *Am. J. Nucl. Med. Mol. Imaging* (2015).

168. Deysine, M., Rosario, E. & Isenberg, H. D. Acute hematogenous osteomyelitis: an experimental model. *Surgery* **79**, 97–99 (1976).

169. Petty, W., Spanier, S., Shuster, J. J. & Silverthorne, C. The influence of skeletal implants on incidence of infection. Experiments in a canine model. *J. Bone Jt. Surg. - Ser. A* (1985). doi:10.2106/00004623-198567080-00015

170. Khodaparast, O. *et al.* Effect of a transpositional muscle flap on VEGF mRNA expression in a canine fracture model. *Plast. Reconstr. Surg.* (2003). doi:10.1097/01.PRS.0000066170.56389.27

171. Salgado, C. J., Jamali, A. A., Mardini, S., Buchanan, K. & Veit, B. A model for chronic osteomyelitis using Staphylococcus aureus in goats. *Clin. Orthop. Relat. Res.* (2005). doi:10.1097/01.blo.0000159154.17131.bf

172. Beardmore, A. A., Brooks, D. E., Wenke, J. C. & Thomas, D. B. Effectiveness of local antibiotic delivery with an osteoinductive and osteoconductive bone-graft substitute. *J. Bone Jt. Surg. - Ser. A* (2005). doi:10.2106/JBJS.C.01670

173. Tran, N. *et al.* In vivo caprine model for osteomyelitis and evaluation of biofilm-resistant intramedullary nails. *Biomed Res. Int.* (2013). doi:10.1155/2013/674378

174. Kieser, D. C. *et al.* The deer femur-A morphological and biomechanical animal model of the human femur. *Biomed. Mater. Eng.* (2014). doi:10.3233/BME-140981

175. Hill, P. F., Clasper, J. C., Parker, S. J. & Watkins, P. E. Early intramedullary nailing in an animal model of a heavily contaminated fracture of the tibia. *J. Orthop. Res.* (2002). doi:10.1016/S0736-0266(01)00163-2

176. Williams, D. L. *et al.* Experimental model of biofilm implant-related osteomyelitis to test combination biomaterials using biofilms as initial inocula. *J. Biomed. Mater. Res. - Part A* (2012). doi:10.1002/jbm.a.34123

177. Passl, R., Muller, C., Zielinski, C. C. & Eibl, M. M. A model of experimental post-traumatic osteomyelitis in guinea pigs. *J. Trauma - Inj. Infect. Crit. Care* (1984). doi:10.1097/00005373-198404000-00007

178. Merritt, K. & Dowd, J. D. Role of internal fixation in infection of open fractures: Studies with Staphylococcus aureus and Proteus mirabilis. *J. Orthop. Res.* (1987). doi:10.1002/jor.1100050105

179. Emslie, K. R., Ozanne, N. R. & Nade, S. M. L. Acute haematogenous osteomyelitis: An experimental model. *J. Pathol.* (1983). doi:10.1002/path.1711410206

180. De Jong, N. W. M., Van Der Horst, T., Van Strijp, J. A. G. & Nijland, R. Fluorescent reporters for markerless genomic integration in Staphylococcus aureus. *Sci. Rep.* (2017). doi:10.1038/srep43889

181. Close, D. M. *et al.* Comparison of human optimized bacterial luciferase, firefly luciferase, and green fluorescent protein for continuous imaging of cell culture and animal models. *J. Biomed. Opt.* (2011). doi:10.1117/1.3564910

182. Cronin, M. *et al.* High resolution in vivo bioluminescent imaging for the study of bacterial tumour targeting. *PLoS One* (2012). doi:10.1371/journal.pone.0030940

183. Mack, D., Rohde, H., Knobloch, J. K.-M., Horstkotte, M. A. & Kaulfers, P.-M. Alcoholic ingredients in skin disinfectants increase biofilm expression of Staphylococcus epidermidis. *J. Antimicrob. Chemother.* **49**, 683–687 (2002).

184. Michalopoulos, A. S., Livaditis, I. G. & Gougoutas, V. The revival of fosfomycin. *International Journal of Infectious Diseases* (2011). doi:10.1016/j.ijid.2011.07.007

185. Williams, R. L. *et al.* Fungal spinal osteomyelitis in the immunocompromised patient: MR findings in three cases. *Am. J. Neuroradiol.* (1999).

186. Malhotra, R., Shu-Yi Chan, C. & Nather, A. Osteomyelitis in the diabetic foot. *Diabetic Foot and Ankle* (2014). doi:10.3402/dfa.v5.24445

187. Cool, S. K., Breyne, K., Meyer, E., De Smedt, S. C. & Sanders, N. N. Comparison of In Vivo Optical Systems for Bioluminescence and Fluorescence Imaging. *J. Fluoresc.* **23**, 909–920 (2013).

188. Enright, E. F., Gahan, C. G. M., Joyce, S. A. & Griffin, B. T. The Impact of the Gut Microbiota on Drug Metabolism and Clinical Outcome. *Yale J. Biol. Med.* **89**, 375–382 (2016).

189. Park, J. Y. *et al.* Genetic engineering of a temperate phage-based delivery system for CRISPR/Cas9 antimicrobials against Staphylococcus aureus. *Sci. Rep.* **7**, 44929 (2017).

APPENDIX A

EVIDENCE OF CRISPR-CAS9 MODIFIED BACTERIOPHAGE EFFICACY IN VITRO

Previously, it was demonstrated that the CRISPR-Cas9 system could be utilized for manipulation of the bacteriophage genome (REF). Thus, treatment of biofilms with bacteriophage modified by CRISPR-Cas9 ("φCas9") compared to traditionally used antibiotics was explored.

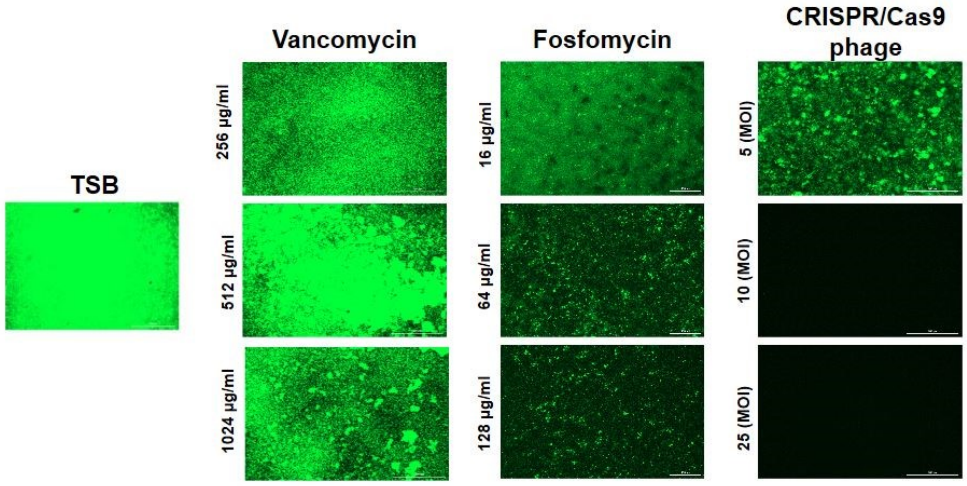

Figure A.1 Cytation5 Investigation of CRISPR-Cas9, Vancomycin, and Fosfomycin Biofilm Treatment

For *in vitro* biofilm studies, a 6-well tissue culture plate was pre-coated with 2% human serum for 24 hours, after which a GFP-integrated strain of S. aureus ATCC 6538 was cultured in tryptic soy broth (TSB) supplemented with 2% glucose for 72 hours. After gentle washing with PBS, TSB supplemented with vancomycin (256, 512, or 1024 µl) or φCas9 (5, 10, or 25 multiplicity of infection (MOI)) was added to the biofilm and incubated for 24 hours before analysis (Cytation 5). For *in vivo* evaluation, a bicortical cylindrical defect was created in the femur diaphysis of female SD rats. Bone wax was used to temporarily seal the ventral portion of the defect, 10 µL of 106 or 107 CFU of S. aureus (n=3) was injected, and a screw was placed in the defect. S. aureus colonization of the femur over time was detected via IVIS Lumina XRMS.

APPENDIX B

ABANDONED ASEPTIC MODELS

As mentioned in the methods, both pin and fixation plate fixation in aseptic pilot studies were considered when trying to identify an appropriate model of osteomyelitis. In the pin fixation model, adequate stabilization to the rat femur was not provided (Fig B.1). In the segmental defection/fixation plate model, bone union was never achieved over 28 days, and thus this model was abandoned.

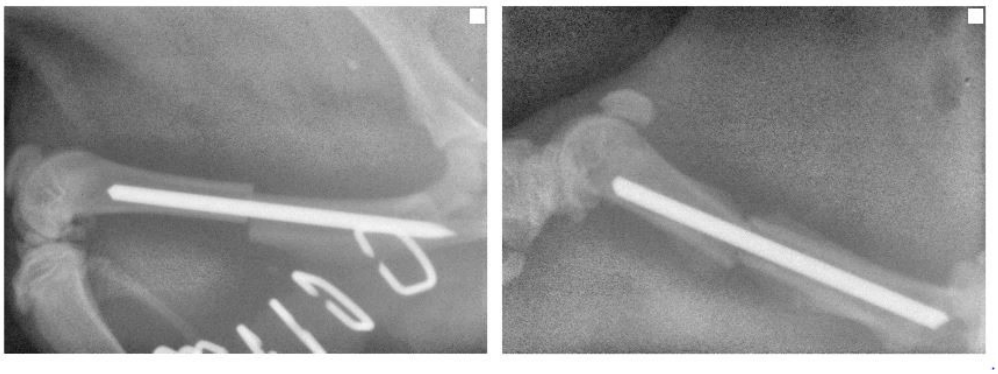

Figure B.1 Pin Fixation in an Aseptic Pilot Study

Two different rats used in the pin fixation aseptic pilot studies were euthanized due to misalignment of femur and lack of stability affecting locomotion.

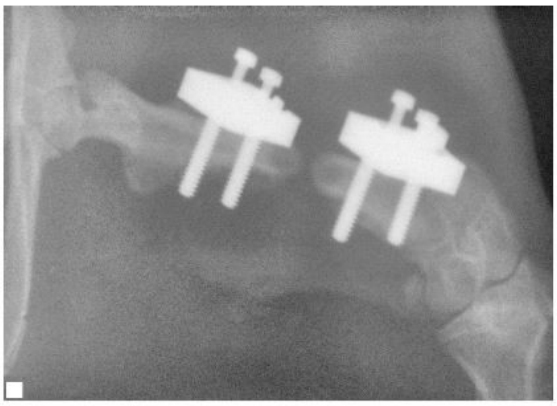

Figure B.2 Segmental defect/ Plate Fixation in an Aseptic Pilot Study(continued)

Although a non-critical segmental defect (3mm) was generated, the proximal and distal femur pieces failed to unite.

APPENDIX C

STATISTICS

All statistical analyses were performed using the GraphPad Prism 8 software system. Significance was confirmed when $p \leq \alpha$ of 0.05.

Model 1: Bacterial Counts

As there were only two groups to compare, an unpaired two tailed t-test was used to compare the two groups.

Model 2: Bacterial Counts

For all bacterial counts in model 2, an Ordinary one-way ANOVA analysis was performed, with a Sidak's multiple comparisons test to compare experimental groups.

APPENDIX D

CHROMOSOMAL INTEGRATION OF GFP INTO ATCC 6538: ADDITIONAL DETAILS & FIGURES

Methods (extended)

Isolation of pTH100, GFP harboring plasmid, from initial *E.Coli* strain

Bacterial strain DH5α harboring plasmid pTH100, the GFP reporter, was purchased for experimental use (Addgene, #84458). This strain was propagated in a 5mL LB + ampicillin culture medium, as the given bacterial strain was characterized by the provider as having ampicillin resistance. To isolate the desired pTH100 plasmid from this strain, 4.5mL of this bacterial culture was first pelleted using a centrifuges and all culture medium was carefully aspirated off. A QIAprep Spin Miniprep kit (QIAGEN) was then used.

Confirmation of DH5α-pTH 100 isolation was then confirmed with standard electrophoresis. A 0.8% agarose gel was generated with Tris acetate and EDTA (TAE) buffer. This solution was then microwaved from 1 min, at which time a 1:10,000 ratio (4uL) of Ethidium Bromide (EtBr) was added. This solution was thoroughly mixed, and casted for loading of DNA samples. 3 μL of the collected DH5α-pTH100 and a 1kB DNA ladder (Thermoscientific, Generuler) were placed into the generated wells with 2uL dye for visualization of ladders. Electrophoresis was then ran for 50 minutes at100V. Residual DH5α-pTH100 was then labelled and placed into a 2-4℃ refridgerator until use.

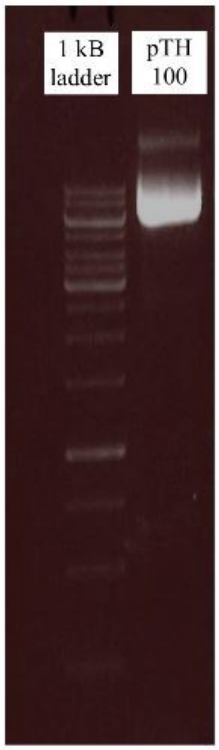

Figure D.1 Electrophoresis of isolated DH5α-pTH100

(Left) A 1 kB DNA ladder serves as a control for this procedure. (Right) A thick ladder forms as a result of our plasmid isolation procedure, indicating successful isolation of the DH5α –pTH 100.

Electroporation of competent *S.aureus* strain RN4220 for DH5α-pTH100 uptake

On ice, 8uL of isolated pTH100 was added to competent *S.aureus* RN 4220 strain, and gently mixed and allowed to sit statically for 30 minutes. 1mL of this mixture was placed into a 2mm gap electroporation cuvette (Fischerbrand, #FB102), which was then placed into a Harvard Apparatus "Electro Cell Manipulator" (ECM 630). The ECM 630 was ran at 2500V, 200Ω. Immediately following this electroporation, 1mL of BHI was added to the cuvette, which was then placed on ice for 30 minutes. The contents of the cuvette were then transferred to a culture tube, and placed into a shaker at 30°C and 200RPM for 4 hours. 100µL of this solution as then

spread onto a BHI with 5mh Chloramphenicol (CM) agar plate and incubated for 22h at 30℃. Five separately resulting bacterial colonies were cultured, resuspended in PBS, and 100µL of this solution was analyzed for fluorescence using a SpectraMax M5 plate reader (Ex. 485 nm, Em.538, bottom read). Controls consisted of: RN4220 (-) and DH5α pTH100 (+). The two colonies with the highest fluorescence (compared to standard RN4220 culture) were selected for future testing.

Table D.2 RN4220/pTH100 Plate Reader Analysis for Fluorescence Uptake

Strain	output
RN 4220 pTH 100- #1	4642.9
RN 4220 pTH 100- #2	2331
RN 4220 pTH 100- #3	5737.6
RN 4220 pTH 100- #4	3197.6
RN 4220 pTH 100- #5	6025.6
RN 4220 (- control)	14.339
DH5α pTH100 (+ control)	368.81

Above are the plate reader results for all 5 isolated RN4220-pTH100 colonies following recovery from electroporation. Compared to the controls and other strains used, RN4220-pTH100 #3 and #5 exhibited the highest apparent fluorescence and were selected for future procedures.

Plasmid isolation from RN4220-pTH100 for uptake in ATCC 6538

RN4220-pTH100 strain #5 was cultured in 5mL BHI/CM culture at 30℃ 200RPM overnight. The pTH100 plasmid was then isolated from this strain using the same methods mentioned above for isolation of pTH 100 from DH5α, utilizing the QIAprep Spin Miniprep kit (QIAGEN). Electroporation was then performed using this isolated pTH100 plasmid with *S.aureus* ATCC 6538 strain in ECM 630 was ran at 2500V, 200Ω. Resulting bacterial culture was then recovered as described above.[180]

Chromosomal Integration of pTH100 into ATCC 6538

Chromosomal integration of pTH100 into ATCC 6538 were performed as previously described. 1 colony of ATCC 6538-pTH 100 was streaked onto an agar plate then incubated at 44℃ to induce the first heat shock event. A single colony from the agar plate that underwent the first heat shock event was then streaked onto a new agar plate, and underwent a second heat shock at 44℃ incubation. 48h later, the agar plate from heat shock #2 was analyzed under hand-held fluorescent light (Cole Palmer). The colony exhibiting the apparent highest fluorescence was then cultured in 5mL BHI at 30℃, 250 RPM. The next day, a 1:1000 dilution of this solution was performed in BHI and returned to 30℃, 250 RPM. 7 hours later, a 1:10 dilution was performed. 10µL of this solution was placed in 1mL fresh BHI and cultured in 30℃, 200 RPM. This dilution procedure was repeated 4-6 times. Resulting ATCC 6538-GFP bacteria was then plated on 1µg/mL anhydrotetracycline agar plates. Bacteria recovered from anhydrotetracylcine plates were then cultured at 37 ℃ in BHI overnight. 4 resulting plates were analyzed under handheld UV light (Cole Palmer UVP-21, #EW-09817-02). All resulting colonies which appeared to exhibit fluorescence under UV light were picked and plated in duplicate, first on BHI then CM agar plates. Bacterial colonies which grew on BHI but not CM were selected for future use. To determine a primary strain for future use, selected colonies were analyzed using SpectraMax M5 plate reader (Ex. 485 nm, Em.538, bottom read).